이학박사학위논문

비만으로부터 유도되는 인슐린 저항성 조절에 관여하는 장내미생물 및 지방조직의 역할 규명

Characterization of gut microbiota and adipose tissues in the regulation of obesity-induced insulin resistance

2018년 2월

서울대학교 대학원

협동과정 유전공학 전공

황 인 재

비만으로부터 유도되는 인슐린 저항성 조절에 관여하는 장내미생물 및 지방조직의 역할 규명

지도교수 김재범

이 논문을 이학박사 학위논문으로 제출함

2018년 2월

서울대학교 대학원

협동과정 유전공학 전공

황 인 재

황인재의 이학박사 학위논문을 인준함

2018년 2월

위 원 장 성 노현 (인)

부위원장 김 재 범 (인)

위 원 이 건수 (인)

위 원 김 민선 (인)

위 원 이 윤희 (인)

Characterization of gut microbiota and adipose tissues in the regulation of obesity induced insulin resistance

A dissertation submitted in partial fulfillment of

the requirements for the degree of

DOCTOR OF PHYLOSOPHY

To the Faculty of

the Interdisciplinary Graduate Program in Genetic Engineering

At

Seoul National University

By

Injae Hwang

February 2018

Date approved

Dec. 21, 2017

ABSTRACT

Characterization of gut microbiota and adipose tissues in the regulation of obesity-induced insulin resistance

Injae Hwang

Chronic energy imbalance leads to obesity, which has been considered as one of a critical risk factor for insulin resistance. Both of gut and adipose tissues have contributed to the regulation of whole body energy homeostasis. For example, small intestine controls the absorption of nutrients and the adipose tissues store extra energy. Recent findings have suggested that gut microbiota is closely linked to adiposity, insulin sensitivity, and glucose metabolism. Studies using germ-free (GF) mice, which are resistant to diet-induced obesity (DIO), have suggested that gut microbiota could play an essential role in the control of host energy homeostasis. Among various phyla in the gut, the abundance ratio of Firmicutes and Bacteroidetes, two major phyla, is altered in the progression of obesity. However, the contribution of Firmicutes and Bacteroidetes in the regulation of insulin resistance has not been

thoroughly understood in obesity.

Adipose tissue inflammation has been implicated in obesity. Among various fat depots, the mass of visceral adipose tissues is correlated with obesity-associated metabolic disorders. On the other hand, subcutaneous adipose tissue is recognized as a beneficial adipose tissue in the regulation of energy homeostasis. Although the physiological differences between visceral and subcutaneous adipose tissues have been documented in clinical and epidemiological studies, the underlying mechanisms elucidating the differential regulation of adipose tissue inflammation in different fat-depots remain unclear.

In chapter one, I have established the diet-induced obese (DIO) mice model which exhibited selective and significant reduction of Firmicutes and Bacteroidetes. Mice with altered gut microbiota ameliorated insulin resistance via increase of glucagon-like peptide 1 (GLP-1), a major gut hormone elevating insulin secretion and insulin sensitivity. Furthermore, alteration of the gut microbiota increased a bile product, taurocholic acid (TCA) which significantly activates GLP-1 secretion in human L-cell (NCI-H716). This study suggests that alteration of gut microbiota would act as an important regulator of obesity-induced insulin resistance. Thus, these findings enhance our understanding of how gut microbiota could interact with host energy homeostasis.

In chapter two, I have examined the underlying mechanisms of fat-depot specific inflammatory responses in obesity. It is of interest to observe that mouse inguinal adipose tissue (IAT) shows the apparent resistance of adipose tissue

macrophage (ATM) infiltration contrast to epididymal adipose tissue (EAT). In this study, I have shown that differential regulations of ATM infiltration between IAT and EAT are due to the intrinsic characteristics of two fat-depots. Gamma (γ)-aminobutyric acid (GABA) signaling pathway was shown to be differentially regulated in EAT and IAT. Pharmacological modulations of $GABA_B$ receptor signaling were solely efficient on ATM infiltration in IAT. Here, I have shown that adipose-derived stem cells (ADSCs) in IAT were responsive to GABA signaling. In accordance with anti-inflammatory roles of GABA in IAT, GABA treatment improved whole body insulin resistance, accompanied by attenuated adipose tissue inflammation in IAT. These data suggest that differential response to GABA between EAT and IAT would contribute to fat-depot specific characteristics in obesity-linked adipose tissue inflammation.

Taken together, I suggest that gut microbiota and IAT are crucial in the regulation of glucose metabolism in obesity. This study provides cellular and physiological understandings how obesity could be linked to systemic insulin resistance. Therefore, it appears that appropriate modulation of gut microbiota and adipose GABA responses might be a prominent strategy for amelioration of insulin resistance associated with various types of metabolic disorders.

Keywords: obesity, gut microbiota, GLP-1, fat-depot specificity, adipose tissue macrophage, gamma-aminobutyric acid

Student Number: 2008-22701

TABLE OF CONTENTS

LIST OF FIGURES

LIST of TABLES

BACKGROUNDS

1. Obesity, insulin resistance, diabetes, and inflammation

1) Obesity-induced insulin resistance and diabetes

The incidence of obese population has been rapidly grown in last decades. 39% of adults are overweight (BMI>25) and 13% are obese (BMI>30) globally (WHO, 2017). The mortality correlated with overweight or obesity becomes increased which leads to severe social costs to deal with the issues (Christakis and Fowler, 2007). Obesity-insulin resistance has been intensively studied to be a major risk factor of metabolic diseases such as type 2 diabetes (Saltiel and Kahn, 2001). Insulin resistance associated hyperglycemia is manifested by elevated hepatic gluconeogenesis, aggravated lipolysis in adipose tissue, and reduced muscle glucose disposals (Kahn and Flier, 2000). In the early stage of obesity, high level of blood insulin maintains normal blood glucose level in spite of presence of insulin resistance. However, chronic hyperinsulinemia induces β-cell failure leading to lack of insulin production and sustained high blood glucose in prolonged obesity (Guilherme et al., 2008). Type 2 diabetes causes various metabolic complications such as cardiovascular disease, renal failure, and retinopathy (Alberti et al., 1998). Thus, obesity is tightly correlated with insulin resistance to induce the pathogenesis of type

2 diabetes.

2) Insulin resistance and inflammation

After the discovery of adipose-derived tumor necrosis factor α (TNFα) secretion in obesity (Hotamisligil et al., 1993), a number of studies suggested that adipose tissues is considered as an immunosensitive organ (Rosen and Spiegelman, 2006). In obesity, adipose tissues increase the expression of pro-inflammatory adipokines and chemokines which recruit and activate immune cells (Kanda et al., 2006). Pro-inflammatory cytokines such as TNFα, interleukin 1β (IL1β), and IL6 in adipose tissues are strongly correlated with insulin resistance (Dandona et al., 2004; Ehses et al., 2009; Hotamisligil et al., 1995). Additionally, these adipokines are linked to insulin resistance of other metabolic organs such as liver, muscle, heart, as well as adipose tissues (Donath and Shoelson, 2011; Olefsky and Glass, 2010b). Pro-inflammatory signaling kinases such as inhibitory κB kinase β (IKKβ) and c-Jun N-terminal kinase (JNK) have been known to suppress insulin signaling cascade via inhibitory serine phosphorylation of insulin receptor substrate 1 (IRS1) and IRS2, one of the most essential downstream mediators of insulin receptor (Chawla et al., 2011; Ferrante, 2007). Moreover, increased phosphorylation of NF-κB and inflammatory kinases stimulate pro-inflammatory genes, which accelerate insulin resistance (Chawla et al., 2011; Wellen and Hotamisligil, 2003). Inhibition or depletion of IKKβ or JNK ameliorates insulin resistance accompanied with distinct

mitigation of inflammatory responses (Austin et al., 2008; Hirosumi et al., 2002; Yuan et al., 2001).

2. Gut, gut microbiota, and host energy metabolism

1) Gut microbiota and obesity

The gut microbiota is a designation of microorganisms such as bacteria, archaea, fungi, and viruses which are colonized at the surface of gut tract (Savage, 1977). It has been perceived intuitively to be necessary for host health (Figure 1). In 1908, Elie Metchnikoff hypothesized that the fermented lactic acid consuming bacteria called ‘probiotics’ would be beneficial to host health (Metchnikoff, 1908). If this mutualism between the host and its microbiota disappeared, dysbiosis can ensue. Barry Marshall and Robin Warren introduced a concept of dysregulated *Helicobacter pylori* in the stomach would cause a noninfectious condition of peptic ulcer disease (Warren and Marshall, 1983). Recently, it has been reported that eating meats induces gut microbiota alteration, and their metabolites, trimethylamine N-oxide, one of the metabolites increasing the risk of atherosclerosis (Tang et al., 2013; Wang et al., 2011). Since most of gut microbiota is anaerobes and uncultivable, there had been a technical limitation of gut microbial studies until the development of next-generation sequencing. In the early 2000s, 16s rDNA metagenome sequencing has revealed that Firmicutes and Bacteroidetes occupy 90% of total gut microbiota

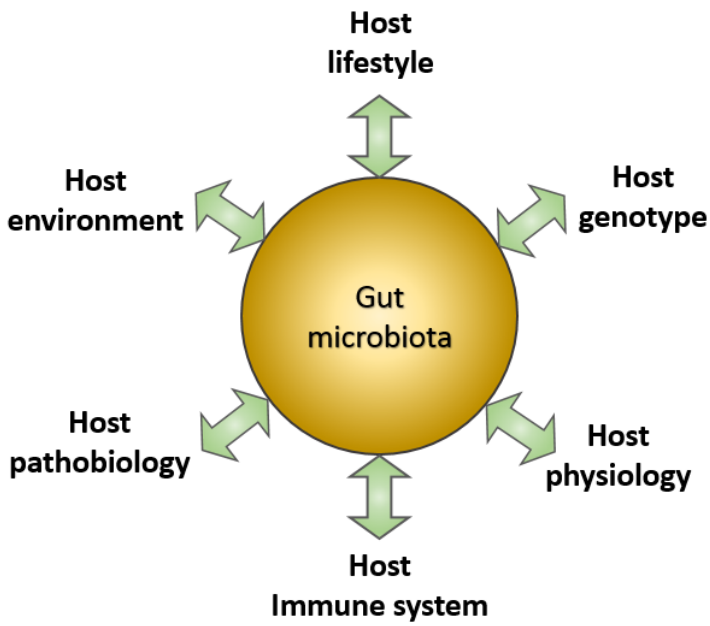

Figure 1.

Interaction between gut microbiota and host. A variety of host factors such as environmental and nutritive condition, lifestyle, genotypes, gender, and disease lead to alteration of the compositions in gut microbiota. Simultaneously, gut microbiota is able to affect various aspects of hosts. Gut microbiota assists the maintenance of host physiology, pathobiology, and immune system via regulation of mucosal immunity, angiogenesis, neuronal activities, and energy metabolism as well as nutrient digestion.

(Ley et al., 2005b). Intriguingly, the relative abundances of Firmicutes and Bacteroidetes denote shifts correlated with the development of obesity (Ley et al., 2005b). In genetically obese mice, obesity is associated with a reduction in the abundance of Bacteroidetes and a relative increase in Firmicutes. The abundance shifts between Firmicutes and Bacteroidetes have been shown in the study of lean and obese human twins (Turnbaugh et al., 2009). In addition, it has been shown that both of germ-free (GF) and pharmacological gut flora depleted mice are resistant to diet-induced obesity (DIO) with improved insulin resistance (Backhed et al., 2004a; Cani et al., 2008a; Murphy et al., 2013b). In DIO mice, treatment of norfloxacin and ampicillin results in a decrease of cecal aerobic and anaerobic bacteria, concurrent with improved insulin resistance and lipid metabolism (Membrez et al., 2008b). Thus, it is of interest to observe whether Firmicutes and Bacteroidetes might be involved in the regulation of body weight and energy metabolism in obesity.

2) Gut microbiota and energy metabolism

In the past two decades, gut microbiota has been recognized as a crucial player interacting with host physiology and pathophysiology (Becattini et al., 2016). The human gut microbiota consists of an estimated one hundred trillion bacteria belonging to hundreds of different species (Rajilic-Stojanovic and de Vos, 2014). Among commensal bacteria in gut, Firmicutes and Bacteroidetes occupy about 90% of total bacterial population (Walter and Ley, 2011). In obesity, it has been well-

studied that relative abundance in Firmicutes increases whereas the occupancy of Bacteroidetes are reduced (Ley et al., 2005b). Additionally, gut microbiota has emerged as an extrinsic factor contributing to host metabolism on the basis of the initial finding that GF mice have reduced adiposity and insulin resistance (Backhed et al., 2004a). Given that gut microbiota is associated with host energy metabolism, several lines of evidence have suggested how gut microbiota has influenced on obesity and insulin sensitivity. First, gut microbiota enhances calories absorption in gut. In obesity, Firmicutes is correlated with increased level of short-chain fatty acids such as acetate, propionate, and butyrate (Turnbaugh et al., 2006). This report has suggested that elevated such short-chain fatty acids could be utilized as extra calories to induce obesity. Second, it has been demonstrated that activations of AMP-activated protein kinase (AMPK) and peroxisome proliferator-activated receptor gamma coactivator 1-α (PGC1α) would accelerate fatty acid oxidation in GF mice. (Backhed et al., 2007). In this report, GF mice gain less body weights upon high-fat diet (HF) feeding, $Fiaf^{-/-}$ GF mice exhibit a similar level of obesity compared to conventionalized wild-type control. Third, gut microbiota in obese mice is a source of adipose tissue inflammation which could induce insulin resistance. Upon HF, the serum level of endotoxin increases with elevated insulin resistance (Cani et al., 2007). The endotoxemia in obesity is able to aggravate inflammation via activation of $CD14^{+}$ monocytes and macrophages. However, the eliminations of gut microbiota by antibiotic-cocktails reduce gut-permeability and rescue endotoxemia accompanied with enhanced insulin sensitivity (Cani et al., 2008a). Lastly, gut microbiota seems to be associated with adipose tissue browning which is responsible

for calories consuming thermogenesis. In antibiotic-treated mice, uptakes of 2-^{14}C deoxyglucose (2-[^{14}C]DG) and ^{18}F fluorodeoxyglucose ([^{18}F]FDG) are increased in inguinal adipose tissue (IAT) and epididymal (EAT) in spite of similar degree of the 2-[^{14}C]DG and [^{18}F]FDG uptakes in interscapular brown adipose tissue (BAT) (Mestdagh et al., 2012; Suarez-Zamorano et al., 2015). These antibiotic-treated mice present significant changes of browning gene expressions such as uncoupling protein 1 (UCP1), cell death activator CIDE-A (CIDEA), PGC1α, peroxisome proliferator-activated receptor γ (PPARγ), and PR domain containing 16 (PRDM16). Consistently, alteration of gut microbiota by intermittent fasting to facilitate browning via elevation of SCFAs (Li et al., 2017).

3) Gut hormones

Primary functions of the gastrointestinal tract are stimulated by nutrient supplements. In response to nutrients, gut produces various hormones involved in digestion, metabolism, and appetite. In stomach, ghrelin secreted from stomach acts as a nutrient sensor for brain to increase appetite (Muller et al., 2015) whereas cholecystokinin (CCK), neurotensin and peptide YY (pYY) inhibit appetites (Svendsen and Holst, 2016). Incretin hormones such as a glucose-dependent insulinotropic polypeptide (GIP), glucagon-like peptide 1 (GLP-1) and 2 (GLP-2) have been isolated and characterized (Campbell and Drucker, 2013b). Among these incretin hormones, GLP-1 is synthesized and secreted by intestinal L-cells

(Campbell and Drucker, 2013b; Lee et al., 1990). Upon nutrients, L-cells increase the expression of proglucagon genes and induce the cleavages of proglucagon into the active form of GLP-1 (7-36 amide) by PKA signaling (Drucker and Brubaker, 1989; Lim and Brubaker, 2006) (Figure 2 and Figure 3). In blood, GLP-1 activates pancreatic β-cells to secrete insulin via GLP-1 receptor (Willms et al., 1996). In addition to the insulinotropic function, GLP-1 also enhances insulin sensitivity (Jinnouchi et al., 2015; Parlevliet et al., 2010). Although beneficial effects of GLP-1 on energy balance in obesity, endogenous GLP-1 is rapidly converted into the inactive form of GLP-1 (9-36 amide) which cannot bind to the GLP-1 receptor (Deacon et al., 1995b). The roles of GLP-1 (9-36 amide) to maintain glucose metabolisms is controversial (Deacon et al., 2002a; Vahl et al., 2003).

4) Bile acids

Bile acids are major constituents of bile. Bile is synthesized and secreted from hepatocytes and stored in gallbladder. Ingested foods enter duodenum elevating the secretion of CCK, which stimulates bile acid secretion in the gallbladder. Bile acids are amphipathic molecules essential for solubilization of lipids and hydrophobic vitamin A, D, E and K. Most of the bile acids are reabsorbed from the intestine and transported back to liver via portal vein. Bile acids are able to activate farnesoid X receptor (FXR) (Makishima et al., 1999; Tu et al., 2000). Bile acids can stimulate FXR to activate fibroblast growth factor 15/19 (FGF15/19)

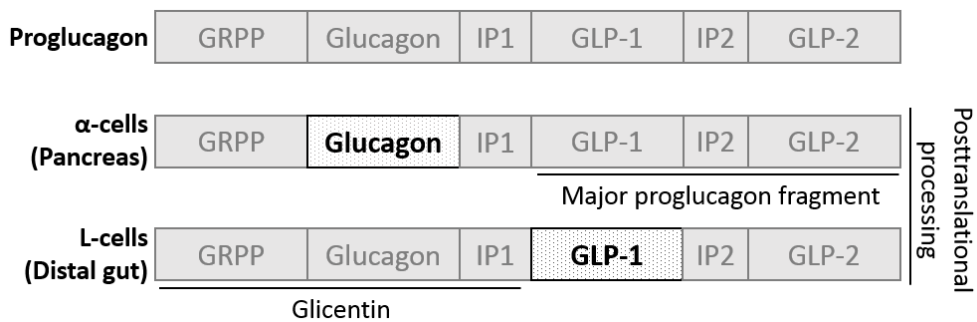

Figure 2.

Tissue-specific processing of proglucagon produces different proglucagon-derived proteins. Proglucagon convertase 2 releases glicentin-related pancreatic peptide (GRPP), glucagon, intervening peptide-1 (IP1), and major proglucagon fragment. In the L-cell of distal gut, proglucagon is separated into glicentin, GLP-1, IP2, and GLP-2.

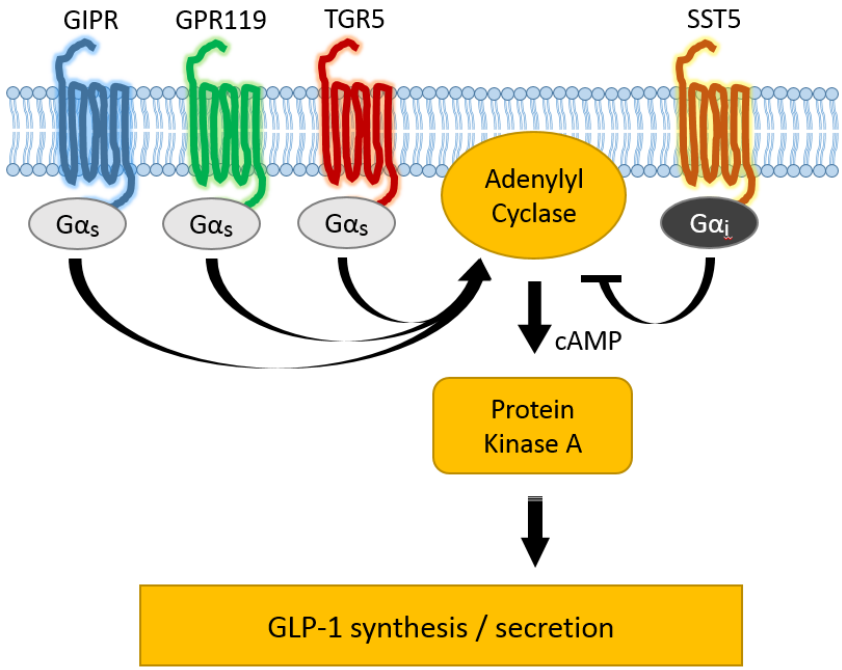

Figure 3.

Various intracellular pathways in the regulation of GLP-1 secretion. Binding of GIP to GIP receptor (GIPR) is associated with stimulation of adenylyl cyclase. Activation of GPR119 via oleoylethanolamide and bile components binding to TGR5/GPR131 activate adenylyl cyclase via stimulatory Gα (Gαs) proteins. Elevation of the cyclic AMP (cAMP) induces PKA phosphorylation to enhance GLP-1 synthesis and secretion. In contrast, somatostatin receptor is coupled with inhibitory Gα (Gαi) protein, which inhibits adenylyl cyclase to suppress PKA activation. Solid arrows; known pathway, dashed arrows; unknown pathway.

(Holt et al., 2003; Inagaki et al., 2005). FGF15/19 binds to FGF receptor 4 (FGFR4), leading to inhibition of cholesterol 7α-hydroxylase (CYP7A1), the rate-limiting enzyme of bile acid synthesis. The composition of bile acids are heterogeneous (Fang et al., 2015; Russell, 2003). Primary bile acids such as cholic acid and chenodeoxycholic acid are synthesized in liver. When these bile acids are secreted, gut microbiota conjugates glycine and taurine to form variable forms of secondary bile acids. Recently, it has been reported that these bile acids are able to activate G-protein coupled receptor 131 (GPR131/TGR5) which accelerate secretion of GLP-1 via PKA activation (Hwang et al., 2015; Pols et al., 2010). Additionally, bile acids agonist (fexaramine) treatment enhances thermogenesis via browning of white adipose tissues (WAT) (Fang et al., 2015).

3. Adipose tissue inflammation and fat-depot specificity

1) Adipose tissue immunity

Adipose tissue is composed of heterogeneous cell types such as adipocytes, fibroblasts, endothelial cells, and innate and acquired immune cells. Innate immune cells are composed of macrophage, neutrophil, eosinophil, and mast cells whereas acquired immune cells include various types of T and B cells. In lean individual, anti-inflammatory immune cells such as alternatively activated (M2) macrophages, eosinophil, and regulatory T cells prevail and regulate energy balance (Ding et al.,

2016; Feuerer et al., 2009; Odegaard et al., 2008). However, in the progression of obesity, pro-inflammatory immune cells such as classically activated (M1) macrophages, cytotoxic T cells, and neutrophil are increased as well as adipocyte hypertrophy. These pro-inflammatory immune cells exacerbate immune imbalance in adipose tissue and promote insulin resistance (Lumeng et al., 2007a; Nishimura et al., 2009; Talukdar et al., 2012) (Figure 4). Among various type of immune cells in adipose tissue, adipose tissue macrophages (ATMs) have been intensively studied to be a major risk factor for obesity-induced insulin resistance.

2) Adipose tissue macrophages

Macrophage is a predominant cell type. In lean animals, M2 macrophages maintain insulin sensitivity in adipose tissues by secretion of anti-inflammatory cytokines such as IL10 and Ym-1 (Chawla et al., 2011; Choe et al., 2016). However, in the progression of obesity, the number of M1 macrophages is increased (Lumeng et al., 2007a). $CD11c^+$ M1 macrophages express inducible nitric oxide synthase (iNOS), TNFα, and IL1β contributing to pro-inflammatory responses in adipose tissues. Further, transplantation of $CD11c^-$ bone marrow into γ-irradiated mice attenuates inflammatory responses and improved body weight gains and insulin resistance supporting the idea that roles of pro-inflammatory ATMs are crucial in the regulation of obesity-induced insulin resistance (Patsouris et al., 2008). Pro-inflammatory ATMs are activated by stimulation of toll-like receptors (TLRs) to

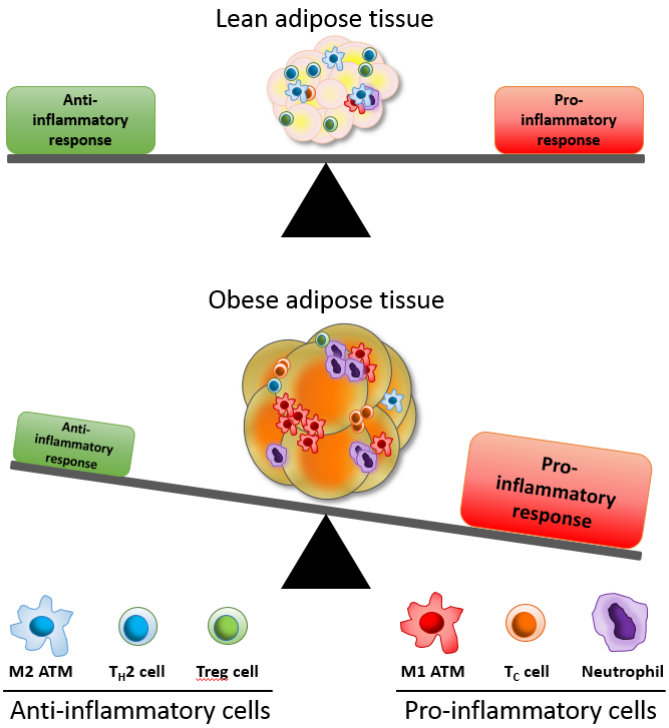

Figure 4.

Alteration of immunity in lean versus obese adipose tissues. Lean adipose tissue harbors various types of anti-inflammatory immune cells such as M2 ATM, helper T type 2 (T_H2) cell, and Treg cells. These immune cells are involved in maintaining insulin sensitivity and store extra energy in the form of triglycerides in adipocytes. In obese animals, the number of pro-inflammatory immune cells including neutrophil, M1 ATM, cytotoxic T (Tc) cell, and neutrophil are elevated. Simultaneously, anti-i6nflammatory immune cells are decreased, leading to aggravation of adipose tissue inflammation and dysfunction.

induce pro-inflammatory responses. Once TLRs are activated, mitogen-activated protein kinases (MAPKs) are phosphorylated to induce inflammatory responses. Representative MAPKs under TLR signaling pathways are extracellular signal-regulated kinases (ERK), JNKs, and the p38 MAP kinases (Bode et al., 2012; Herlaar and Brown, 1999). Simultaneously, nuclear factor κB (NF-κB) also plays crucial roles in the regulation of inflammatory responses (Baeuerle and Henkel, 1994; Xie et al., 1994). In the resting status, inhibitory κB tethers NF-κB components in the cytoplasm. However, upon inflammatory stimuli, IKKβ phosphorylates IκB for ubiquitin-dependent degradation to release NK-κB into nucleus for transcription of various inflammatory genes. In addition to regulation of energy metabolism, several lines of evidence have suggested that ATMs are crucial for development of adipose tissues. First, M2 ATMs contribute to tissue repair and angiogenesis (Nguyen et al., 2007). Second, ATMs are reported to be recruited into the tips of the gonadal adipose tissue to promote tissue outgrowth (Cho et al., 2007). Third, ATMs surrounding adipogenic progenitors are important for adipogenesis (Lee et al., 2013). Accordantly, a mouse with suppression of inflammatory responses showed less adipogenic activity *in vivo* (Asterholm et al., 2014).

3) Fat-depot specific characteristics in obesity

Adipose tissues are present in whole body and store excess energy in the form of lipid metabolites. In human and rodents, there are two different adipose-depots

with physiological roles, WAT and BAT. Anatomically, WAT is largely divided into two major depots, subcutaneous and visceral adipose tissues. Visceral adipose tissues are located in the abdominal cavity and can be further subdivided into mesenteric, omental, perirenal, and perigonadal depots in mice. Although both subcutaneous and visceral adipose tissues belong to WAT, they are fundamentally different. For instance, the expression profiles of lipid metabolism-related genes and inflammatory genes between human omental and subcutaneous adipose tissues are significantly different (Montague et al., 1998). Subcutaneous adipose tissue is highly vascularized compared to visceral adipose tissue (Gealekman et al., 2011). In addition, the number of adipose-derived stem cells (ADSCs) and their characteristics are differentially regulated (Chau et al., 2014; Jeffery et al., 2015; Joe et al., 2009). Since the degree of visceral obesity is positively correlated with the incidence of diabetes, visceral adipose tissue has been intensively subjected to study (Gesta et al., 2007; Kissebah and Krakower, 1994). In contrast, subcutaneous adipose tissue has been considered against metabolic complications. It has been shown that in HF feeding, the subcutaneous adipose tissue transplanted mice exhibit resistance to DIO and less insulin resistance (Hocking et al., 2014; Tran et al., 2008). Another report has revealed that subcutaneous adipose tissue plays crucial roles in the prevention of atherosclerosis (Siviero-Miachon et al., 2015). Moreover, cold exposure induces vigorous browning of subcutaneous adipose tissue compared to visceral adipose tissue (Cohen and Spiegelman, 2015). It has been demonstrated that browning of subcutaneous adipose tissues could facilitate fatty acid consumption to improve obesity and energy metabolisms (Kim and Plutzky, 2016). However, the underlying

mechanisms how subcutaneous adipose tissue contributes to obesity-induced insulin resistance are largely unknown.

4. Purpose of this study

Insulin resistance is a crucial risk factor for most metabolic disorders. Particularly, obesity-induced insulin resistance is accompanied by numerous physiological changes which are mechanically linked to alteration of energy metabolism. Gut microbiota and adipose tissues undertake dynamic changes in response to excess nutrients. Gut microbiota in host gut epithelial cells has been implicated in the regulations of energy homeostasis and inflammation in obesity. However, it has not been verified whether and how specific gut phyla would affect obesity-induced insulin resistance. In parallel, visceral adipose tissue undertakes rapid changes in fat-components, adipocyte size, and structures in obesity. The clinical and epidemiological clues led to focus on the role of visceral adipose tissue rather than subcutaneous adipose tissue. However, the previous reports of adipose tissue transplantation led me to investigate the roles of subcutaneous fat-depot in the regulation of metabolic disorder.

In the first chapter, I have established a model of DIO mice with depletion of Firmicutes and Bacteroidetes by using antibiotics. With these antibiotics treated animal model, I was able to test the involvement of those two major phyla in the regulation of obesity and insulin resistance. Unexpectedly, alteration of gut

microbiota did not change the progression of obesity compared to control group. However, ablation of Firmicutes and Bacteroidetes significantly improved insulin resistance. Further, GLP-1 was discovered to be a key mediator between gut microbiota alteration and amelioration of insulin resistance in DIO animals

In the second chapter, I have examined IAT and EAT in obesity. Among numerous changes, inflammation and the number of ATM accumulation were the most obvious differences between subcutaneous IAT and visceral EAT. To explore which factor might be involved in fat-depot specific ATM accumulation, transcriptome analyses have been conducted. Interestingly, I have discovered that gamma (γ)-aminobutyric acid (GABA) signaling would be considerably distinct in IAT compared to EAT. Modulation of GABAergic signaling improved insulin resistance in subcutaneous IAT. Taken together, I would like to propose the idea that Firmicutes and Bacteroidetes and GABA response in subcutaneous adipose tissue would be crucial to regulate energy metabolism in obesity.

CHAPTER ONE:

Alteration of gut microbiota by antibiotics improves insulin resistance via GLP-1 in diet-induced obesity

Summary

Firmicutes and Bacteroidetes, two major phyla of gut microbiota, are involved in lipid and bile acid metabolism to maintain systemic energy homeostasis in host. Recently, accumulating evidence has suggested that dietary changes promptly induce the alteration of abundance of both Firmicutes and Bacteroidetes in obesity and its related metabolic diseases. Nevertheless, the metabolic roles of Firmicutes and Bacteroidetes on such disease states remain unclear. The aim of this study was to determine the effects of antibiotic-induced depletion of Firmicutes and Bacteroidetes on dysregulation of energy homeostasis in obesity. Treatment of C57BL/6J mice with the antibiotics (vancomycin and bacitracin; V + B), in the drinking water, before diet-induced obesity (DIO) greatly decreased both Firmicutes and Bacteroidetes in the gut as revealed by pyrosequencing of the microbial 16S rRNA gene. Concomitantly, systemic glucose intolerance, hyperinsulinemia, and insulin resistance in DIO were ameliorated via augmentation of GLP-1 secretion (active form; 2.03 fold, total form; 5.09 fold) independently of obesity as compared with untreated DIO controls. Furthermore, there were increases in metabolically beneficial metabolites derived from the gut. Together, my data suggest that Firmicutes and Bacteroidetes potentially mediate insulin resistance through modulation of GLP-1 secretion in obesity.

Introduction

Obesity and obesity-related metabolic diseases including cancer, type 2 diabetes, and cardiovascular diseases impose a high social burden in terms of quality of life (Christakis and Fowler, 2007; Ludwig, 2002; Schulz et al., 2014). Many groups have investigated the effects of genetic and environmental factors on the development of obesity and demonstrated that several factors such as adipose tissue inflammation and hepatic lipid metabolism are associated with the etiology of obesity (Jo et al., 2013; Olefsky and Glass, 2010a).

A number of studies suggest that gut microbiota is closely linked to adiposity, insulin sensitivity, and glucose metabolism (Backhed et al., 2004b; Ley et al., 2005a). Studies performed in germ-free (GF) mice, which are resistant to diet-induced obesity (DIO), suggested that gut microbiota plays a key role in the regulation of adiposity and host energy homeostasis (Backhed et al., 2004b; Backhed et al., 2007). Furthermore, modulation of gut microbiota with the antibiotic treatment leads to a reduction of glucose intolerance, adiposity and adipose tissue inflammation (Cani et al., 2008a). For instance, treatment of a combination of norfloxacin and ampicillin to obese mice resulted in a decrease in the number of cecal aerobic and anaerobic bacteria followed by improved glucose tolerance and liver lipid metabolism

independently of obesity (Membrez et al., 2008a). Among the various phyla in the gut, it has been noted that a shift in the abundance of two major phyla, Firmicutes and Bacteroidetes, correlates with the development of obesity (Hildebrandt et al., 2009; Ley et al., 2005a). In genetically obese *ob/ob* mice, the development of obesity is associated with a reduction in the abundance of Bacteroidetes and a proportional increase in Firmicutes (Ley et al., 2005a). Moreover, analogous differences in gut microbiota have been reported in studies of lean versus obese humans (Turnbaugh et al., 2009). However, accumulating evidence has suggested that there is no correlation between the proportions of Firmicutes and Bacteroidetes and obesity (Collado et al., 2008; Schwiertz et al., 2010). Schwietz et al., reported that there is more Bacteroidetes in the gut of overweight and obese humans as compared to lean humans (Schwiertz et al., 2010). Another group also suggested that higher abundance of Firmicutes is present in lean people relative to obese people (Collado et al., 2008). Therefore, there is controversy regarding changes in the relative abundance of Firmicutes and Bacteroidetes in gut microbiota are related to obesity. Intriguingly, Firmicutes and Bacteroidetes have been implicated in the regulation of lipid and bile acid metabolism, maintaining energy homeostasis in the host (Martin et al., 2007; Turnbaugh et al., 2006; Van Eldere et al., 1996). Notably, both phyla are enriched with genes encoding multiple enzymes that govern carbohydrate and lipid metabolism

(Turnbaugh et al., 2006). In addition, both Firmicutes and Bacteroidetes promptly engage in the regulation of bile acid (BA) modification and govern BA-controlled endocrine functions including triglyceride, cholesterol, and glucose homeostasis (Van Eldere et al., 1996). Importantly, it has been demonstrated that perturbations of BA-mediated signaling pathway influence risk of metabolic complications such as obesity and diabetes (Martin et al., 2007). In spite of of such common features shared by Firmicutes and Bacteroidetes, it has not been precisely elucidated the possible roles of Firmicutes and Bacteroidetes in dysregulation of energy homeostasis in obesity and its related disorder.

Gut hormones, glucose-dependent insulinotropic polypeptide (GIP), glucagon-like peptide 1 (GLP-1) and 2 (GLP-2), are crucial regulators of processes that contribute to whole body energy metabolism, including satiety, gut motility, insulin secretion, and glucose uptake (Campbell and Drucker, 2013a). Among the three hormones, GLP-1 is known to have anti-diabetic effects and secreted by several cell types such as L-cells in the posterior gut tract and neurons in the brain (Brubaker, 2006; Pols et al., 2010). Although short-chain fatty acids produced by certain types of gut microbiota stimulate GLP-1 secretion through G-protein-coupled receptor signaling (Tolhurst et al., 2012), it is largely unknown whether changes in gut microbiota in response to nutrient cues would modulate GLP-1 secretion.

In this study, I demonstrated that treatment with the antibiotics, vancomycin (V) and bacitracin (B), before DIO depleted Firmicutes and Bacteroidetes in the gut and ameliorated insulin resistance. Notably, I found that such beneficial effect on systemic energy homeostasis in the host was mediated by stimulation of GLP-1 secretion. Furthermore, there were increments of gut metabolites, which positively regulate host energy metabolism.

MATERIALS AND METHODS

Animal experiments

C57BL/6J mice were obtained from Central Lab Animal Inc. (Seoul, South Korea) and were housed in colony cages under a 12 hour (h) - light/12 h - dark cycle with free access to food and water. Mice were allowed for acclimate for 2 weeks before the study. To assess the impact of antimicrobial strategies on metabolic changes in DIO mice, 8-week-old male mice were fed normal chow (NC) for 4 weeks and then fed a high fat diet (HF) for 4 weeks (NH group). For mice with changes in gut microbiota (Ab-NH group), these mice were administered drinking water containing vancomycin hydrochloride (0.5 g/L; v2002; Sigma, St. Louis, MO, USA) and bacitracin zinc salt (1.0 g/L; B5150; Sigma). After 4 weeks, NH and Ab-NH mice were switched from a NC to a HF comprising 60% kcals from fat composed of soybean oil and lard (Research Diets Inc., New Brunswick, NJ, USA). Ab-NH group continued to receive water with vancomycin + bacitracin (V + B). Age-matched NC fed mice were maintained without antibiotics (V + B) and HF. In the experimental set, glucose tolerance tests, insulin tolerance tests, and plasma insulin measurements were performed for each group (NC, NH, and Ab-NH groups). After 2 weeks of recovery, on the day of sacrifice, various metabolic parameters of Ab-NH group were compared with NC and NH group. 3 to 10 mice were used for each experimental group. All experiments were approved by the Seoul National University Institutional Animal Care and Use Committees (IACUC).

Body weight, food intake, and water consumption

Body weight, food intake, and water consumption were measured every week after the start of antibiotics or HF treatment during the indicated time periods. Pre-measured amounts of food were placed in the cage. After 24 h, food was reweighted and the amount of consumed food was calculated by difference. The average food consumption was calculated from four repeated experiments. To measure water consumption, the volume of water consumed was quantified once a week for eight weeks after the start of antibiotics (V + B) administration. Water (100 mL) with or without antibiotics was provided in a sterile bottle. After 24 h, the remaining water was measured by mass cylinder.

Pyrosequencing data analyses

The basic analyses were performed on cecal contents according to procedures described in other studies (Chun et al., 2010). The obtained reads from the different samples were sorted by the unique barcodes of each PCR product. The sequences of the barcode, linker, and primers were removed from the original sequencing reads. Any reads containing two or more ambiguous nucleotides, a low quality score (average score < 25), or reads shorter than 300 bp were discarded. The taxonomic classification of each read was assigned using the EzTaxon-e database (http://eztaxon-e.ezbiocloud.net), which contains the 16S rRNA gene sequence of type strains that have valid published names and representative species level

phylotypes of either cultured or uncultured entries in the GenBank database with complete hierarchical taxonomic classification from the phylum to species level (Kim et al., 2012). This experiment was performed at Chunlab Inc. (Seoul, South Korea).

Glucose tolerance test

As described previously (Lee et al., 2011), mice fasted for 7 h were administered a glucose solution (2 g/kg glucose, 20% glucose solution) through intraperitoneal injections or oral gavages. Blood samples were collected at 15, 30, 60, 90, 120, and 150 minutes (min) after injection and blood glucose level was measured. For exendin 9-39 amide injection study using NH and Ab-NH mice, these groups were intraperitoneally injected with either glucose alone or glucose mixed with exendin 9-39 amide (25 nmol/kg; ab141101; Abcam, Cambridge, UK). Glucose tolerance test was performed by intraperitoneal injection of glucose at 2 g/kg body weight, followed by measurement of blood glucose at 0, 15, 30, 45, 60, 75, 90 and 120 min after intraperitoneal injection.

Insulin tolerance test

As described previously (Lee et al., 2011), mice fasted for 7 h were injected with insulin (I-5500; Sigma) via the peritoneal cavity at a dose of 0.4 U/kg. Blood

was sampled at 15, 30, 60, 90, and 120 min after injection by drawing 3 μL of blood from the tip of the tail vein.

Western blot analyses

Muscle tissues and livers isolated from each mouse were homogenized with modified immunoprecipitation assay (RIPA) buffer (50 mM Tris-HCl [pH 7.4], 150 mM NaCl, 1 mM EDTA, 1 mM PMSF, 1% (v/v) NP-40, 0.25% (w/v) Na-deoxycholate, and protease inhibitor cocktail with 1 mM NaF and 10 mM Na_3VO_4 as phosphatase inhibitors) and subjected to 8% SDS-PAGE. As previously described (Kim et al., 2009), membranes were blotted with antibodies against the following proteins: phospho-Akt (Ser473) (Cell Signaling Technology, Beverly, MA, USA), Akt (Cell Signaling Technology), phospho-GSK3β (Ser 9) (Cell Signaling Technology), GSK3β (BD, NJ, USA), GAPDH (AbFrontier, Gasan-dong, Seoul, Korea), and β-actin (Sigma, St. Louis, MO, USA).

RNA isolation and quantitative real-time PCR (qPCR)

As described previously (Kim et al., 2009; Lee et al., 2011), each tissue was homogenized with TRI Reagent (Molecular Research Center, Cincinnati, OH, USA). cDNA was synthesized using M-MuLV reverse transcriptase (Fermentas, Glen Burnie, MD, USA). Q-RT-PCR was performed using the MyiQ quantitative real-time PCR detection system (Bio-Rad Laboratories Inc.) with SYBR Green I

(BioWhittaker Molecular Applications; Rockland, ME, USA). The level of each mRNA was normalized to the level of 18S rRNA or cyclophilin mRNA. The primer sequences are available upon request.

Micro-computed topography (CT) image acquisition

Each mouse was maintained under anesthesia with isoflurane (2.5% flow rate) for the duration of the scan. Animals were positioned prone in the standard mouse bed. Limbs were positioned laterally to the body to acquire uniform CT images. Whole body CT images were obtained with a Micro-SPECT/CT scanner (NanoSPECT/CT, Bioscan Inc., Washington DC, USA). For CT image acquisition, the X-ray source was set to 200 μA and 45 kVp with 0.5 mm. The CT images were reconstructed using cone-beam reconstruction with a Shepp filter with the cutoff at the Nyquist frequency and a binning factor of 4, resulting in an image matrix of 480 × 480 × 632 and a voxel size of 125 μm.

Adipose tissue volume measurement and lean body mass measurement

To measure lean body mass (LBM), the weight of each mouse was measured before image acquisition. On the whole, body image, total adipose tissue and visceral adipose tissue volume were measured as reported previously (Judex et al., 2010). LBM was defined as the weight of the body excluding the weight of fat. In this study, LBM was calculated as follows:

$$\mathbf{LBM} = \left\{ \boldsymbol{body\ weight}\ (\boldsymbol{g}) - \left(\boldsymbol{total\ adipose\ tissue\ volume}\ (\boldsymbol{cm^3}) \times \mathbf{0.9}\ (\boldsymbol{g/cm^3}) \right) \right\}$$

where 0.9 g/cm^3 is the density of fat. Detailed methods were described in a previous report (Judex et al., 2010).

Adipose tissue fractionation and flow cytometry analyses

Adipose tissue was fractionated as previously described (Huh et al., 2013). Briefly, EAT were weighed, chopped, and incubated in collagenase buffer for 30 min at 37°C with shaking. After centrifugation, adipocytes in the supernatant were removed. The pelleted stromal vascular cell (SVC) fraction was used for flow cytometry. Adipose tissue SVC pellets were incubated with red blood cell lysis buffer (a 1:9 mixture of 0.17 M Tris (pH 7.65) and 0.16 M NH_4Cl), centrifuged at 1300 rpm for 5 min, and resuspended in PBS. For macrophage analyses, SVCs were stained with CD11b (BD Bioscience, San Jose, CA, USA), F4/80 (eBioscience, San Diego, CA, USA), and CD11c (eBioscience) monoclonal antibodies for 30 min at 4°C. Cells were gently washed with and resuspended in PBS. SVCs were analyzed using a FACS Canto II (BD Bioscience).

Gut permeability test in vivo

This examination is based on the intestinal permeability to 4000-Da fluorescent-dextran (46944; Sigma) as previously described (Cani et al., 2008a). 4 h-fasted mice were orally administered with fluorescein isothiocyanate (FITC)-

dextran (600 mg/kg body weight, 125 mg/mL). After 1 h, 300 μL of the blood were collected from the heart. The blood was centrifuged at 4°C, 6,000 rpm, for 10 min. Collected serums were diluted with same volume of PBS and analyzed for FITC concentration at excitation wavelength of 485 nm and the emission wavelength of 535 nm. Standard curves of the FITC-dextran concentration were obtained by continuous diluting FITC-dextran solution with PBS (0 – 12.5 μg/mL).

Liver triglyceride measurement

Liver triglycerides were measured according to the manufacturer's protocol (Bioassay Systems, Hayward, CA, USA). Liver tissue samples (90 – 120 mg) were homogenized in 500 μL of 5% Triton X-100 with a tissue homogenizer. Total tissue extracts were incubated in a water bath to 80°C and cooled to room temperature. This step was repeated. After centrifugation of the total tissue extract, the supernatant was collected and measured optical density at 570 nm using spectrophotometer (infinite M200; TECAN, Männedorf, Switzerland) in 96-well plates as previously described (Jo et al., 2013).

Cell culture experiments

NCI-H716 L-cell line was kindly provided by Dr. Young Min Cho in Seoul National University. Cells were grown in suspension in RPMI-1640 medium supplemented with 10% fetal bovine serum. Cells were treated with fresh medium

every 2-3 days at a 1:3 dilutions. NCI-H716 cells were seeded in 24-well plates (10^5 cells, 1 mL per one well) with fresh RPMI-1640 medium without serum supplementation. To test GLP-1 secretion, NCI-H716 cells were treated with or without taurocholic acid sodium salt hydrate (1 mM; T4009; Sigma), putrescine dihydrochloride (1 mM; P5780; Sigma) and creatine monohydrate (1 mM; C3630; Sigma) followed by 2 h incubation. H-89 dihydrochloride hydrate (40 μM; B1427; Sigma) was either treated alone or co-treated with taurocholic acid sodium salt hydrate for 2 h incubation. Each conditioned medium from cells treated with different metabolites was carefully harvested and centrifuged. 200 μL supernatant was collected for GLP-1 measurement as described below.

Biochemical analyses for metabolic markers

Serum insulin, endotoxin, TNFα, and cholesterol were measured using a mouse insulin ELISA kit (AKRIN-011T; Shibayagi, Gunma Pref., Japan), ToxinSensor™ Chromogenic Endotoxin Assay Kit (L00350; Genscript, Piscataway, NJ, USA), mouse TNFα detection kit (KMC3011; Invitrogen, Carlsbad, CA, USA), and cholesterol detection reagent (TR13421; Thermo Scientific, Waltham, MA, USA), respectively, following the manufacturers' instructions. Active GLP-1 and total GLP-1 in serum were measured using GLP-1 ELISA (Active 7-36) (43-GP1HU-E01; ALPCO, Salem, NH, USA) and Total GLP-1 (7-36 and 9-36) ELISA (43-GPTHU-E01; ALPCO), respectively. In order to measure endotoxin, serums were diluted in PBS 1/50 to 1/100 ratio (v/v). For measurement of the GLP-1 active form, glucose

solution (2 g/kg) was administered to mice by oral gavage. Mice rested 30 min before sacrifice and blood collection. To inhibit dipeptidyl peptidase IV (DPP-IV) activity, blood samples were placed in BD P700 tubes containing DPP-IV inhibitors (BD Bioscience) immediately. Blood samples were centrifuged at 2500 rpm for 10 min at 4°C to isolate serum. Serum samples were used for measurement of active GLP-1 in samples that were never frozen.

Immunohistochemistry

After isolation from NC, NH, and Ab-NH mice, ileum was dissected and washed with PBS (0.1 M). They were then fixed in 10% neutral buffered formalin overnight at room temperature. After dehydration with a graded alcohol series and clearing, tissues were embedded in paraffin. Tissue sections were cut to a thickness of 4 μm and were immunostained with anti-rabbit GLP-1 antibody (1:1000; Abcam, Cambridge, UK). Before heat-induced antigen retrieval with Tris-EDTA, pH 9.0 (Thermo-Scientific, Rockford, IL, USA) for 15 min, endogenous peroxidase activity was blocked with 0.3% H_2O_2 in methanol. Sections were blocked in normal goat serum and incubated in primary antibody overnight at 4°C. They were then incubated in Alexa Fluor 488 donkey anti-rabbit IgG (1:300; Invitrogen, Carlsbad, CA, USA) for 2 h at room temperature and mounted in Vectashield containing DAPI. Immunoreactivity was visualized with a confocal microscope system (LSM 510; Carl Zeiss, Oberkochen, Germany).

Capillary ethanol-mass spectrometry (CE-MS)-based metabolomics

Frozen ileal and cecal contents were homogenized with Dulbecco's phosphate-buffered saline (D-PBS) immediately after thawing. Supernatants were collected without precipitation. Supernatants (100 μL) were centrifuged and filtered using Ultrafree-MC filter units (Millipore, Billerica, MA, USA). Samples were analyzed by CE-MS at Human Metabolome Technologies, Inc. (Yamagata, Japan). Detailed methods were described in a previous report (Matsumoto et al., 2012).

Statistical analyses

Data are presented as the mean with SEM. Differences between two groups were assessed by using the Student's *t*-test. Data involving more than two groups were analyzed by ANOVA (GraphPad Prism; GraphPad, San Diego, CA, USA). Significant ANOVA results were followed by *post hoc* tests (one-way; Tukey, two-way; Bonferroni). A value of $p < 0.05$ was considered significant.

RESULTS

Treatment with vancomycin (V) and bacitracin (B) depletes Firmicutes and Bacteroidetes in the mouse gut

To investigate whether the modulation of intestinal microbial communities, with selective reduction of two major gut phyla, Firmicutes and Bacteroidetes, protects against obesity and insulin resistance, I challenged mice with antibiotics before DIO. Eight-week-old C57BL/6J male mice were fed NC for 4 weeks and then fed a high-fat diet (HF) for 4 weeks (NH). As shown in Figure 5, one NH group (Ab-NH) was given free access to drinking water containing a V + B cocktail throughout the experiment to alter the gut microbiota. V and B were selected because of their strong sterilizing effects, especially on Gram-positive bacteria and anaerobes, which include major gut phyla such as Firmicutes and a considerable number of species belonging to Bacteroidetes (Bacon et al., 1991; Hall, 1994; Wolf et al., 2004). Moreover, V and B are minimally absorbed by the host gastrointestinal tract after oral administration (Eng et al., 1993; Rao et al., 2011). I verified the depletion of Firmicutes and Bacteroidetes at 4 weeks of antibiotic (V + B) treatment NC fed mice before HF feeding (data not shown). In agreement with previous reports (de La Serre et al., 2010), there was a downward trend in the absolute abundance of gut microbiota upon HF challenge as compared to NC fed group Figure 6. Furthermore, the absolute abundance of bacterial DNA in the Ab-NH was significantly reduced relative to the NH group, suggesting that absolute richness of gut microbiota is altered by V + B. As shown in Figure 7, HF increased the proportion of Firmicutes and decreased the

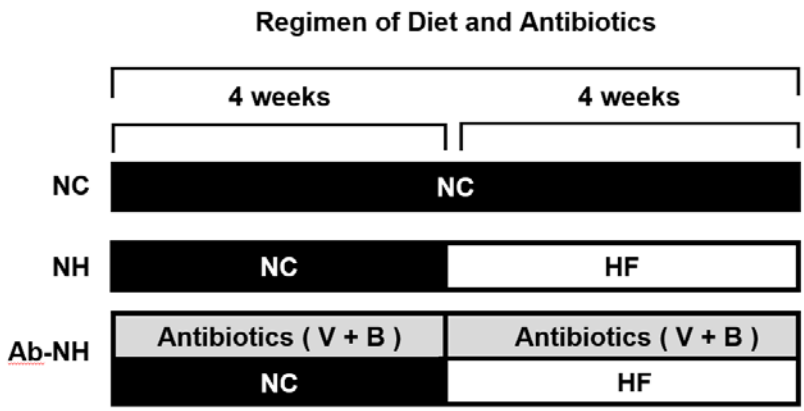

Figure 5.

Illustration depicting the experimental strategies used in this study. C57B6L/J 8 week-old male mice were given drinking water with or without V + B for 4 weeks. In next 4 weeks, NC group was fed NC. Meanwhile, HF fed mice were separated into vehicle (NH) and V + B treated group (Ab-NH).

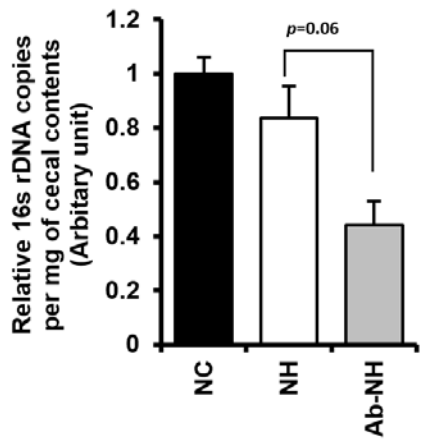

Figure 6.

Relative amounts of gut microbiota by analyses of 16s rDNA. Each cecal contents of NC, NH, and Ab-NH mice were collected to isolate bacterial DNA. 16s rDNA levels of the experimental groups were measured and compared. Each bar represents the mean ± S.E. of the individual samples.

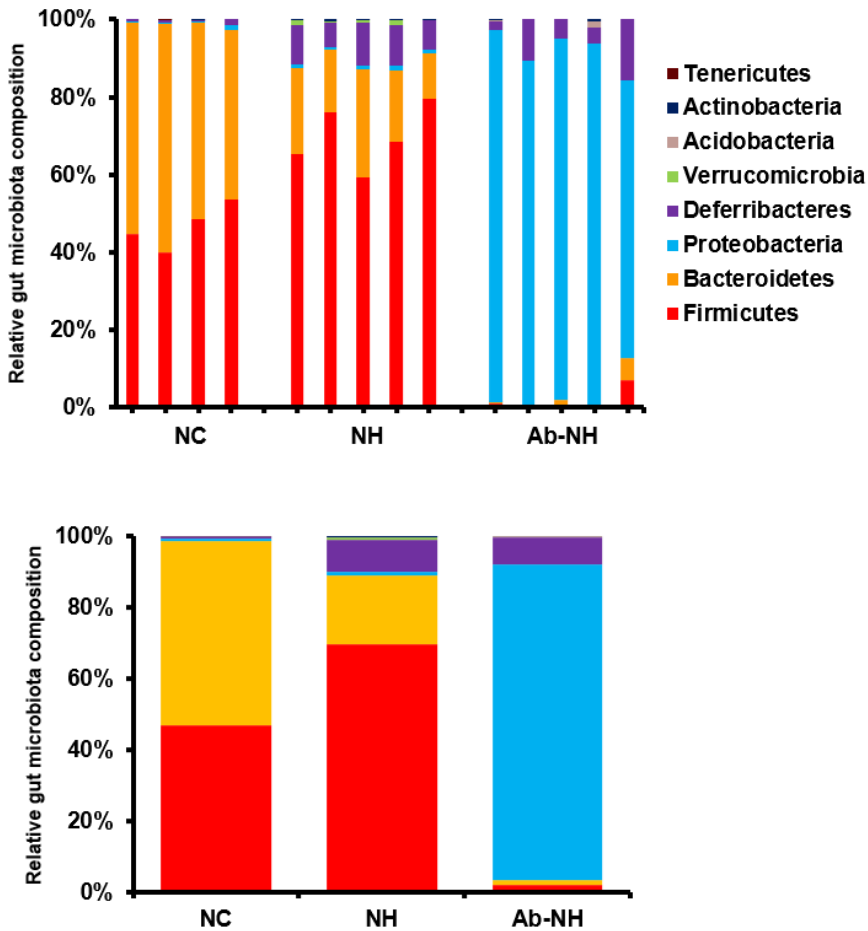

Figure 7.

Gut microbiota metagenomics compositions of NC, NH, and Ab-NH mice. Bacterial 16s rDNA pyrosequencing analyses of the cecal contents of the NC, NH, and Ab-NH groups. Upper bar-graphs imply gut microbiota in individual mouse and group average values are indicated in the lower panel. The percentage of the community contributed by each phylum is indicated. Each phylum is denoted by a color, as shown beside the graph.

proportion of Bacteroidetes, compared to the populations in NC group while V + B greatly reduced the proportions of Firmicutes and Bacteroidetes in DIO. With the substantial decrease in these phyla, the proportion of Proteobacteria increased markedly Figure 7. Furthermore, at the class and species levels, *Escherichia coli* comprised more than half of the total bacteria (52.95%), whereas the population of EF098132_g_uc, belonging to the family Lachnospiraceae of Firmicutes, and Porphyromonadaceae_uc_s, belonging to the family Porphyromonadaceae of Bacteroidetes, decreased considerably in the Ab-NH group Figure 8.

Gut microbiota alteration with V + B treatment ameliorates insulin resistance in DIO mice

To examine the effects of V + B-mediated modulation of gut microbiota on insulin sensitivity in DIO mice, a glucose tolerance test (GTT) and an insulin tolerance test (ITT) were performed. As expected, the NH group displayed impaired glucose tolerance and insulin tolerance compared to the NC group. In contrast, both of glucose and insulin intolerance were improved in the Ab-NH group as compared to NH group (Figure 9). Furthermore, the serum insulin levels in the Ab-NH group were lower than those in the NH group (Figure 10). Also, upon insulin treatment, phosphorylation of Akt (Ser 473) and GSK3β (Ser 9), two major components of the insulin-signaling cascade, slightly increased in the muscle and liver in the Ab-NH group (Figure 11). Since obesity-induced insulin resistance is closely associated with

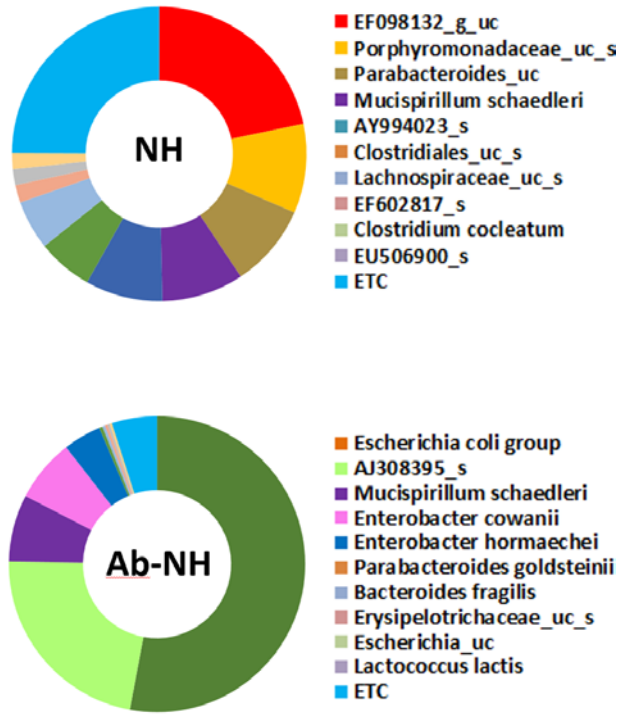

Figure 8.

Comparison of cecal microbial species compositions in NH and Ab-NH mice. In NH group, the prevalence (%) of each species, from top to bottom, was 21.72%, 9.79%, 9.15%, 9%, 8.48%, 6.07%, 5.43%, 1.93%, 1.76%, 1.73%, and 24.91%. In the Ab-NH group, the prevalence (%) of each species, from top to bottom, was 52.95%, 22.35%, 7.33%, 6.85%, 4.13%, 0.36%, 0.29%, 0.29%, 0.25%, 0.25%, and 4.93%.

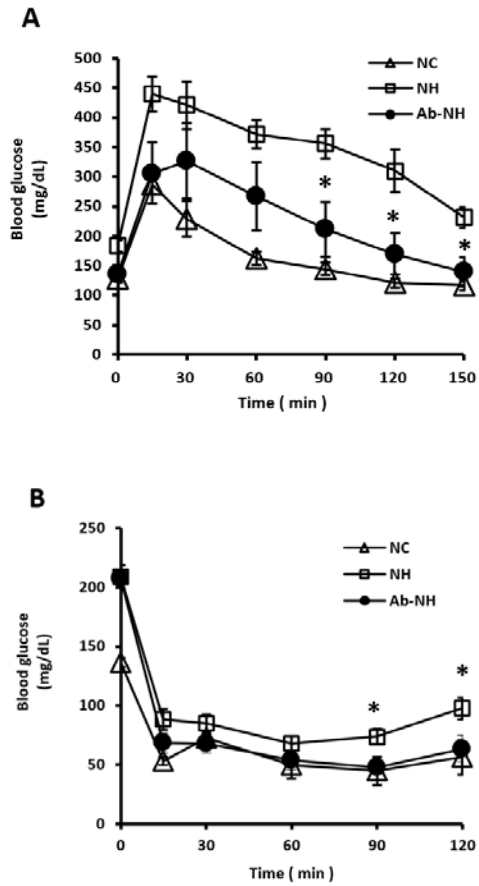

Figure 9.

Improvement of insulin resistance in NC, NH, and Ab-NH mice. A, at the end of the experimental period, mice were given an intraperitoneal glucose tolerance test. N=4 per time point for NC group and N=5 per time point for NH and Ab-NH group. B, the same mice tested in panel A were given an insulin tolerance test (ITT) after two weeks of recovery. N=4 per time point for NC group and N=5 per time point for NH and Ab-NH group.

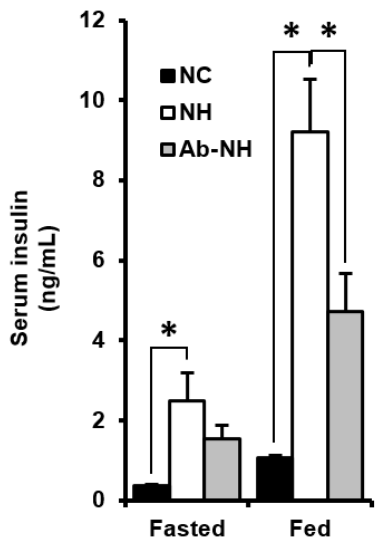

Figure 10.

Comparison of serum insulin level by V + B treatment. Blood samples were collected from the tail vein of each mouse after 7 h or fasting or normal feeding to measure the serum insulin concentration.

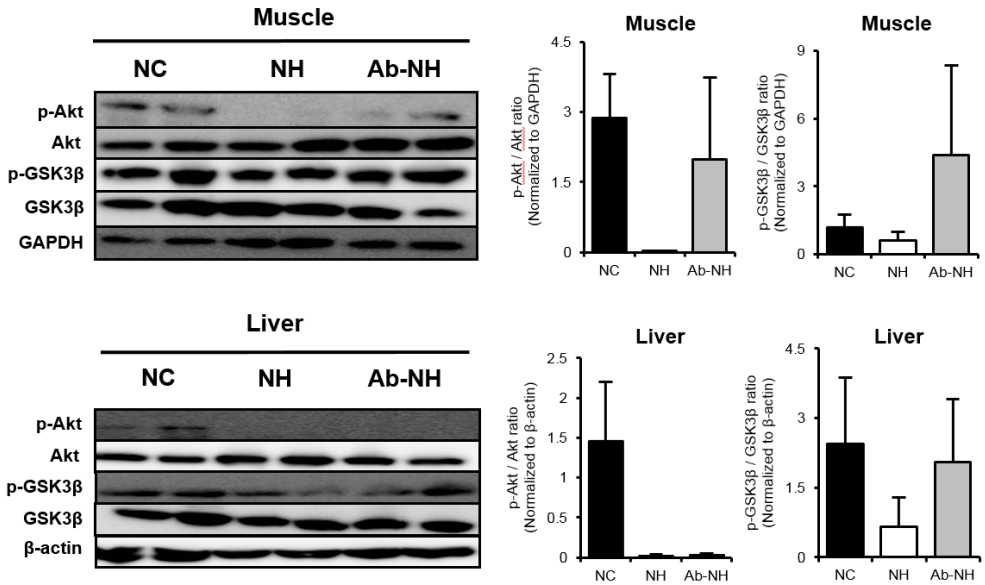

Figure 11.

Improvement of insulin signaling in V + B treated mice. Western blot images (left) and bar-graphs (right) showing quantitative analyses of western blot data using ImageJ software of insulin signaling marker proteins p-Akt (s473) and p-GSK3β (S9) in the muscle and liver. Total Akt, total GSK3β, GAPDH in muscle and β-actin in liver were used as controls.

pancreatic islet hypertrophy (Lingohr et al., 2002), the size of pancreatic islets was investigated. As shown in Figure 12, treatment with V + B alleviated pancreatic islet hypertrophy in Ab-NH mice. Together, these data suggest that the prominent reduction in the abundance of Firmicutes and Bacteroidetes with V + B would ameliorate insulin resistance in DIO.

Depletion of Firmicutes and Bacteroidetes does not affect body weight gain and adiposity in DIO

Because it has been reported that the relative abundance of Firmicutes and Bacteroidetes is correlated with obesity (Backhed et al., 2004b), I have asked whether depletion of Firmicutes and Bacteroidetes with V + B changed the body weight gain in DIO. Interestingly, as shown in Figure 13, body weight gain in the Ab-NH group was comparable to that in the NH group. When I examined the mass of several different fat depots, there was no significant difference between the NH and Ab-NH groups (Figure 14). In addition, adiposity, abdominal fat area, whole body fat volumes, and lean body mass were similar in the NH and Ab-NH groups (Figure 15). Further, food intake and water consumption were not affected by V + B in DIO mice (Figure 16). These data propose that significant reduction of Firmicutes and Bacteroidetes by V + B would not be associated with obesity and adiposity.

Reduction of Firmicutes and Bacteroidetes by V + B treatment does not affect

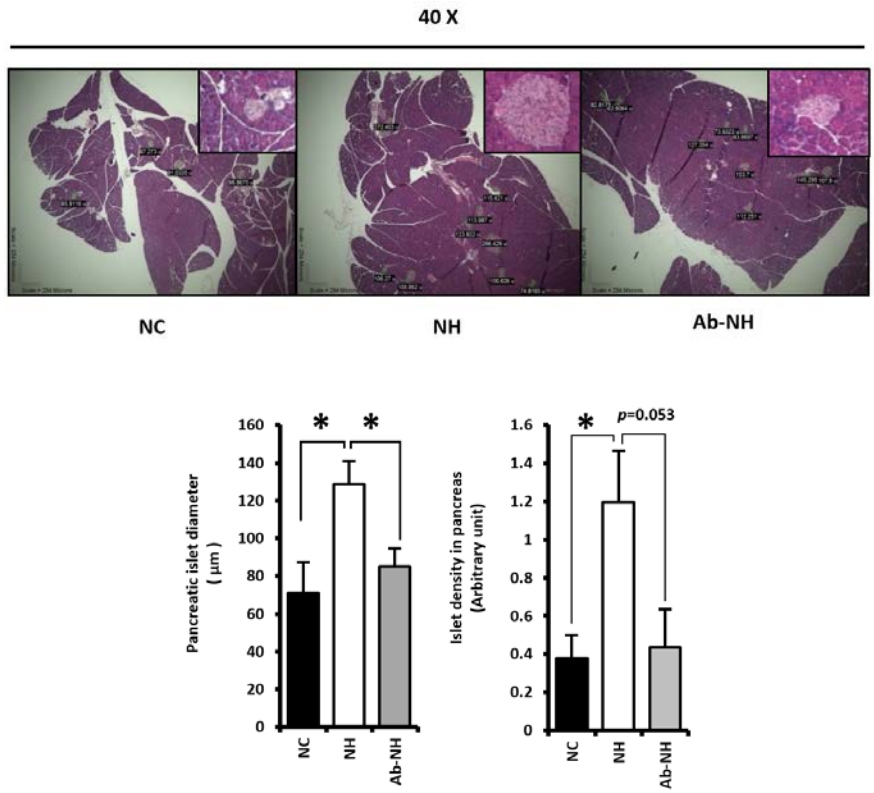

Figure 12.

Reduction of the islet hypertrophy by gut microbiota alteration. Pancreatic islets from mice in the NC, NH, and Ab-NH groups were isolated and stained with hematoxylin and eosin. Representative images of the pancreas are shown, with enlarged images of pancreatic islets displayed in the upper right. Islet diameters (μm) (N = 33, 31, and 35 for NC, NH, and Ab-NH, respectively) and density were measured by ImageJ software. Each bar represents the mean ± standard error (S.E.) of the individual samples. Mean values with $*p < 0.05$ were considered significant

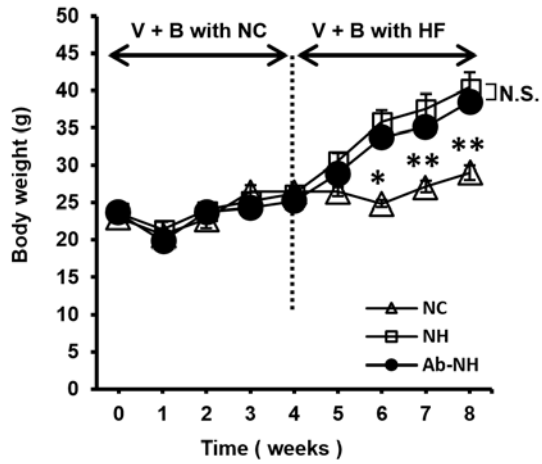

Figure 13.

Antibiotic treatment does not affect body weight change in DIO. Body weights were measured every week from zero to eight weeks during the experimental period. '*' exhibits difference between NC and NH group. Each bar represents the mean ± standard error (S.E.) of the individual samples. Mean values with *$p < 0.05$ and **$p < 0.01$ were considered significant. N.S., not significant.

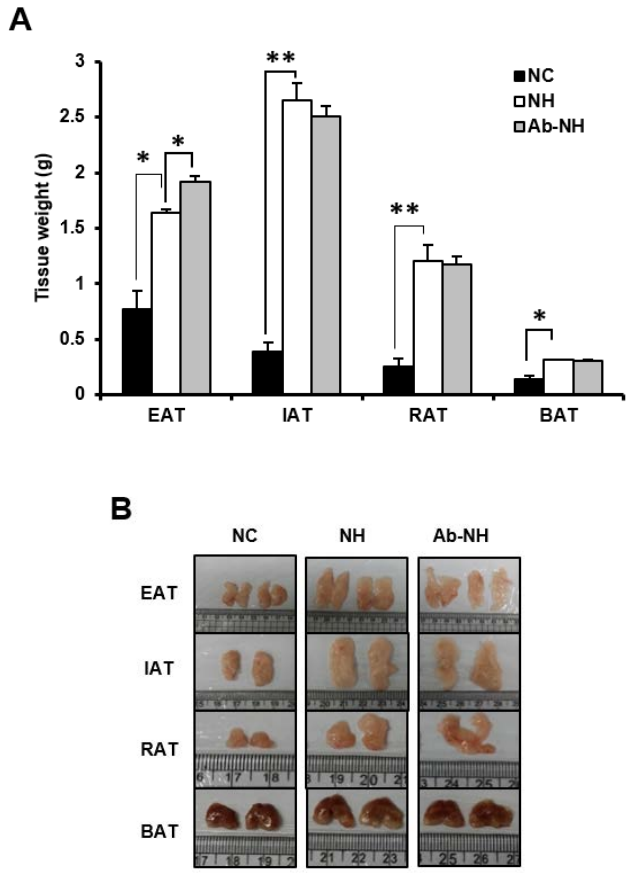

Figure 14.

Antibiotic-treatment did not influence fat-depot mass changes in DIO mice. (A) Major adipose tissue depots, including EAT, IAT, renal adipose tissue (RAT), and BAT, were isolated and weighed after the experimental period. (B) Representative images of EAT, IAT, RAT, and BAT in NC, NH, and Ab-NH are shown (scale; 1 mm). Each bar represents the mean ± standard error (S.E.) of the individual samples. Mean values with $*p < 0.05$ and $**p < 0.01$ were considered significant.

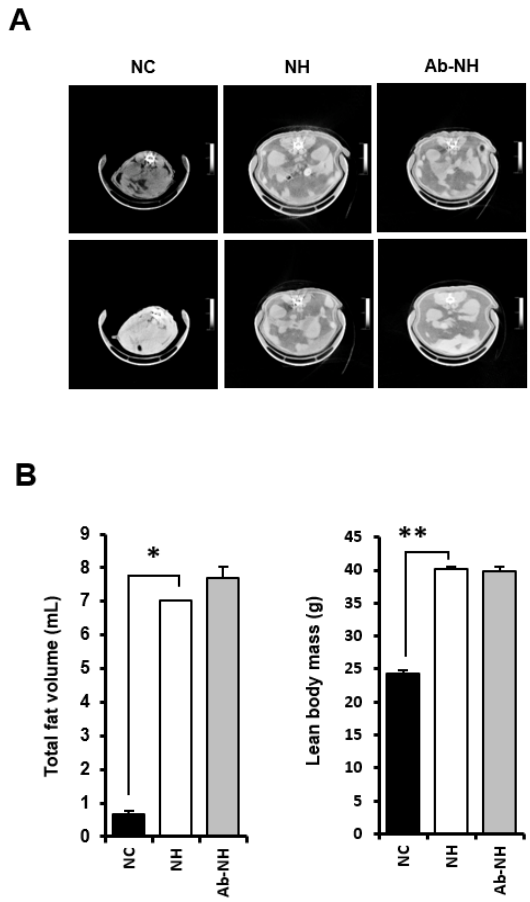

Figure 15.

Total body adiposity and lean mass were not altered in V + B treatment. A, representative transverse cross-sectional micro-computed tomography (micro-CT) images of NC, NH, and Ab-NH abdominal areas. B, total fat volume (left) and lean body mass (right) were quantified from Micro-CT scans. Mean values with $*p < 0.05$ and $**p < 0.01$ were considered significant.

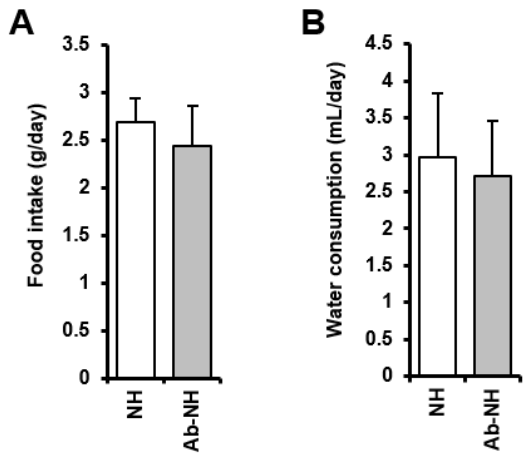

Figure 16.

Antibiotic treatment did not affect food and water consumption in DIO mice. A, Daily food intake was measured once a week for eight weeks after the start of antibiotics administration to the Ab-NH group. Mice in the Ab-NH group consumed 2.85, 2.7, 3.15, 2.4, 2.05, 2.05, 2, and 2.35 g of food per day, respectively, similar to mice in the NH group. The average daily food intake over 8 weeks is shown. B, Water consumption was quantified once a week for eight weeks after the start of antibiotics administration to the Ab-NH group. Water (100 mL) with or without antibiotics was provided in a sterile bottle. After 24 h, the remaining water was measured by mass cylinder. Ab-NH mice drank 2.65, 2.75, 3.65, 2.35, 1.9, 1.9, and 2.1 mL of water in each 24 h period sampled, similar to mice in the NH group. The average daily water consumption is shown. Each bar represents the mean ± standard error (S.E.) of the individual samples.

the risk factors related to insulin resistance in DIO mice

In severe obesity, chronic adipose tissue inflammation is closely associated with insulin resistance (Patsouris et al., 2008; Permana et al., 2006). In particular, an increase in pro-inflammatory macrophages (F4/80+, CD11b+, and CD11c+) in the adipose tissue of obese mice aggravates systemic insulin resistance (Patsouris et al., 2008). To test the hypothesis that adipose tissue inflammation contributes to improved insulin resistance in the Ab-NH group, inflammatory gene expression and macrophage infiltration were analyzed in adipose tissue. The expression of pro-inflammatory genes such as *Tnfα* and *Il6* in EAT was higher in the NH and Ab-NH groups than in the NC group (Figure 17). Similarly, the expression of macrophage surface marker genes such as *F4/80*, *Cd11b*, and *Cd11c* was comparable in the Ab-NH and NH groups (Figure 17). Consistent with the changes in gene expression profiling data, the number of F4/80+ and CD11b+ macrophages in the adipose tissues of the HF-treated groups (NH and Ab-NH) was higher than that in the NC group (Figure 18).

It is well recognized that a complex interplay between the host and the bacteria modulates systemic inflammation in obesity (Cani et al., 2007). For instance, in addition to structural imbalance and perturbation of the function of gut microbiota, disruption of gastrointestinal barrier integrity has been reported to be a critical change in the host to aggravate inflammation induced by dysbiosis of gut microbiota (Cani et al., 2007). However, there were no significant changes in the extent of gut inflammation indicated by retained expression of *Tnfα* and *Il10* in the Ab-NH group

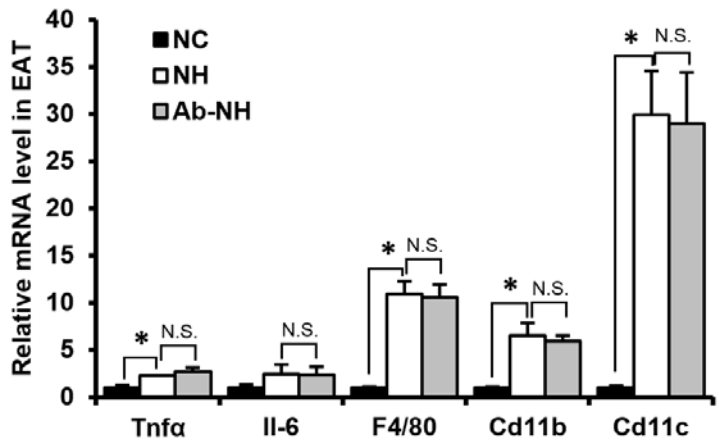

Figure 17.

Inflammatory gene expressions in antibiotic-treated mice. A, Relative mRNA levels in EAT were measured. Pro-inflammatory cytokines, *Tnfα* and *Il6*, and macrophage markers, *F4/80*, *Cd11b*, and *Cd11c*, were measured by quantitative real time-PCR. Mean values with $*p < 0.05$ was considered significant. N.S., not significant.

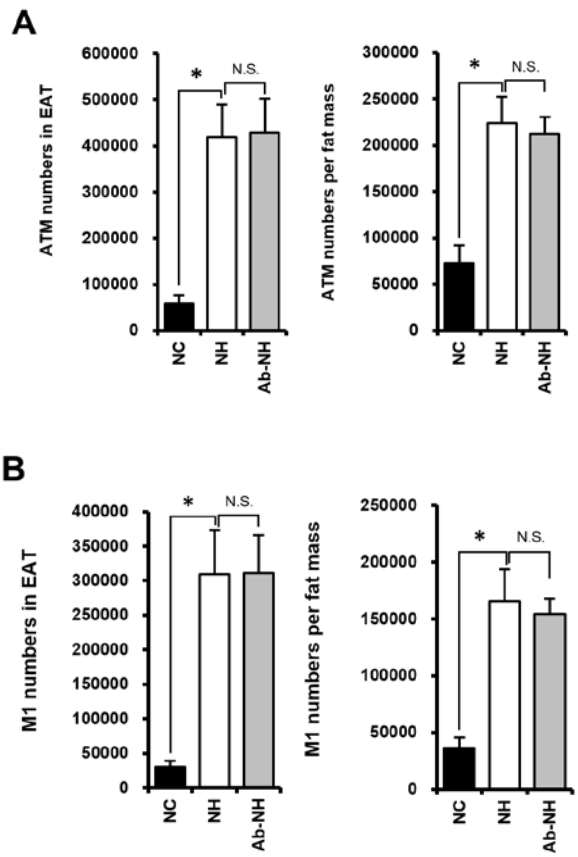

Figure 18.

Comparison of ATM accumulation in adipose tissue. A, flow cytometry of adipose tissue macrophages (F4/80+ and CD11b+) in EAT. Total ATM number in EAT, (left) and ATM number per fat mass (right) are calculated based on total SVC cell counts. B, flow cytometry of M1 type macrophages (F4/80+, CD11b+, and CD11c+) in EAT. Total cell numbers are indicated in the left graph, and the number of cells per gram of adipose tissue is shown in right graph. Mean values with $*p < 0.05$ was considered significant. N.S., not significant.

relative to NH group (data not shown). Furthermore, the expression of the gut barrier gene *mucin 6* and tight junction genes such as *occludin* (*Ocln*) and *claudin 10* (*Cldn10*) was not greatly different between the NH and Ab-NH group (Figure 19). Also, HF-mediated elevation of gut leakage was substantially reduced in the Ab-NH group (Figure 20). In turn, serum endotoxin and serum TNFα, markers of systemic inflammation were similar in the NH and Ab-NH groups (Figure 21).

Previous studies demonstrated that dysregulation of lipid metabolism in liver was associated with obesity and its related disorders (Jo et al., 2013; Petersen et al., 2005). In the present study, the levels of serum cholesterol and hepatic triglyceride were trended upward regardless of V + B treatment upon HF feeding indicating that HF-induced dysregulation of lipid metabolism in the liver would not be affected by the modulation of the gut microbiota by V + B treatment (Figure 22). Thus, these results suggest that amelioration of insulin resistance in the Ab-NH group is not related to the alleviation of chronic inflammation or hepatic lipid dysregulation.

V + B-mediated alteration of gut microbiota improves glucose tolerance via stimulating GLP-1 secretion in DIO mice

GLP-1 is a prominent gut hormone that modulates whole body insulin sensitivity (Baggio and Drucker, 2007). To investigate whether GLP-1 was involved in the improvement of insulin resistance in the Ab-NH group, serum levels of GLP-1 (7-36 amide and 9-36 amide) were measured. Intriguingly, the level of total GLP-

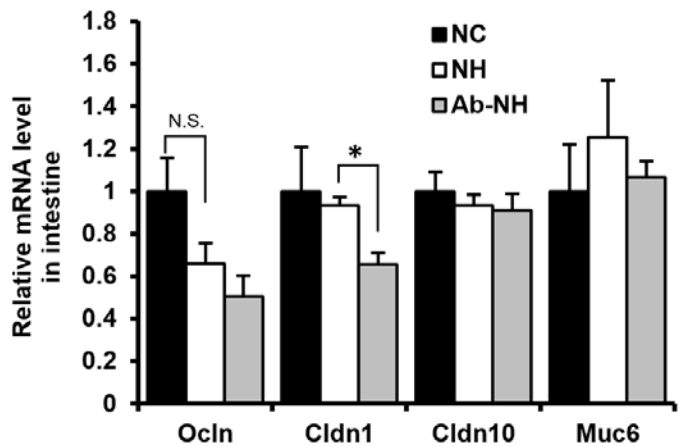

Figure 19.

Gut barrier gene expressions in NC, NH, and Ab-NH mice. Relative expression of gut barrier genes in the intestine: *occludin* (*Ocln*), *claudin 1* (*Cldn1*), *claudin 10* (*Cldn10*), and *Mucin 6* (*Muc6*). Mean values with $*p < 0.05$ was considered significant. N.S., not significant.

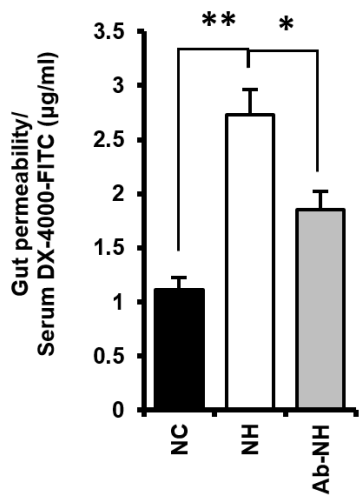

Figure 20.

Alteration of gut microbiota alters gut leakages. After oral administration of DX-4000, serum levels of DX-4000 were measured in NC, NH and Ab-NH group. Mean values with $*p < 0.05$ and $**p < 0.01$ was considered significant.

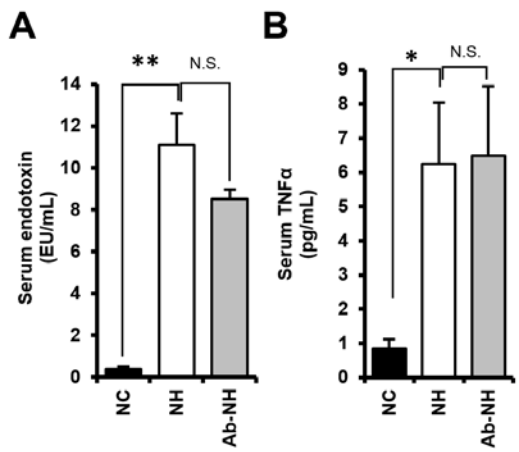

Figure 21.

V + B treatment does not alter serum endotoxemia and TNFα in DIO. Serum of each group was isolated to measure (A) endotoxin and (B) TNFα. Mean values with $*p < 0.05$ and $**p < 0.01$ was considered significant. N.S., not significant.

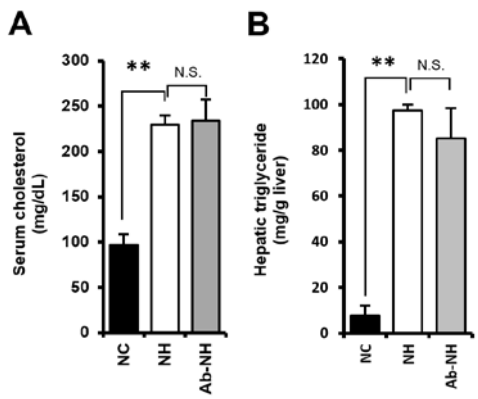

Figure 22.

V + B mediated gut microbiota alteration does not affect metabolic profiles in DIO mice. Serums and liver of NC, NH, and Ab-NH were extracted to measure (A) cholesterol and (B) hepatic triglyceride. Mean values with $^{**}p < 0.01$ was considered significant. N.S., not significant.

1 in fasting status increased in the Ab-NH group to an extent comparable to NC mice (Figure 23). To determine whether the increase in total GLP-1 in basal status of the Ab-NH group was resulted from the different ability of L-cells to secret GLP-1 upon glucose challenge, GLP-1 release was examined after oral glucose administration. As shown in Figure 23, the levels of active GLP-1 in the serum were significantly higher in the Ab-NH group than in the NH group. The reduction in active GLP-1 upon HF feeding (Figure 23) is consistent with previous report that GLP-1 secretion is suppressed in obese humans (Ranganath et al., 1996). In addition, the degree of GLP-1 staining in the ileum increased in the Ab-NH group compared to NH group, suggesting that the production of GLP-1 in the ileum was augmented in the Ab-NH group (Figure 24).

I next examined the involvement of GLP-1 in the enhancement of glucose tolerance in Ab-NH group. Treatments of exendin 9-39 amide (Ex(9-39)), a well-known GLP-1 receptor antagonist, led to aggravation of glucose intolerance in NH mice relative to the NH mice treated with vehicle (Figure 25). Additionally, Ab-NH group with Ex(9-39) exhibited significantly impaired glucose intolerance to an extent comparable to NH mice treated with Ex(9-39) (Figure 25). These data imply that amelioration of obesity-induced glucose intolerance in Ab-NH mice would be attributable to GLP-1-mediated beneficial effects on energy metabolism.

Modulation of two major phyla stimulates production of metabolically beneficial metabolites

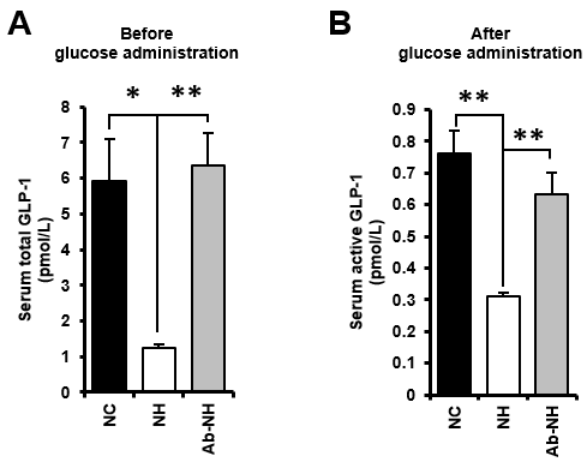

Figure 23.

GLP-1 is elevated in serum of Ab-NH group. A, Measurement of total (7-36 and 9-36 amide) GLP-1 under fasting status in the NC, NH, and Ab-NH groups. N=5 per group. B, Measurement of active (7-36 amide) GLP-1 after oral glucose administration (2 g/kg, 20% glucose solution). Mean values with *$p < 0.05$ and **$p < 0.01$ were considered significant. N.S., not significant.

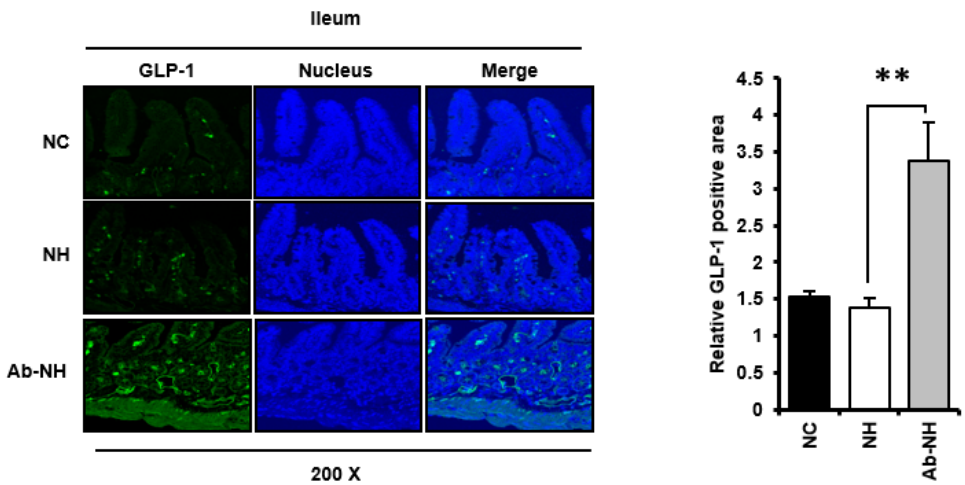

Figure 24.

Intestinal GLP-1 measurement in NC, NH, and Ab-NH mice. Representative immunofluorescence images of L-cells in the ileum (left) stained with anti-GLP-1 (green) and DAPI (blue). GLP-1 positive area (right) were measured using ImageJ software. Mean values with $^{**}p < 0.01$ were considered significant.

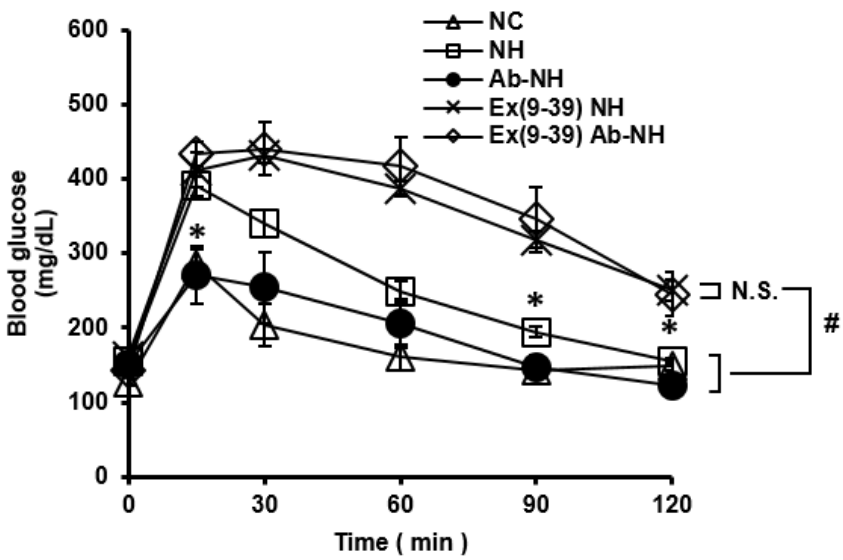

Figure 25.

GLP-1 receptor antagonism diminishes the insulin sensitization effect on Ab-NH group. Mice were given glucose tolerance test with exendin (9-39) amide (Ex(9-39)) in NH and Ab-NH group. Blood glucose levels of Ex(9-39) treated groups showed statistical significance against vehicle treated groups from the 30 min to 120 min after glucose administration (#). '*' exhibited difference between NH and Ab-NH group. Each bar represents the mean ± S.E. of the individual samples. Mean values with $^{*,\#}p < 0.05$ was considered significant. N.S., not significant.

Microbial communities actively produce various metabolites, which have the potential to affect energy homeostasis (Matsumoto et al., 2012). As shown in Figure 26, capillary ethanol mass spectrometry (CE-MS) analyses revealed distinct gut metabolite patterns in the NH and Ab-NH groups. In contrast, serum metabolite profiles were not markedly different in the NH and Ab-NH groups (Figure 27). Among the metabolites selectively up-regulated in the Ab-NH group (Table 1), eight metabolites including succinic acid, creatine, putrescine, sulfotyrosine, taurocholic acid (TCA), mucic acid putrescine, and 1-methylnicotinamide (Figure 28) were known to benefit host energy metabolism ('t Eijnde et al., 2001; Desmarais et al., 1998; Enrique-Tarancon et al., 2000; Kobayashi et al., 2007; Macdonald and Fahien, 1988; Mendez and Balderas, 2001; Rose, 1911; Watala et al., 2009). Given previous studies reported that gut-derived metabolites are able to stimulate GLP-1 secretion (Lauffer et al., 2009; Wu et al., 2013a), I tested the effects of gut metabolites induced by removal of Firmicutes and Bacteroidetes on GLP-1 section in L-cells. Among three metabolites prominently induced in the Ab-NH group, TCA overtly enhanced GLP-1 secretion in L-cells, indicating that alteration of gut metabolites in Ab-NH group, in part, contributes to an increase in GLP-1 secretion in DIO (Figure 29). Further, PKA was appeared to be engaged in TCA-mediated GLP-1 secretion as treatment of H-89 dihydrochloride hydrate (H-89), a well-known PKA inhibitor, substantially reduced the positive effect of TCA on GLP-1 secretion (Figure 30). Collectively, these results suggest that depletion of Firmicutes and Bacteroidetes with V + B in DIO would alter gut metabolites and subsequently augments insulin sensitivity via increasing GLP-1 secretion.

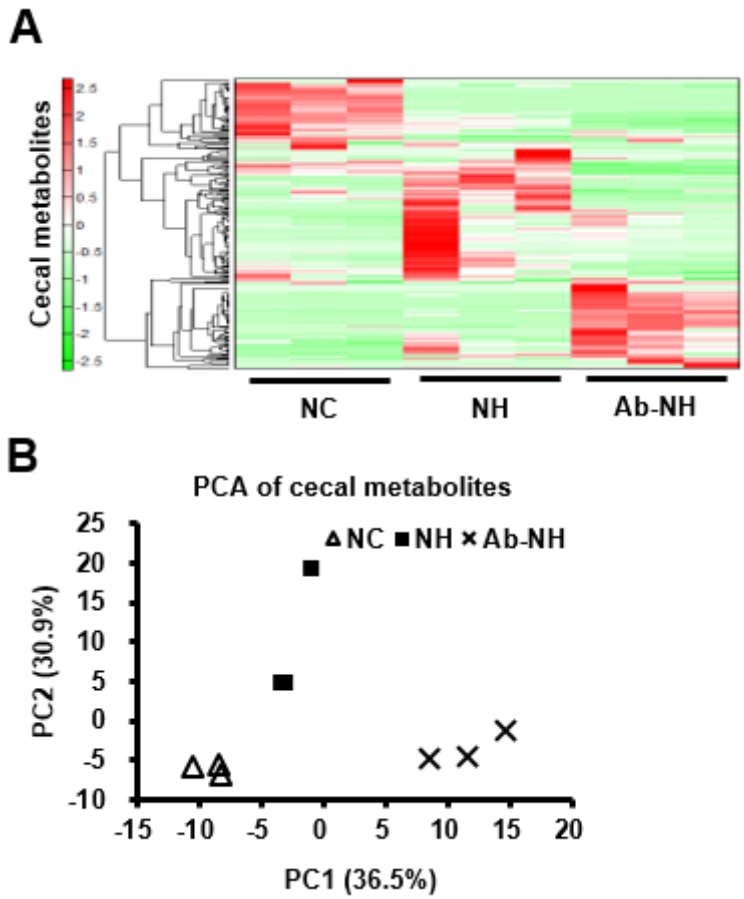

Figure 26.

Ileal metabolomes were analyzed in NC, NH, and Ab-NH group. A, heat-maps of the relative amounts of metabolites identified in the ileal contents by capillary ethanol-mass spectrometry (CE-MS). B, the relative amount of each individual metabolite was indicated by color intensity: red for positive correlation and green for inverse correlation.

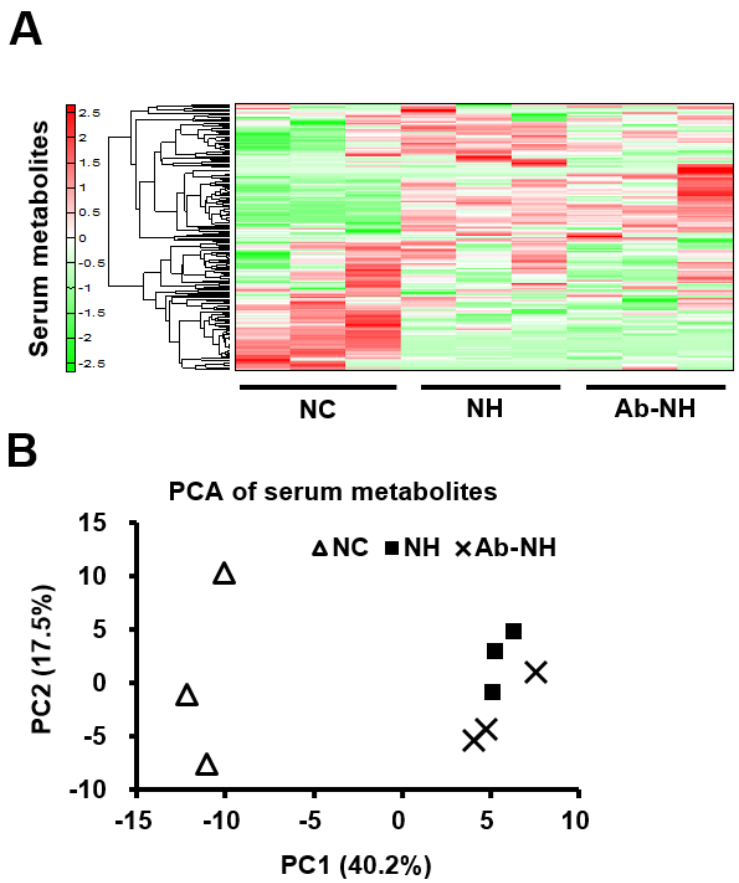

Figure 27.

Serum metabolomes were analyzed in NC, NH, and Ab-NH group. Heat-maps of the relative amounts of metabolites identified in serum contents by capillary ethanol-mass spectrometry (CE-MS). The relative amount of each individual metabolite was indicated by color intensity: red for positive correlation and green for inverse correlation.

Table 1. Metabolites exclusively up-regulated in the Ab-NH group

No.	Compound Name	KEGG ID	Relative Folds of Inductions (Average ± standard error, Log_2 scale, N=3)			P-value Student's t-test (NH vs Ab-NH)
			NC	NH	Ab-NH	
1	Succinic acid	C00042	-0.585±0.075	0.583±0.075	1.167±0.548	0.082969
2	Creatine	C00300	-0.679±0.046	-0.501±0.213	1.180±0.483	0.056252
3	Pro	C00148 C00763 C16435	-0.689±0.003	-0.527±0.103	1.216±0.455	0.05556
4	*N*-Acetylputrescine	C02714	-0.660±0.062	-0.573±0.075	1.233±0.426	0.0475
5	XC0065	-	-0.623	-0.623	1.246±0.412	0.04535
6	Sulfotyrosine	No ID	-0.633	-0.633	1.266±0.362	0.034368
7	XA0036	-	-0.634	-0.634	1.267±0.359	0.033863
8	3-Methyladenine	C00913	-0.638	-0.638	1.276±0.335	0.029358
9	Imidazolelactic acid	C05568	-0.651	-0.625±0.026	1.276±0.332	0.02857
10	Glucuronic acid	C00191	-0.885	-0.380±0.261	1.265±0.043	0.021719
11	Putrescine	C00134	-0.638±0.018	-0.655±0.004	1.294±0.278	0.019725
12	Taurocholic acid	C05122	-0.648	-0.648	1.296±0.273	0.019123
13	Homovanillic acid	C05582	-0.331±0.479	-0.810	1.141±0.264	0.017773
14	Mucic acid	C00879 C01807	-0.649	-0.649	1.299±0.262	0.017548
15	1-Pyrroline 5-carboxylic acid	C03912	-0.650	-0.650	1.300±0.255	0.016711
16	1*H*-Imidazole-4-propionic acid	No ID	-0.724	-0.566±0.081	1.289±0.272	0.014741
17	*S*-Hexylglutathione	C02886	-0.655	-0.655	1.310±0.216	0.011908
18	N^1-Methyl-4-pyridone -5-carboxamide	C05843	-0.655	-0.655	1.310±0.214	0.011624
19	7-Methylguanine	C02242	-0.740	-0.514±0.226	1.254±0.300	0.010997
20	XC0126	-	-0.657	-0.657	1.313±0.200	0.010143
21	XA0035	-	-0.657	-0.657	1.314±0.198	0.009986

22	**Urea**	**C00086**	**-0.657**	**-0.657**	**1.314±0.196**	**0.009728**
23	**Carboxymethyllysine**	**No ID**	**-0.503±0.024**	**-0.789±0.062**	**1.291±0.240**	**0.009505**
24	**1-Methylnicotinamide**	**C02918**	**-0.661**	**-0.661**	**1.322±0.147**	**0.005459**
25	**Cadaverine**	**C01672**	**-0.722±0.014**	**-0.602±0.017**	**1.324±0.121**	**0.003372**
26	**Gluconolactone**	**C00198**	**-0.664**	**-0.664**	**1.329±0.094**	**0.002235**
27	**Creatinine**	**C00791**	**-0.760±0.069**	**-0.547±0.164**	**1.307±0.098**	**0.001635**
28	**Gluconic acid**	**C00257**	**-0.292±0.173**	**-0.937±0.160**	**1.229±0.204**	**0.001428**
29	**Isethionic acid (2-hydroxyethanesulfonic acid)**	**C05123**	**-0.654±0.073**	**-0.666±0.068**	**1.320±0.130**	**0.000838**
30	***N*-Acetylhistidine**	**C02997**	**-0.673±0.149**	**-0.636±0.093**	**1.309±0.128**	**0.000425**

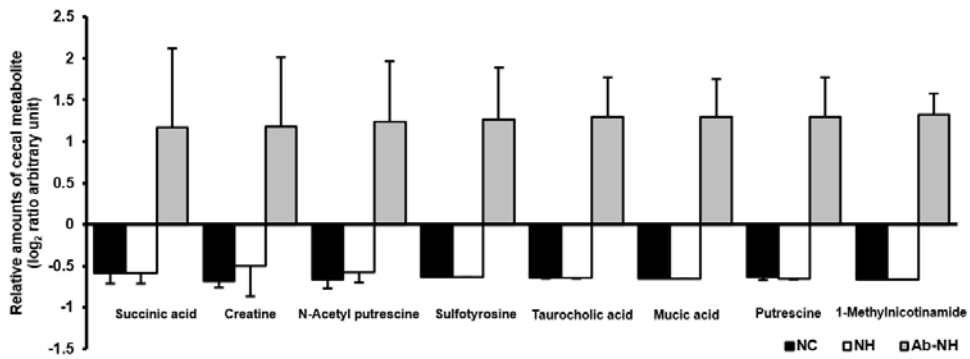

Figure 28.

Target metabolite candidates upregulated in Ab-NH group. The cecal levels of eight metabolites metabolically beneficial in diabetes are shown. These metabolites only increased in the Ab-NH group. CE-time-of-flight/MS (CE-TOF/MS) scans of cationic and anionic metabolites covered a 50–1000 *m/z* range. The y-axis represents the relative peak area (metabolite peak area / (internal standard peak area × sample amount) or (measured value − theoretical value) / (measured value × 10^6) in the case of putative metabolites) converted to $\log_2$ ratio.

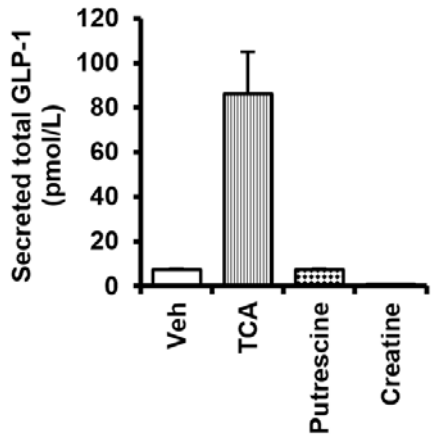

Figure 29.

A bile component activates secretion of GLP-1. The levels of GLP-1 in conditioned media. NCI-H716 cells were treated with taurocholic acid, putrescine and creatine in a time- and concentration- dependent manner.

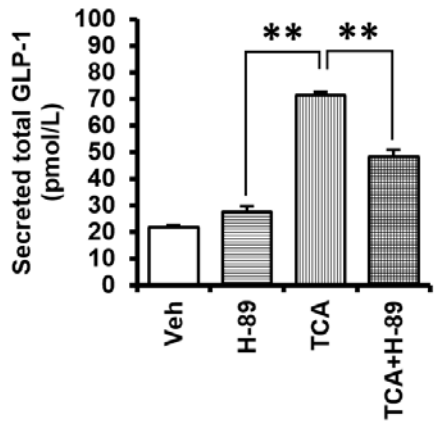

Figure 30.

Taurocholic acid mediated GLP-1 secretion is mediated by PKA activation. The levels of GLP-1 in conditioned media. TCA and H-89 dihydrochloride hydrate (H-89) were either treated alone or co-treated. Each bar represents the mean ± S.E. of the individual samples. Mean values with $^{**}p < 0.01$ were considered significant.

DISCUSSION

Compelling evidences indicate that Firmicutes and Bacteroidetes, two major phyla of gut microbiota, play a significant role in the regulation of host energy metabolism (Backhed et al., 2004b; Cani et al., 2008b), although the association of relative abundance of Firmicutes and Bacteroidetes with obesity and its related metabolic diseases has been controversial. To elucidate the roles of Firmicutes and Bacteroidetes on obesity and its related metabolic complications, I developed a mouse model in which gut microbiota is altered by treatment with an antibiotic cocktail of V + B before the establishment of DIO. V + B treatment in DIO altered gut microbiota, selectively by reducing the population of Firmicutes and Bacteroidetes, and improved insulin resistance, without affecting obesity. Of note, serum GLP-1 levels and GLP-1 expression in intestinal L-cells were significantly augmented upon the V + B-mediated alteration of gut microbiota. Additionally, depletion of Firmicutes and Bacteroidetes increased production of particular metabolites in the gut, which would contribute to beneficial changes in the host energy metabolism including GLP-1 secretion. These data suggest that distinct shifts in gut microbial composition by V + B treatment would ameliorate insulin resistance in DIO by stimulating GLP-1 secretion.

Gut microbiota, particularly Firmicutes and Bacteroidetes, are involved in the control of host energy metabolism including carbohydrate, lipid and bile acid metabolism (Swann et al., 2011; Turnbaugh et al., 2006). More importantly, Firmicutes and Bacteroidetes share roles to regulate the response of host to dynamic

changes in diets (Muegge et al., 2011). Previously, it has been suggested that there is a correlation between obesity and relative proportion of Firmicutes and Bacteroidetes (Ley et al., 2005a). However, several lines of evidence indicated that such correlation is not always implicated in obesity and changes in the relative abundance of Firmicutes and Bacteroidetes may not be sufficient for the onset of obesity (Arumugam et al., 2011; Vijay-Kumar et al., 2010). In present study, I observed that body weight gains and adiposity upon HF were not attenuated when Firmicutes and Bacteroidetes were concurrently depleted. On the other hand, I observed that obesity-induced insulin resistance was improved in parallel with the reduction in the abundance of Firmicutes and Bacteroidetes, indicating a potential role of Firmicutes and Bacteroidetes in the regulation of insulin sensitivity in DIO.

Previously, it has been reported that patients with type 2 diabetes are relatively enriched with Gram-negative bacteria belonging to the phyla Bacteroidetes and Proteobacteria (Larsen et al., 2010; Suez et al., 2014). Additionally, it has been shown that such increases in gut microbiota are associated with metabolic endotoxemia through increasing plasma LPS, leading to oxidative stress, macrophage infiltration markers and most inflammatory markers inducing insulin resistance (Cani et al., 2007). In particular, disruption of gastrointestinal barrier integrity appeared to cause a critical change in the host to aggravate inflammation induced by dysbiosis of the microbiome (Bode and Bode, 2005; Cani et al., 2007). In the present study, there was an increase in the relative abundance of Proteobacteria in conjunction with the reduction of Firmicutes and Bacteroidetes in Ab-NH group. However, my data suggest that such modulation in gut microbiota would have

limited effects on obesity-mediated increment of gut leakage as well as endotoxemia (Figure 20 and 21). Nevertheless, future studies are required to reveal the extent to which Proteobacteria modulate changes in the systemic energy homeostasis in response to V + B in DIO.

Various biological pathways facilitate the crosstalk between host energy homeostasis and gut microbiota. Here, my data suggest that V + B-induced alteration of gut microbiota modulates insulin sensitivity by promoting GLP-1 secretion. GLP-1 is a gut hormone mainly secreted from L-cells in the gut in response to nutrient status (Baggio and Drucker, 2007; Campbell and Drucker, 2013a). Particularly, the active form of GLP-1 (7-36 amide) governs systemic energy homeostasis by regulating satiety in brain, insulin secretion in pancreatic islets, and glucose uptake in muscle (Holst, 2007). Although previous report has shown that GLP-1 secretion is reduced in patients with type 2 diabetes (Muscelli et al., 2008), the dynamics of GLP-1 secretion in non-diabetic obese rodent models have not been well documented. In Figure 23B, the level of active GLP-1 in the NH group was lower than that in the NC group. Notably, treatment of Ex(9-39) aggravated glucose intolerance in Ab-NH group, indicating the significance of GLP-1-mediated beneficial effects on energy metabolism in the improvement of glucose intolerance in the Ab-NH group. Previous studies showed that several kinds of prebiotics stimulate GLP-1 secretion and that gut microbiota acts as a mediator by fermenting indigestible prebiotics to short-chain fatty acids (Cani et al., 2009; Musso et al., 2010). Consequently, short chain fatty acids induce GLP-1 release from L-cells and modulate systemic energy homeostasis (Tolhurst et al., 2012). Here, I demonstrated

that depletion of Firmicutes and Bacteroidetes in DIO increased production of gut-derived metabolites including TCA, creatine, and protein tyrosine phosphatase 1B (Figure 28). In consistent with previous studies demonstrating that TCA stimulates GLP-1 secretion in humans (Wu et al., 2013a; Wu et al., 2013b), TCA treatment promoted GLP-1 secretion in L-cells. Thus, findings both in my results and from those human data suggest that an increase in TCA after depletion of Firmicutes and Bacteroidetes would be associated with GLP-1 dependent amelioration of insulin resistance in DIO. In addition to TCA, other metabolites have been reported to have beneficial effects on host energy metabolism ('t Eijnde et al., 2001; Desmarais et al., 1998; Enrique-Tarancon et al., 2000; Macdonald and Fahien, 1988; Mendez and Balderas, 2001; Rose, 1911; Watala et al., 2009). For instance, sulfotyrosine represses protein tyrosine phosphatase 1B and contributes to the regulation of insulin signaling (Desmarais et al., 1998) and creatine is linked with increased GLUT4 expression in muscle ('t Eijnde et al., 2001). Therefore, it is of particular interest to investigate the potential roles of these metabolites in the alleviation of insulin resistance mediated by alteration of Firmicutes and Bacteroidetes in DIO in the future.

In this study, the serum insulin levels of the Ab-NH group were lower than those in the NH group in fasting and feeding conditions, implying that alternative mechanisms might enhance insulin sensitivity, independent of active GLP-1-mediated stimulation of insulin release. In the pancreas, active GLP-1 (7-36 amide) binds to GLP-1 receptor to activate protein kinase A signaling, induces insulin secretion, and promotes β-cell survival (Baggio and Drucker, 2007). However, after

secretion into the blood, active GLP-1 is rapidly degraded into the inactive GLP-1 (9-36 amide) metabolite within 1~2 min by dipeptidyl peptidase IV (Deacon et al., 1995a). Although the role of inactive GLP-1 in glucose metabolism is still unclear, it has been recently suggested that inactive GLP-1 may be involved in the regulation of glucose homeostasis (Deacon et al., 2002b; Nikolaidis et al., 2005). For instance, inactive GLP-1 alone lowers the blood glucose level in anesthetized pigs (Deacon et al., 2002b). In dogs, inactive GLP-1 significantly increases myocardial glucose uptake with dilated cardiomyopathy (Nikolaidis et al., 2005). Furthermore, inactive GLP-1 is highly stable in blood, which would prolong the effects of active GLP-1 to improve insulin resistance (Wu et al., 2013a). These findings are consistent with my data that an increment of insulin sensitivity in V + B-treated DIO mice is potentially attributable to increased levels of both active and inactive forms of GLP-1.

Increased adipose tissue inflammation correlates with insulin resistance in obese individuals. Moreover, depletion or aggravation of gut microbiota with various antibiotics alleviates insulin resistance and obesity by reducing inflammatory responses (Cani et al., 2008b; Murphy et al., 2013a). In this study, adipose tissue and whole body inflammation were similar between NH and Ab-NH groups. However, in a recent study, mice treated with sub-therapeutic levels of antibiotics displayed increased adiposity and insulin resistance with subtle but significant changes in gut microbiota (Cho et al., 2012). These conflicting results might be derived from the selection and concentration of antibiotics, which would influence metabolic changes and adipose tissue dysregulation.

In conclusion, I demonstrated that alteration of gut microbiota, with significant depletion of Firmicutes and Bacteroidetes, by treatment with V + B would improve insulin resistance in DIO mice. Apparently, such modulation in gut microbiota alters profiles of gut-derived metabolites and consequently augments GLP-1 secretion. Taken together, these findings may provide an insight into the understanding of biological mechanisms involved in the regulation of insulin sensitivity in obese subjects.

CHAPTER TWO:

Gamma (γ)-aminobutyric acid response mediates resistance to adipose tissue inflammation in obese IAT

Summary

Obesity is one of risk factors for insulin resistance, which leads to most of the metabolic syndromes such as type 2 diabetes. Studies in both human and animal models reveal that metabolic disorders are positively correlated with an increase of visceral fat tissues including EAT. On the contrary, subcutaneous adipose tissues including IAT have been proposed to play beneficial roles in the regulation of host metabolism. In this study, I have demonstrated that macrophage infiltration was significantly reduced in IAT, versus EAT in the progression of obesity. Further, the different degrees of macrophage recruitment between two fat-depots were derived from the intrinsic characteristics of each fat tissue rather than the microenvironment of adipose tissues. Through transcriptome analyses, the pathway of gamma (γ)-aminobutyric acid (GABA) response was proposed as one of the potential etiologies to exhibit differential inflammatory responses between IAT and EAT. In IAT, GABA signaling modulated monocyte chemotaxis implying that GABA response might be a causality to determine fat-depot specific inflammatory responses. Moreover, I have demonstrated that IAT originated adipose-derived stem cells (ADSCs) seemed to be the primary cell type to mediate GABA response against macrophage recruitment. Taken together, these data suggest that differential GABA responses in IAT would contribute to less-inflammatory responses in obesity.

INTRODUCTION

The obese population has grown rapidly worldwide in last several decades (Christakis and Fowler, 2007; Ludwig, 2002). A considerable number of obese population is closely associated with metabolic disorders such as hyperlipidemia, type 2 diabetes, and cardiovascular diseases (Grundy, 2004; Ludwig, 2002; Meigs et al., 2005). Insulin resistance induced by obesity is known to be a major factor to stimulate most metabolic diseases, and is linked with increased reactive oxygen species (ROS), endoplasmic reticulum (ER) stress, mitochondrial dysfunction, hypoxia, and low-grade chronic inflammation in obesity (Guilherme et al., 2008; Saltiel and Kahn, 2001).

In clinical viewpoints, obesity is largely subdivided into two types, visceral obesity and subcutaneous obesity and two types of obesity exhibit different outcomes in metabolic diseases (Kissebah and Krakower, 1994; Pouliot et al., 1992). Enlargement of visceral adipose tissue shows a strong correlation with metabolic syndromes and mortality (Gesta et al., 2007; Kissebah and Krakower, 1994). On the other hand, subcutaneous adipose tissue contributes to metabolic benefits in obesity (Siviero-Miachon et al., 2015; Tran et al., 2008). For instance, activation of adipogenesis with pioglitazone results in a reduction of visceral adipose tissue and improves metabolic index. At the same time, pioglitazone selectively increases subcutaneous adipose tissue (Miyazaki et al., 2002). MitoNEET is a protein located in outer mitochondrial membrane, and is named according to its C-terminal amino

acid sequence, Asn-Glu-Glu-Thr (NEET) (Colca et al., 2004). Leptin deficient (*ob/ob*) mice is a model of obesity, but overexpression of mitoNEET in *ob/ob* mice has shown further increase of body weights upon HF feeding (Kusminski et al., 2012). Intriguingly, mitoNEET transgenic *ob/ob* mice exhibit significant improvement of insulin resistance accordant with increased IAT weight. Also, metabolic parameters were improved by overexpression of adiponectin in spite of extra body weight gains (Kim et al., 2007). These results indicate the beneficial roles of subcutaneous adipose tissue in the regulation of energy metabolism. Numerous studies have shown the different degrees of cold-induced thermogenic- (Seale et al., 2011), angiogenic- (Gealekman et al., 2011) and adipogenic properties (Jeffery et al., 2015; Joe et al., 2009) between visceral and subcutaneous adipose tissue. Although inflammatory responses are the most distinct in subcutaneous adipose tissue compared to visceral adipose tissue in obesity (Cartier et al., 2008; Miller et al., 2011; Montague et al., 1998; Xu et al., 2012), it still remains unclear why and how subcutaneous and visceral fat-depots are different in metabolic regulation particularly in obesity-induced inflammation.

After a discovery of increased adipose-derived TNFα secretion in obesity (Hotamisligil et al., 1993), numerous studies have supported the idea that adipose tissue is one of the immunosensitive organs (Schaffler et al., 2006). In obesity, adipose tissue immune cells have been reported to orchestrate adipose tissue inflammatory responses (Donath and Shoelson, 2011). For instance, neutrophil, $CD8^+$ effector T-, mast- and B-cells are increased and induce pro-inflammatory responses in adipose tissues (Liu et al., 2009; Nishimura et al., 2009; Talukdar et al.,

2012; Winer et al., 2011). In contrast, regulatory T cells contribute to anti-inflammatory responses in obesity (Feuerer et al., 2009). Among the various kind of immune cells, adipose tissue macrophages (ATMs) have been intensively studied to mediate obesity-induced insulin resistance (Lumeng et al., 2007a; Patsouris et al., 2008; Weisberg et al., 2003). In lean subjects, alternatively activated M2 macrophages in adipose tissue contribute to metabolic homeostasis by lowering fat tissue inflammation via HIF-2α, IL10, and Arginase (ARG) I (Choe et al., 2014; Odegaard and Chawla, 2011). In obesity, adipose tissues show elevated classically activated $CD11c^+$ M1 macrophages (Lumeng et al., 2007a). M1 ATMs promote pro-inflammatory cytokines such as TNFα, IL1β, and IL6, which are strongly associated with systemic insulin resistance (Despres and Lemieux, 2006; Lumeng et al., 2007a). Consistently, $CD11c^+$ cell deficient mice restore abnormal metabolic parameters in obesity (Patsouris et al., 2008) demonstrating that pro-inflammatory ATMs are crucial in obesity-induced insulin resistance.

In obesity, pro-inflammatory macrophages produce various inflammatory cytokines to inhibit insulin signaling pathway in adipocytes (Chawla et al., 2011; Ferrante, 2007). In obesity, the origin of ATMs has previously been attributed to the recruitment of blood monocytes into adipose tissues (Lumeng et al., 2007b; Oh et al., 2012). However, several lines of evidence have suggested that other possibilities of the ATM origins would be possible in obesity. First, the number of $Ki67^+$ proliferative ATMs are increased in obesity (Amano et al., 2014). Second, netrin-1, a secreted laminin-related molecule is elevated in obesity and contribute to retention of ATMs (Ramkhelawon et al., 2014). Last, the survival rates of ATMs are increased

in obesity (Hill et al., 2015). Since these studies have demonstrated that ATMs are increased in visceral EAT, it has not been thoroughly studied how subcutaneous ATMs and inflammatory responses are regulated in subcutaneous IAT in obesity.

Given that subcutaneous IAT has shown beneficial roles in the regulation of energy metabolism and resistance to inflammatory responses in obesity, I decided to investigate why and how subcutaneous IAT and visceral EAT exhibits a different degree of adipose tissue inflammation in obesity. In the progression of obesity, the number of ATMs was significantly lower in IAT compared to EAT. Notably, I found that gamma (γ)-aminobutyric acid (GABA) response was differentially regulated in IAT, unlike EAT in obesity. Furthermore, I have shown that chemotactic activity of ATMs was reduced in IAT originated adipose-derived stem cells (ADSCs) in response to GABA stimulation. Subsequently, GABA dependent regulation of ATM infiltration in IAT improved insulin resistance in DIO. Taken together, these data suggest that fat-depot selective GABA responses would contribute to regional differences in adipose tissue inflammation and whole body energy metabolism.

MATERIALS AND METHODS

Animal experiments

Six-week-old C57BL6/J and C57BLKS/J-Lepr^{db}/Lepr^{db} (*db/db*) male mice were obtained from Central Lab Animal Inc (Seoul, Korea). Ds-Red^{+} transgenic mice were generously provided by Gou Young Koh (KAIST, Daejeon, South Korea). These mice were housed in colony cages for 12 hours (h) light/12 h dark cycles with free access to food and water. C57BL6/J wild-type mice were allowed for acclimation for 2 weeks before the start of HF feeding. The eight-week-old male mice were fed 60% kcals of fat contained HF (Research Diets Inc., New Brunswick, NJ, USA) with free drinking water. On the day of sacrifice, all of the experimental groups of mice were compared to age-matched control (NC) group mice. All experiments were approved by the Seoul Natl. Univ. Institutional Animal Care and Use Committees (IACUC).

Chemicals

For animal experiments, 50 mg/kg of GABA (A2129; Sigma-Aldrich, St. Louis, MO, USA) and 1.5 mg/kg of saclofen (Sac) (0246; Tocris, Bristol, UK), $GABA_B$ selective antagonist were used to be intraperitoneally injected in animal. For *ex vivo* condition, GABA (100 nM) and baclofen (Bac; 10 μM) were used to stimulate

$GABA_{(B)}$ receptor signaling. Sac (20 μM and CGP35348 (CGP; 50 μM) (1245; Tocris) was treated to inhibit $GABA_B$ responses. Bicuculline methiodide (Bicu; 50 μM) (2503; Tocris) was tested to repress $GABA_A$ receptor mediated signaling.

GABA measurement

Each of adipose tissue was homogenized in 2 mL of PBS. After centrifugation in the condition of 12000 rpm and 4°C for 10 min, the middle layer was carefully isolated. The tissue extracts in PBS were mixed with 10% trichloroacetic acid in cold acetone (1:4 ratio v/v) and incubated for overnight in -20°C freezer. To remove proteins, the samples were centrifuged in the condition of 14000 rpm and 4°C for 30 min. The supernatants were carefully taken and dried using SpeedVac™ (Thermo Fisher Scientific, Waltham, MA, USA). Each dried sample is reconstituted with 0.1% formic acid in distilled water. The reconstituted samples were analyzed by liquid chromatography-mass spectrometry (LC-MS) in National Instrumentation Center for Environmental Management (Seoul, South Korea).

Serum metabolome analyses by capillary ethanol-mass spectrometry (CE-MS)

Blood by heart puncture was collected and centrifuged to isolate serum. The serum was centrifuged and filtered using Ultrafree-MC filter units (Millipore, Billerica, MA, USA). Samples were analyzed by CE-MS at Human Metabolome

Technologies, Inc. (Yamagata, Japan). Detailed methods were described in a previous report (Matsumoto et al., 2012).

Adipose tissue transplantation

10-week NC fed and HF littermates were used as recipients. Age matched DIO mice were used as donors. Fat transplantation was performed using fat-pads from EAT and IAT. Extracted fat-pads were cleaved into approximately 0.6 g for visceral- or 0.3 g and kept in 37°C incubator with 3 mL of phosphate-buffer saline (PBS) until transplantation. The recipient mice were anesthetized with muscle by injection with 0.2 mL/kg with Rompun and 0.4 mL/kg of Zoletil up to 200 μL with addition of PBS. Each fat-slices were transplanted into visceral EAT and subcutaneous IAT (Tran et al., 2008). Adipose tissues were not added in NC and HF sham group. The recipient mice were fed either NC or HF up to 3 weeks. Body weight and blood glucose were measured until the sacrifice of the recipients.

RNA-sequencing analyses

All libraries were sequenced with 101-bp paired-ends on an Illumina HiSeq instrument. Read pairs were aligned using RSEM v.1.2.25 (Li and Dewey, 2011) and Bowtie 2.2.6 (Langmead and Salzberg, 2012) to the Mus musculus genome (GRCm38/mm10) (Waterston et al., 2002). I estimated the expected number of fragments from each transcript and gene with RSEM. Limma (Voom) (Law et al.,

2014) was used to perform statistical tests for pairwise differential expression between samples (EAT and IAT; NC and HF), calculate log_2 fold change (log_2FC) values and select differentially expressed genes (DEGs) with adjusted p-value cutoff <0.05.

Pathway analyses

SPIA (Tarca et al., 2009) was used for pathway analysis. 314 pathways annotated in Kyoto Encyclopedia of Genes and Genomes (KEGG) database (Kanehisa and Goto, 2000) were analyzed. Among three statistics (pNDE: P-value from the number of differentially expressed genes, pPERT: P-value from perturbation factor, pINT: Integrated p-value of pNDE and pPERT) generated by SPIA, significance of pathways was determined by pINT. Average absolute log fold change (FC) of pathway genes and pINT are used to generate half-volcano plots of pathways.

In vivo ATM migration

Leukocyte pools from Ds-Red$^+$ transgenic mice, blood by heart puncture were collected in 1.5 mL-tube and mixed with 20 μL of 0.5 M EDTA to prevent blood clotting. Each blood samples were pooled to 3 mL of Greiner Leucosep tube (GN163290; Sigma Aldrich) with pre-equilibration of 3 mL of NycoPrep 1.077 (1114550; Axis-Shield PoC AS, Oslo, Norway). In room temperature, after a

centrifugation of 2500 rpm and 10 min condition, middle layer was carefully isolated and washed with RoboSep buffer (20104; STEMCELL, Vancouver, Canada). 1×10^6 mononuclear cells (MNCs) in RoboSep buffer were intravenously injected to recipient mice. After resting period, each fat-depots were extracted from the recipient mice to test exogenous MNC infiltration into adipose tissues.

Adipose tissue fractionation

Adipose tissue was fractionated as previously described (Huh et al., 2013). Briefly, EAT and IAT were chopped and incubated in collagenase buffer for 30 min at 37°C with shaking. After centrifugation, adipocytes in the supernatant were collected separately. Simultaneously, the pelleted stromal vascular cells (SVCs) were incubated with red blood cell lysis buffer (a 1:9 mixture of 0.17 M Tris (pH 7.65) and 0.16 M NH_4Cl), centrifuged at 1300 rpm for 5 min, and resuspended in PBS to remove red blood cell derived components.

Flow cytometry analyses

The SVCs were stained with CD11b (BD Bioscience, San Jose, CA, USA), F4/80 (eBioscience, San Diego, CA, USA), and CD11c (eBioscience) monoclonal antibodies for 30 min at 4°C. After staining of the ATM surface markers, Ki67 (eBioscience) or Annexin V (BD Bioscience) were stained by following manufacturer's protocols. For the analyses of ADSCs, SVCs were incubated with

CD31 (eBioscience), CD34 (eBioscience), and Sca-1 (eBioscience). After incubation, cells were gently washed and resuspended in PBS. The stained cells were analyzed or sorted for ADSCs using the fluorescence-activated cell sorting (FACS) Canto II™ or Aria II™ instrument (BD Bioscience). The primary adipocyte size was measured by using BioSorter™ (Union Biometrica, Holliston, MA, USA)

Whole mount immunohistochemistry

Adipose tissues were mounted after fixation by vascular perfusion of 1% paraformaldehyde in PBS. The whole-mounted tissues were incubated for 1 h in room temperature with a blocking solution containing 5% goat serum (005-000-121; Jackson ImmunoResearch, West Grove, PA, USA) in 0.3% PBS-T. After blocking, the whole-mounted adipose tissues were incubated overnight at 4 °C with antibodies against CD31 (MAB1398Z; Merck, Billerica, MA, USA), CD11b (14-0112-81; eBioscience), and CD11c (14-0114-81; eBioscience). After several washes with PBS-T, the whole-mounted tissues were incubated for 1 h at room temperature with secondary antibodies, namely FITC, Cy3- or Cy5-conjugated anti-Armenian hamster antibody, anti-rat antibody or anti-rabbit antibody (diluted 1:500; Jackson ImmunoResearch). The lipid droplet of adipocytes was visualized by coherent anti-strokes Raman scattering (CARS). Pump and Strokes lasers were tuned to 14140 cm^{-1} (or 707nm) and 11300 cm^{-1} (or 885nm), respectively, to be in resonance with the CH_2 symmetric stretch vibration at 2840 cm^{-1}. Glucose Bioprobe (GB-Cy3) was stained as previously studied (Kim et al., 2015). The signals were visualized, and

digital images were obtained using Zeiss (LSM700, Carl Zeiss, Oberkochen, Germany) and Leica microscope (TCS SP8 CARS, Leica Microsystems, Wetzlar, Germany).

hematoxylin and eosin (H&E) staining

Adipose tissues dissected from the mice were incubated with 4% paraformaldehyde in PBS solution for one day. Paraffin-embedded tissues were sliced into 4 μm (Probe-On-Plus Slides; Fisher Scientific). After drying, Xylene, 100%, 95%, 80% and 70% alcohol were used step by step to wash the slides to remove paraffin. Harris hematoxylins were stained for 10 min. 1% HCl and 0.5% ammonia was treated with slides progressively. Eosins were stained followed by dehydration with treatment of 70% to 100% concentration of xylene gradually. The staining processes were carried out at ABION CRO, Inc. (Seoul, Korea).

Monocyte chemotaxis

The conditioned medium from each group was loaded to lower layer of 8 μm pore size trans-well (CLS3428; Sigma Aldrich), and THP-1 cells stained with 2 μM of Cell Tracker^{TM}-CMPTX (C34552; Thermo Fisher Scientific, Waltham, MA, USA) in 37°C incubator for 1 h were washed with PBS. In each sample, 3×10^5 cells were loaded on the upper surface of 8 μm pore size trans-well (upper layer). After 12 h incubation, upper layer was removed to remain chemotactic cells. The chemotactic

cells were stained with Hoechst dye (H3570; Thermo Fisher Scientific) for 30 min. After removal of the staining dye with washing, 10% FBS DMEM-high glucose medium were filled, and the plates were read with a confocal microscope (LSM700, Carl Zeiss, oberkochen, Germany). In randomized microscope images, Cell Tracker™ (Red) and Hoechst (Blue) positive cells were counted and quantified.

RNA isolation and Q-PCR

As described previously (Huh et al., 2013; Jeong et al., 2010), each tissue was homogenized with TRIzol reagent (Molecular Research Center, OH, USA). cDNA was synthesized with M-MuLV reverse transcriptase (Fermentas, MD, USA). Then, the cDNA was mixed with TOPreal™ qPCR 2X PreMIX (RT500M; Enzynomics, Daejeon, South Korea). Quantitative real-time PCR was performed using the CFX96™ real-time system (Bio-Rad Laboratories, CA, USA). The threshold cycle (Ct) values of each mRNA were normalized to Ct value of cyclophilin. The quantitative real time-PCR primers used in this study were synthesized from Bioneer (Daejeon, South Korea).

Glucose tolerance test

As described previously (Lee et al., 2011), 4 h fasted mice were administered with glucose through intra-peritoneal (IP) injections or oral gavages (2 g/kg glucose,

20% glucose solution). Blood samples were drawn at 15, 30, 60, 90, and 120 min after injection by taking 3 μL of blood collected from the tip of the tail vein.

Western blot analyses

EAT and IAT extracted from each groups were homogenized with modified immunoprecipitation assay (RIPA) buffer (50 mM Tris-HCl [pH 7.4], 150 mM NaCl, 1 mM EDTA, 1 mM PMSF, 1% (v/v) NP-40, 0.25% (w/v) Na-deoxycholate, protease inhibitor cocktail with 1 mM NaF and 10mM Na_3VO_4 as phosphatase inhibitor) and subjected to 10% SDS-PAGE. As previously described (Kim et al., 2009), separated proteins were blotted with antibodies followed: phosphorylation of c-Jun N-terminal kinase (p-JNK) (SC6254; Santa Cruz Biotechnology, Dallas, TX, USA), JNK (SC474; Santa Cruz Biotechnology), phosphorylation of p38 mitogen-activated protein kinase (p-p38) (9211; Cell Signaling Technology, Danvers, MA, USA) , p38 (9212; Cell Signaling Technology), and β-actin (A5316; Sigma-Aldrich, St. Louis, MO, USA) were used.

Statistical analyses

Data are presented as the mean with standard error means (S.E.). All statistical analyses were performed using Student's t-test.

RESULTS

IAT exhibits resistance to obesity-induced ATM infiltration in obesity

To investigate changes of subcutaneous IAT and visceral EAT in obesity, C57B6L/J mice were fed HF. While body weights were gradually increased upon HF periods, the pattern of fat mass in IAT versus EAT was significantly different (Figure 31A and 31B). In addition, there were different in population of fat cell size and degree of vascularization (Figure 31C and 31D). Given that expression of inflammatory cytokines in EAT and IAT are dissimilar in obesity (Cartier et al., 2008; Miller et al., 2011; Montague et al., 1998; Xu et al., 2012), I have investigated whether IAT and EAT might differentially express inflammatory genes in DIO. Whereas IAT expressed a relatively lower level of pro-inflammatory genes than EAT, the level of anti-inflammatory gene expression in IAT was higher than that of EAT (Figure 32). Consistent with differential expression of inflammatory gene in IAT and EAT in DIO, I examined macrophage accumulation in IAT and EAT. As shown in Figure 33A and 33B, ATMs ($CD11b^+$ and $F4/80^+$) and M1 ATMs ($CD11b^+$, $F4/80^+$, and $CD11c^+$) macrophage number was gradually elevated in EAT. However, IAT showed significant less level of ATM accumulation compared to EAT in the progression of obesity. In addition to DIO mice, I also observed *db/db*, genetically obese mice, exhibited less accumulation of ATM and M1 ATM in IAT than EAT (Figure 33C). These data imply that pro-inflammatory ATMs are accumulated differentially between IAT and EAT.

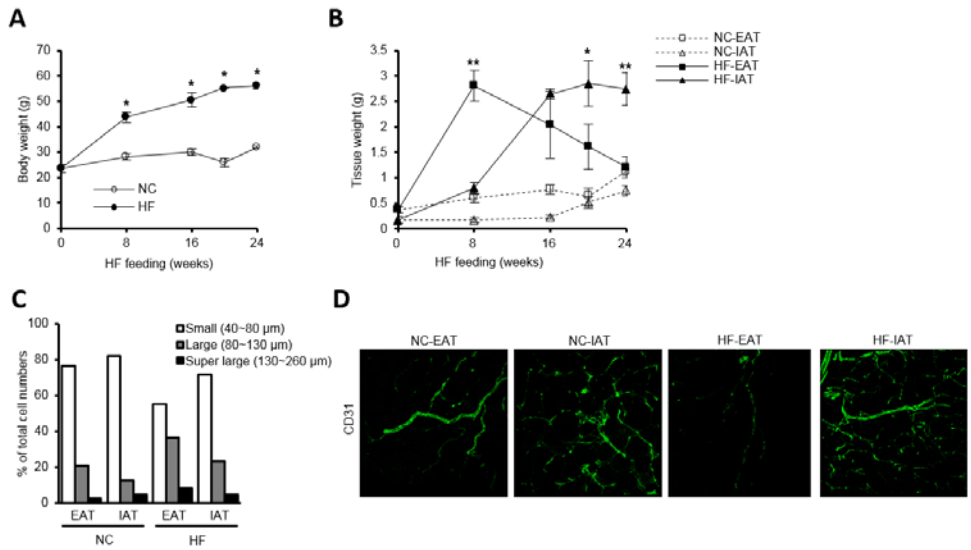

Figure 31

Multiple analyses of differential fat-depots in obesity. (A) Body weight changes in NC- and HF-fed mice. Each mouse was measured body weight at 0, 8, 16, 20, and 24 weeks after NC- or HF-feeding (B) Weights of EAT and IAT upon HF feeding period. Individual adipose tissues were isolated from mice above. (C) Measurement of adipocyte size upon NC- or HF-feeding. Primary adipocytes isolated from NC and HF fed mice were counted and separated into small (40~80 μm), large (80~130 μm), and super large group (130~260 μm) upon cell size by using BioSorter^{TM}. (D) Whole mount immunohistochemistry of $CD31^{+}$ endothelial cells in EAT and IAT.

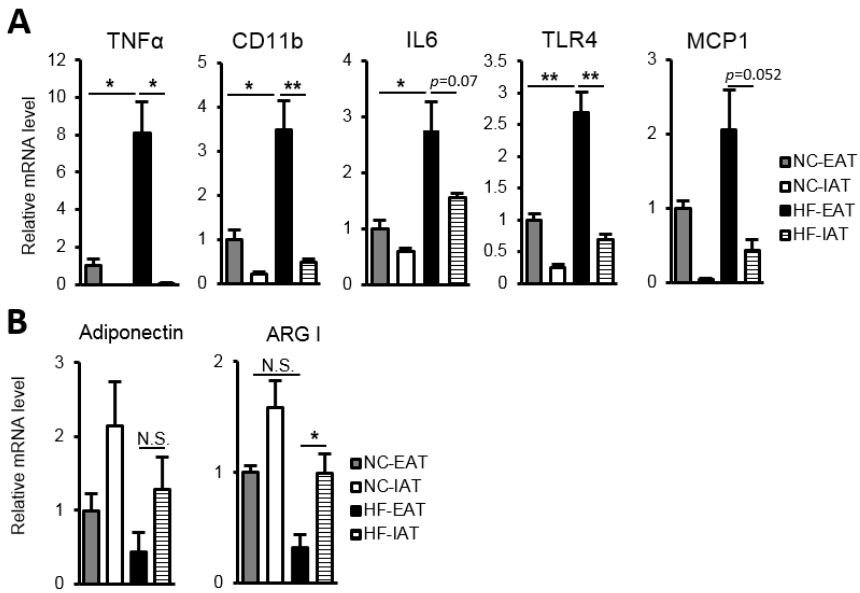

Figure 32

Fat-depot specific patterns of inflammatory gene expression. (A) Relative mRNA level of inflammatory genes such as TNFα, CD11b, IL6, TLR4, and MCP1. (B) Relative mRNA level of anti-inflammatory genes such as adiponectin and ARG I.

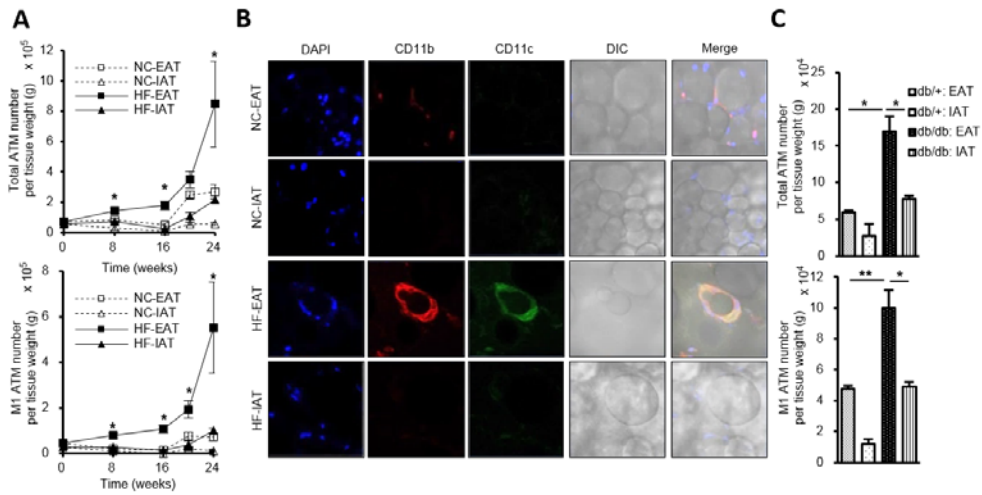

Figure 33

Distinct patterns of ATM accumulation in the progression of obesity. (A) Flow cytometry analyses of $CD11b^+$ and $F4/80^+$ ATMs (upper panel) and $CD11b^+$, $F4/80^+$, and $CD11c^+$ M1 ATM in EAT and IAT at 0, 8, 16, 20, and 24 weeks of HF feeding. (B) Relative mRNA level of anti-inflammatory genes such as adiponectin and ARG I. (C) Representative whole mount images (×400) of $CD11b^+$ (Red) and $CD11c^+$ (Green) in EAT and IAT of NC and HF fed mice. (D) Fat-depot specific accumulation of ATM (upper panel) and M1 ATM (lower panel) in *db/db* mice.

As ATM accumulation in obesity could be increased by three processes such as proliferation (Amano et al., 2014), apoptosis (Hill et al., 2015), and infiltration (Lumeng et al., 2007b; Oh et al., 2012), I decided to test these processes in IAT and EAT of DIO. First, the ratio of $Ki67^+$ proliferative macrophage was not different between IAT and EAT implying that proliferation of ATM might not be a major factor to exhibit fat-depot specific ATM accumulation in obesity (Figure 34A). In addition, while the number of annexin V^+ apoptotic macrophages was significantly reduced in DIO group, the annexin V^+ macrophage counts were similar both in EAT and IAT (Figure 34B). Next, when exogenous Ds-Red^+ mononuclear cells (MNCs) were injected into recipient mice (Figure 35A), there was a significant difference of Ds-Red^+ macrophage numbers in IAT and EAT. As shown in Figure 35B, in DIO mice, exogenous ATM and M1 ATM infiltration were significantly elevated in EAT whereas the number of Ds-Red+ ATM and M1 ATM were not altered in IAT. These data suggest that subcutaneous adipose tissues would be less susceptible to ATM accumulation probably via reduced macrophage infiltration rather than proliferation or apoptosis.

Intrinsic characteristics of adipose tissues affect fat-depot specific ATM infiltration

IAT is localized under dermis with abundant extracellular matrix whereas EAT is surrounded by internal organs. To distinguish whether the source of dissimilar ATM infiltration might be originated from tissue environments or intrinsic tissue

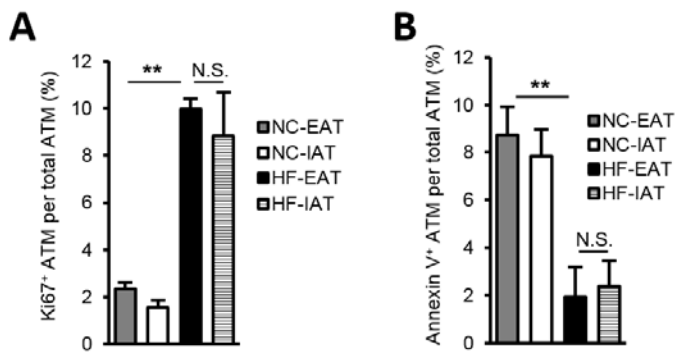

Figure 34

Degrees of proliferative- and apoptotic ATM ratios between EAT and IAT. The ratio of (A) proliferative ($Ki67^+$), and (B) dead (Annexin V^+) ATM was measured in EAT and IAT of NC and HF fed mice.

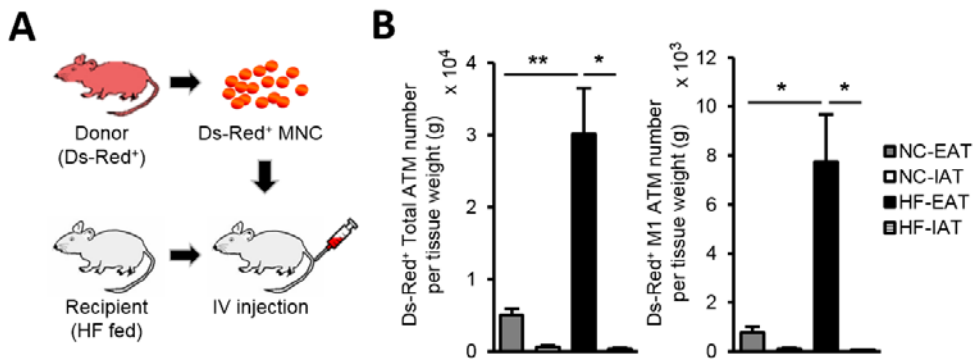

Figure 35

Fat-depot specific exogenous ATM infiltration in EAT and IAT of obesity. (A) An experimental strategy of *in vivo* ATM infiltration. The recipient mice were intravenously injected with either PBS or Ds-Red^{+} MNC isolated from Ds-Red transgenic mice. These mice were rested for 24 h and analyzed the number of ATM infiltration in EAT and IAT. (I) Flow cytometry analyses of Ds-Red+ ATM and M1 ATM in EAT and IAT.

inherency, I separated IAT and EAT into two pieces, and transplanted each of these adipose fragments into HF fed recipient mice (Figure 36). Again, the recipient mice are subdivided as 'EAT transplantation; (1)', and 'IAT transplantation; (2)' group. As previously reported (Foster et al., 2013; Tran et al., 2008), I observed the beneficial effects on metabolic parameters such as glucose metabolism in a (2) group. (Figure 37). To investigate whether macrophage infiltration into exogenous transplanted adipose tissue might be dependent on the location of transplantation, Ds-Red$^+$ MNCs were intravenously injected into (1) and (2) group mice. As shown in Figure 38A, donor EAT transplanted to the IAT locus (EAT→IAT), donor EAT to the EAT locus (EAT→EAT), donor IAT to the IAT locus (IAT→IAT), and donor IAT to the EAT locus (IAT→EAT) were well-vascularized in recipient mice. I observed a higher number of Ds-Red$^+$ ATMs in EAT→EAT and EAT→IAT groups than IAT→EAT and IAT→IAT groups (Figure 38B) without any significant effect on Ds-Red$^+$ ATM infiltration in recipient adipose tissues of (1) and (2) group mice (Figure 38C). Meanwhile, anatomical location of transplantation did not affect exogenous Ds-Red$^+$ macrophage infiltration (Figure 38B). Consistent with these findings, H&E staining of transplanted donor adipose tissues showed no differences by the location of transplantation (Figure 39). Together, these results demonstrated that the origin of fat-depot specific ATM infiltration would be mainly associated with certain intrinsic adipose factors rather than the environmental effect surrounding adipose tissues.

In obesity, GABAergic response is differentially regulated in IAT versus EAT.

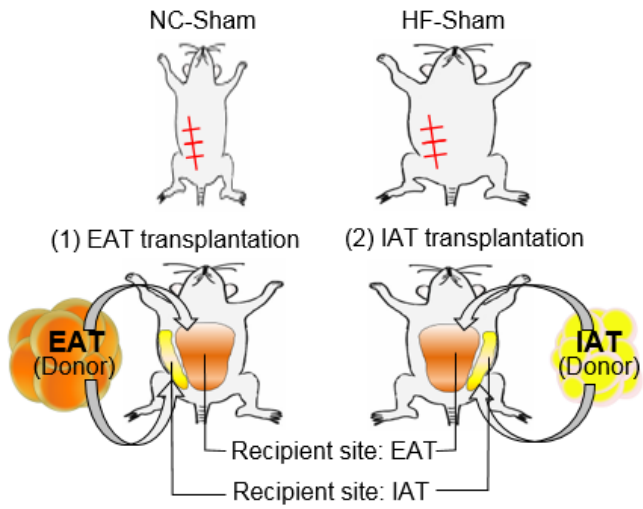

Donor	Recipient		Tissue Group
	Group Number	Target Location	
EAT	(1)	Subcutaneous	EAT → IAT
		Visceral	EAT → EAT
IAT	(2)	Subcutaneous	IAT → IAT
		Visceral	IAT → EAT

Figure 36

An experimental strategy of adipose tissue transplantation. An illustration of adipose tissue transplantation. Donor adipose tissues (EAT and IAT) were transplanted into either subcutaneous or visceral location of the recipient mice. The EAT transplanted recipients are symbolized as ‘group (1)’ and the IAT transplanted recipients are denoted as ‘group (2)’. Information for each fat-depot is indicated in the panel below.

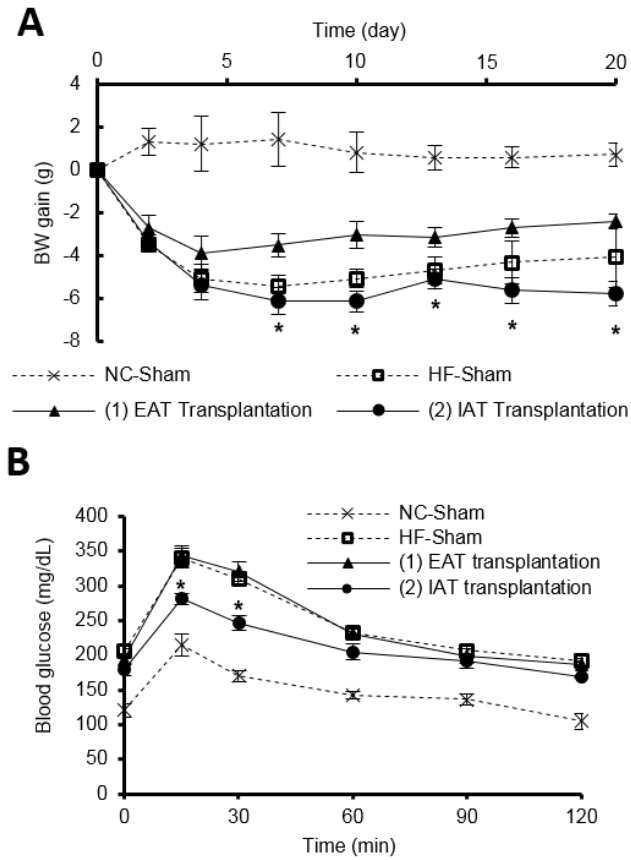

Figure 37

Metabolic phenotypes by adipose tissue transplantation. (A) In each group, body weights changes were denoted until 20 days of adipose tissue transplantation. (B) After 2 weeks of the surgery, 6 h fasted mice were tested for glucose tolerance.

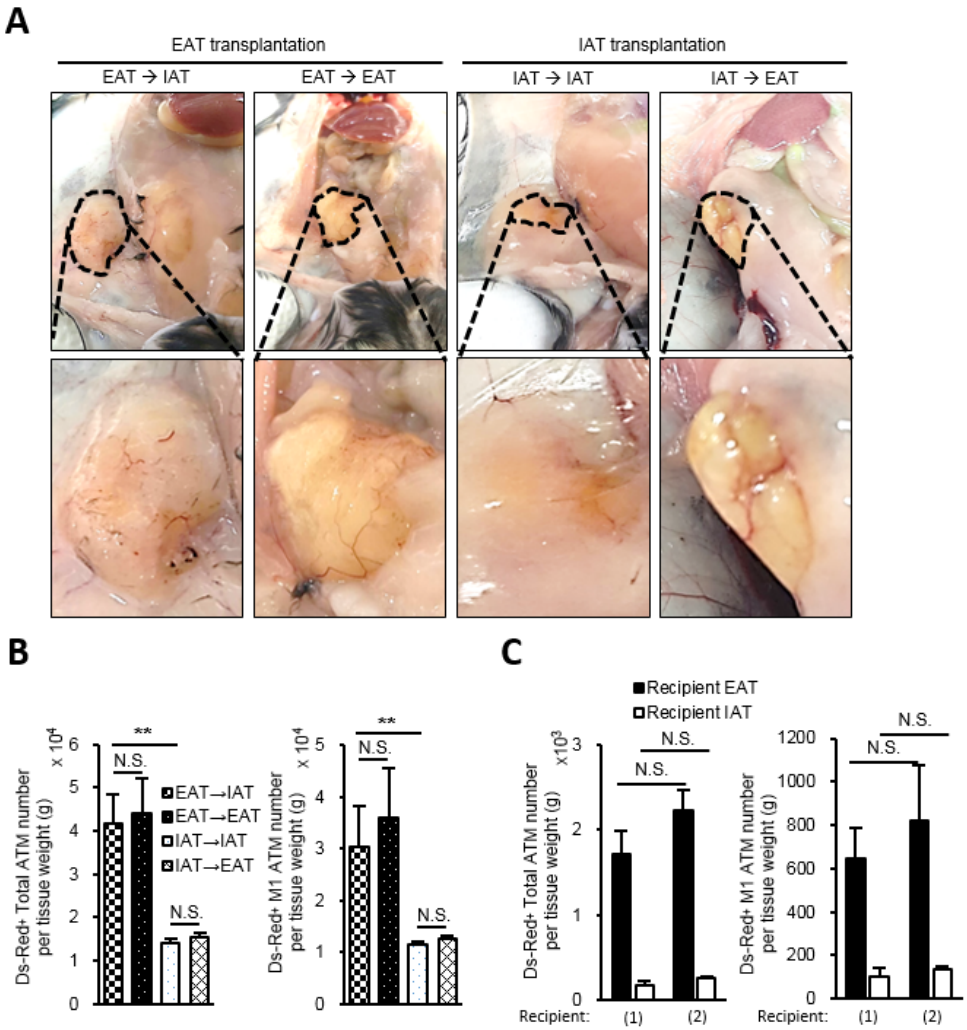

Figure 38

Phenotypes of donor fat-depots and exogenous ATM infiltration test in each fat-depot. (A) Representative images of transplanted adipose tissues in recipient mice. (B) Comparison of exogenous Ds-Red^{+} ATM infiltration (left) and M1 ATM (right) in donor adipose tissues. (C) Flow cytometry analyses of Ds-Red^{+} ATM (left) and M1 ATM (right) in adipose tissues of (1) and (2) groups.

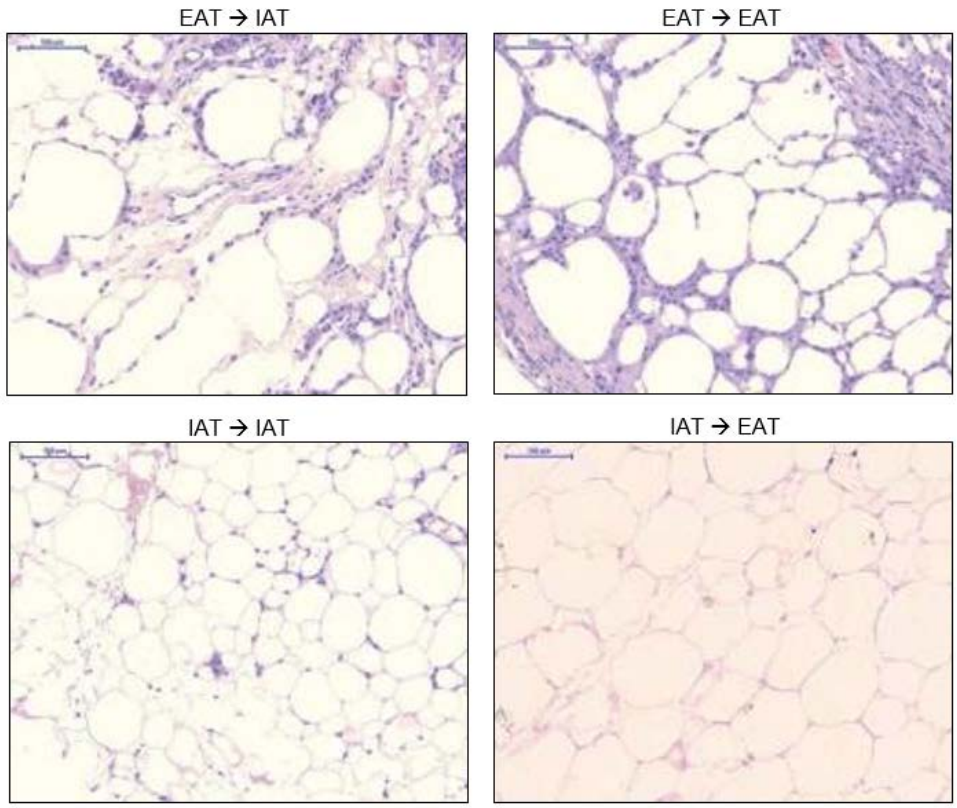

Figure 39

H&E staining of donor adipose tissues. Representative images (×150) of H & E staining of donor adipose tissues.

Adipose tissue is composed of adipocytes and SVCs with various cell types. In order to distinguish the different capacity to recruit macrophages into each fat-depot or SVCs between adipocytes and SVCs from each fat-depot, I tested monocyte chemotaxis in conditioned media of adipocytes and SVC. As shown in Figure 40, differential extent of monocyte chemotaxis was observed in conditioned media of SVCs. Given that different degree of macrophage infiltration was intrinsically originated in adipocytes and SVCs from EAT and IAT, I decided to examine the transcriptomes of adipocyte and SVC from EAT and IAT. By the comparative analyses of adipocyte and SVC from each fat-depot in DIO mice (Figure 41A and 41B), I discovered that expression profiles of 'GABAergic synapse' among the lists of KEGG pathways were dissimilarly regulated in IAT versus EAT (Figure 41C and 41D). Further, it appeared that the GABAergic synapse pathway showed significant differences in transcriptomes of SVCs compared with adipocytes.

In the central nervous system, gamma (γ)-aminobutyric acid (GABA) is well known inhibitory neurotransmitter synthesized by glutamate decarboxylase 1 (GAD1) and 2 (GAD2) (Bu et al., 1992; Roberts and Frankel, 1950). When GABA is secreted by pre-synaptic neuron, the post-synaptic signal is regulated via binding of GABA to either $GABA_A$ or $GABA_B$ receptor (Kerr and Ong, 1995; Macdonald and Olsen, 1994). Given that both of GABA receptors could regulate activities of neuronal synapse, I have asked whether GABA receptor mediated cellular signaling might be present in adipose tissues. As shown in Figure 42A and 42B, $GABA_B$ receptor, a heterodimer composed of $GABA_B$ receptor 1 (GABBR1) and $GABA_B$ receptor 2 (GABBR2), showed notable levels of gene expression in adipose tissues

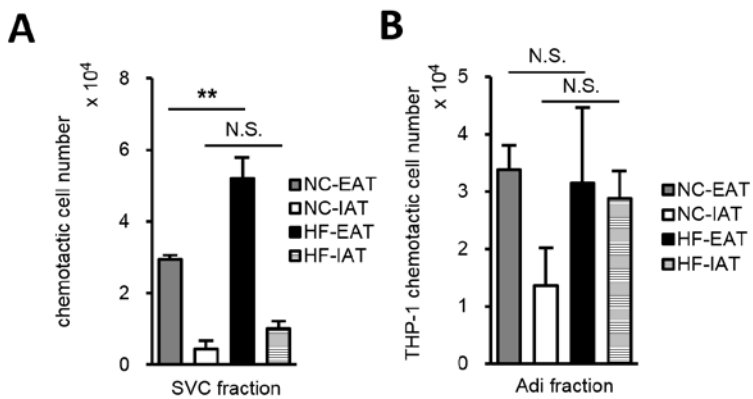

Figure 40

Fat-depot specific monocyte migration in adipocytes and SVCs fraction. EAT and IAT of NC and HF fed mice were fractionated into adipocytes and SVCs. Each sample was cultured in media. The conditioned media was used to test THP-1 human monocyte chemotaxis by using 8 μm pore sized trans-well. Chemotactic cells were analyzed in the group of (A) SVC and (B) adipocyte (Adi) derived conditioned media.

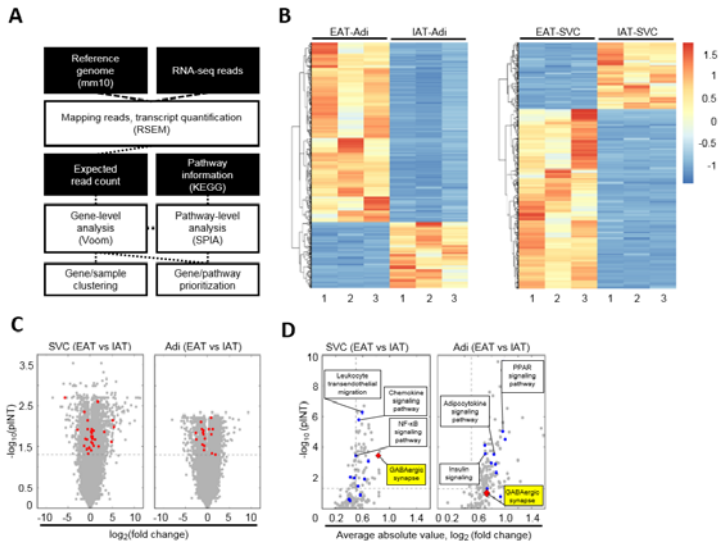

Figure 41

Transcriptome analyses of IAT and EAT in DIO mice. (A) An algorithm of RNA-sequencing data analyses. (B) Each heat-map displays expression patterns of differentially expressed genes (DEGs) between EAT and IAT in adipocytes and SVCs. Genes are represented as horizontal lines and hierarchically clustered by z-transformed expression patterns. (C) Volcano plots from DEG patterns between EAT and IAT in adipocyte (left) and SVCs (right). Differentially expressed GABAergic pathway genes in KEGG pathway are shown in red. (D) Half-volcano plots show significance of KEGG pathway comparing EAT and IAT in SVCs (left) and adipocytes (right). The *x* axis indicates the average absolute $\log_2$ fold change of pathway genes. The *y* axis represents the negative $\log_{10}$ p value (pINT) from the SPIA analyses result. Circular dots (blue) designate the pathways involved in inflammation and energy metabolism. The rhombus dot (red) indicates 'GABAergic synapse'.

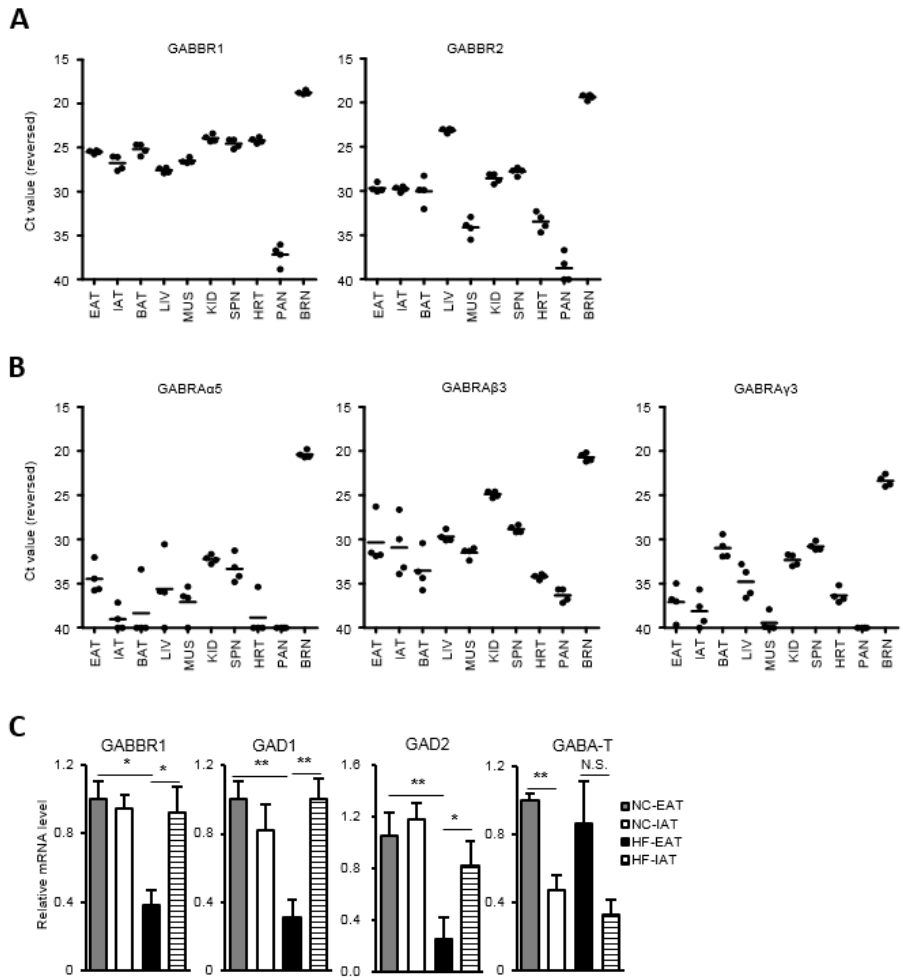

Figure 42

GABAergic gene expressions in mice. mRNA level (Ct values) of (A) $GABA_B$ receptor genes and (B) $GABA_A$ receptor subunits. (C) Relative mRNA level of GABAergic gene expressions in EAT and IAT of obesity.

whereas subunits of $GABA_A$ receptor were rarely expressed. In obese mice, I also observed that GABA related genes such as GABBR1, glutamate decarboxylase 1 (GAD1), glutamate decarboxylase 2 (GAD2), and GABA transaminase (GABA-T) were differentially expressed between EAT and IAT of DIO mice (Figure 42C). Since GAD1 is a rate-limiting enzyme synthesizing GABA (Roberts and Frankel, 1950), a functional difference of GABAergic responses between EAT and IAT was tested by measurement of GABA concentrations. As shown in Figure 43A, the level of GABA was significantly higher in IAT of DIO mice. Consistently, GABA concentration was still higher in IAT of genetically obese mice (Figure 43B). Furthermore, I found that the level of circulating GABA was reduced in DIO mice (Table 2). These data proposed the idea that dissimilar patterns of GABAergic actions between obese IAT and EAT might be involved in fat-depot specific ATM infiltration in obesity. To test whether GABA stimulation would influence fat-depot specific ATM infiltrations, each of adipose tissue was stimulated by GABA and measured monocyte chemotaxis (Figure 44A). As shown in Figure 44B, the number of migrated monocytes was significantly reduced in IAT. However, such effect was not observed in EAT. These results indicate that GABA responses in IAT might contribute to fat-depot selective ATM infiltration in obesity.

GABA dependent regulation of ATM infiltration is associated with $GABA_B$ receptor signaling in IAT.

Since GABAergic response to ATM infiltration appeared to be differentially

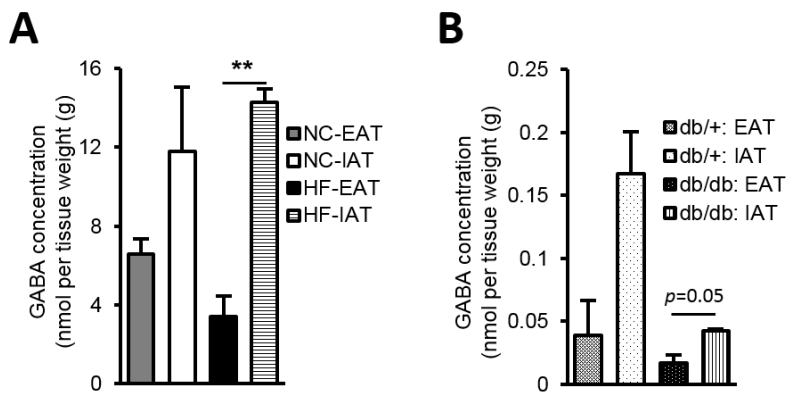

Figure 43

GABA concentration in adipose tissues. Fat-depot specific GABA concentration of (A) DIO and (B) *db/db* mice.

Table 2. A list of serum metabolites significantly changed in HF fed mice

No.	Compound Name	KEGG ID	Relative Folds of Inductions (Average ± standard error, Log_2 scale, N=3)		P-value Student's t-test (NH vs Ab-NH)
			ND	HD	
1	10-Hydroxydecanoic acid	C02774	-1.301	0.735±0.179063	0.00765
2	2-Aminobutyric acid	C02261,C02356	-1.102±0.342555	0.909±0.103344	0.020523
3	2-Hydroxybutyric acid	C05984	-1.074±0.246211	0.511±0.062588	0.018239
4	2-Oxobutyric acid	C00109	-1.277	0.339±0.096665	0.00356
5	2-Oxoglutaric acid	C00026	1.241±0.308649	-0.635±0.222267	0.010018
6	3-Hydroxy-3-methylglutaric acid	C03761	-1.304	0.731±0.143139	0.004911
7	3-Indoxylsulfuric acid	No ID	1.233±0.248622	-0.400±0.19012	0.007716
8	3-Ureidopropionic acid	C02642	-1.255	0.642±0.177242	0.008615
9	4-Methyl-2-oxovaleric acid 3-Methyl-2-oxovaleric acid	C00233 C00671,C03465	-1.168±0.054497	0.537±0.111277	0.000976
10	5-Aminovaleric acid	C00431	1.281±0.321594	-0.640	0.026904
11	Arg	C00062,C00792	1.073±0.507148	-0.367±0.201478	0.089629
12	Asn	C00152,C01905,C16438	-0.951±0.477486	1.066±0.055302	0.050031
13	Carboxymethyllysine	No ID	1.315±0.191113	-0.657	0.009258
14	Cholic acid	C00695	1.240±0.425	-0.620	0.048517
15	Creatine	C00300	1.166±0.451162	-0.500±0.132408	0.056357
16	Cystine	C00491,C01420	-1.106±0.500199	0.758±0.225108	0.047695
17	GABA	C00334	1.320±0.165462	-0.660	0.006915
18	Hippuric acid	C01586	1.311	-0.588±0.135389	0.000715
19	Imidazolelactic acid	C05568	-1.029±0.143103	0.517±0.114921	0.001327
20	Myristoleic acid	C08322	1.254±0.384909	-0.653±0.039178	0.037227
21	N^1-Methyl-4-pyridone-5-	C05843	-1.005±0.215923	0.779±0.406116	0.029496

	carboxamide				
22	N^5-Ethylglutamine	C01047	1.328±0.086448	-0.704±0.02503	0.000875
23	N^6-Methyllysine	C02728	1.137±0.396193	-0.725±0.285309	0.022517
24	*N*-Acetylalanine	No ID	-1.048±0.156148	0.869±0.284556	0.008803
25	*N*-Acetylleucine	C02710	1.245±0.350648	-0.546±0.170946	0.02089
26	*N*-Acetyllysine	C12989	1.326±0.118029	-0.663	0.003501
27	Nicotinamide	C00153	1.109±0.197933	-0.334±0.096073	0.008064
28	Ophthalmic acid	No ID	1.244±0.414723	-0.622	0.045988
29	Perillic acid	C11924	-1.328	0687±0.044241	0.000482
30	Phenaceturic acid	C05598	-0.663	1.326±0.124414	0.003892
31	Phosphorylcholine	C00588	-1.164±0.120911	0.421±0.162235	0.001968
32	SDMA	No ID	-1.201±0.383463	0.800±0.197099	0.019046
33	*S*-Methylcysteine	No ID	-1.226±0.018734	0.703±0.259049	0.017151
34	Stachydrine	C10172	1.327±0.108758	-0.664	0.00297
35	Trigonelline	C01004	1.322±0.152799	-0.661	0.005888
36	Trimethylamine *N*-oxide	C01104	1.304±0.188833	-0.585±0.036175	0.008041
37	Trp	C00078,C00525,C00806	-1.005±0.303209	-0.585±0.036175	0.014791
38	Tyr	C00082,C01536,C06420	-0.831±0.314284	1.216±0.23614	0.007945
39	XA0027	-	1.250±0.260321	-0.782±0.032557	0.014889
40	β-Ala	C00099	1.227±0.332601	-0.473±0.151706	0.021858

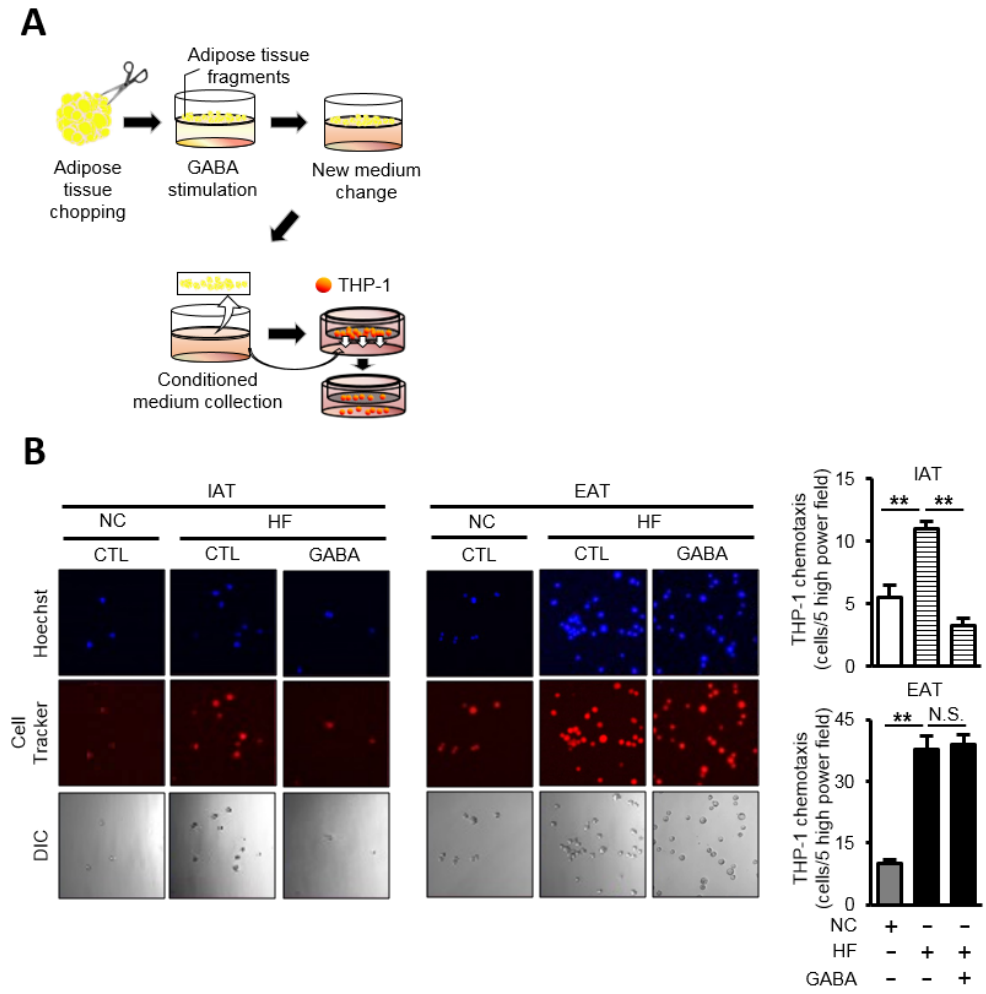

Figure 44

Monocyte chemotaxis by GABA stimulation in EAT and IAT. (A) An illustration of THP-1 chemotaxis upon GABA treatment. (B) Microscopic images of migrated cells in IAT (left) and EAT (middle). The quantification of chemotaxis of GABA stimulated IAT (upper right) and EAT (lower right).

regulated in IAT versus EAT, I examined the involvement of GABA responses in the regulation of fat-depot specific macrophage infiltration by selective modulation of $GABA_A$ and $GABA_B$ receptor signaling. Among GABA receptor modulating chemicals, baclofen (Bac) has been known to selectively activate $GABA_B$ receptor (Cook and Nathan, 1967; Drew et al., 1984). On the other hand, saclofen (Sac) and CGP35348 (CGP) were developed as specific antagonists of $GABA_B$ receptors (Kerr et al., 1988; Olpe et al., 1990). As shown in Figure 45A, selective stimulation of $GABA_B$ receptor signaling by Bac treatment inhibited monocyte chemotaxis in conditioned media from IAT. Inversely, specific inhibition of $GABA_B$ responses by pre-treatment of $GABA_B$ receptor selective antagonists, Sac and CGP, elevated the capacity of monocyte migration in conditioned media of IAT (Figure 45B). However, these $GABA_B$ signaling effects were not observed in EAT (Figure 45C and 45D). As GABA binds to $GABA_A$ receptor as well as $GABA_B$ receptor, I have further tested whether $GABA_A$ receptor selective blockage by bicuculline methiodide (Bicu) would affect monocyte migration. In contrast to $GABA_B$ responses in IAT, neither IAT nor EAT did not alter the capacity of monocyte recruitment by $GABA_A$ receptor signaling antagonism (Figure 46). To verify fat-depot specific $GABA_B$ signaling effects *in vivo*, the recipient mice were either intraperitoneally injected GABA or Sac prior to intravenous injection of Ds-Red^+ MNCs (Figure 47A). As shown in Figure 47B and 47C, I observed selective suppression of ATM and M1 ATM infiltration in IAT by GABA stimulation. Simultaneously, inhibition of $GABA_B$ receptor with Sac augmented ATM and M1 ATM infiltration of IAT even in the presence of GABA. Together, these data indicate that $GABA_B$ signaling of IAT would contribute to fat-

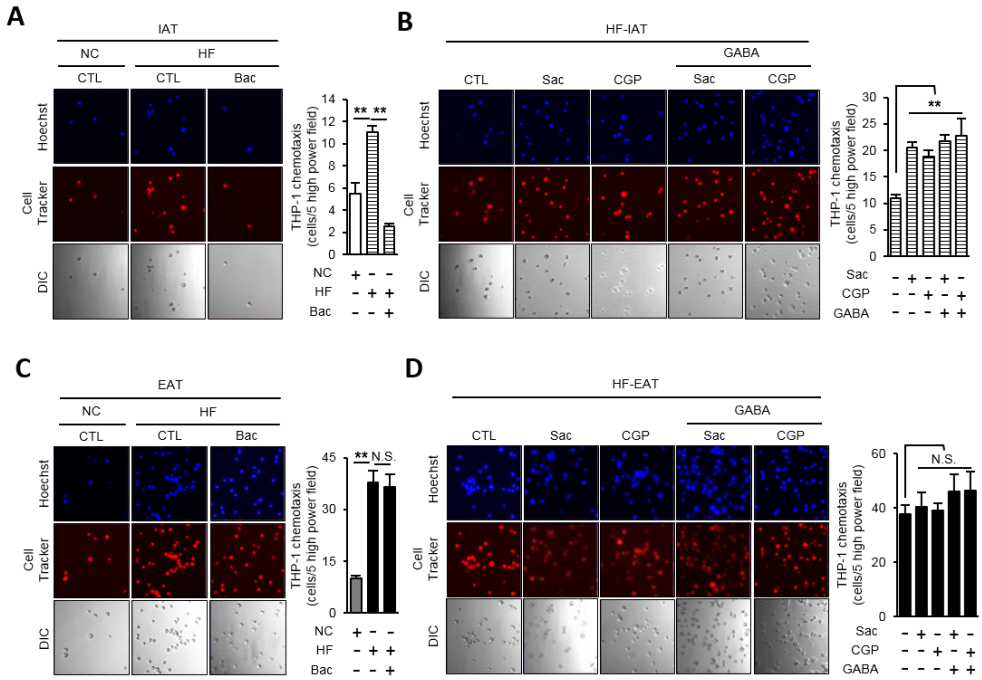

Figure 45

Selective regulation of monocyte chemotaxis in IAT by modulation of $GABA_B$ signaling. The effect of either activation of $GABA_B$ signaling via (A and C) Bac treatment or inhibition of $GABA_B$ signaling using (B and D) Sac and CGP on THP-1 monocyte chemotaxis. The adipose-derived conditioned media were individually collected from IAT (A and B) and EAT (C and D).

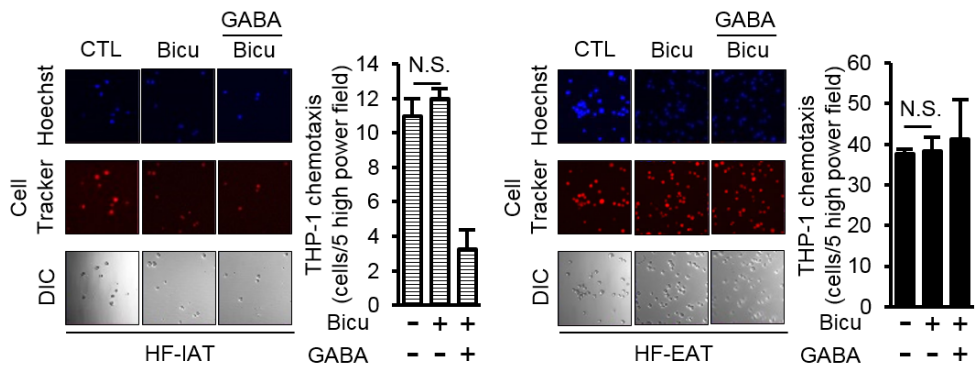

Figure 46

$GABA_A$ antagonism does not affect monocyte chemotaxis in adipose tissue. The effect of inhibition of $GABA_A$ signaling using Bicu on THP-1 migration. The adipose-derived conditioned media were individually collected from IAT and EAT.

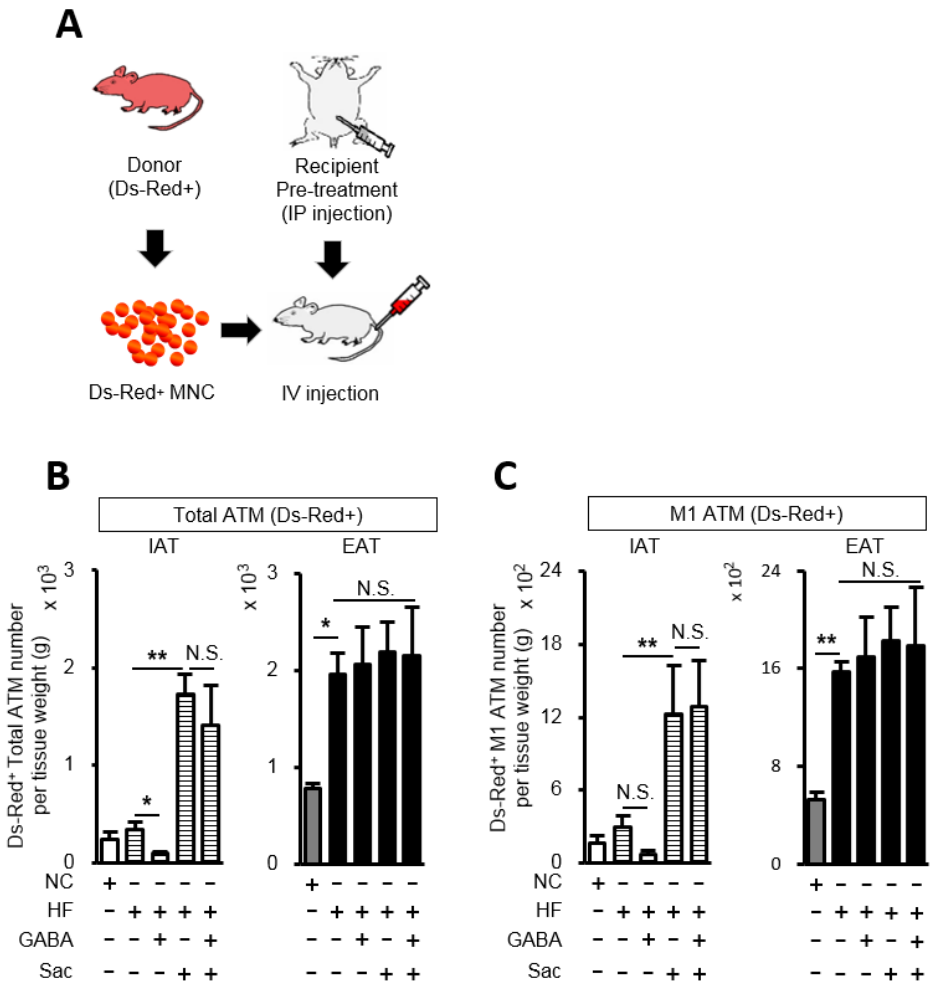

Figure 47

The effect of $GABA_B$ response on *in vivo* exogenous ATM infiltration in IAT versus EAT. (A) An experimental scheme of *in vivo* ATM migration of $GABA_B$ signaling modulated DIO mice. Vehicle, GABA, and Sac were intraperitoneally injected twice prior to intravenous injection of Ds-Red|+ MNCs. These mice were sacrificed after 12 h of chemical injection. (B) ATM and (C) M1 ATM infiltration into IAT (left) and EAT (right) in response to alteration of $GABA_B$ signaling

depot selective ATM infiltration in obesity.

In obesity, GABA response in IAT is involved in adipose tissue inflammation.

Since ATM infiltration is closely linked with pro-inflammatory responses in obesity (Turner et al., 2014), I have asked whether $GABA_B$ signaling in IAT would suppress inflammatory responses in obesity. As shown in Figure 48A, mRNA levels of pro-inflammatory cytokine genes were reduced by GABA treatment in IAT. Conversely, the mRNA levels of anti-inflammatory genes such as ARG I, and IL10 showed a reverse correlation by Sac (Figure 48B). In accordance with inflammatory gene expression profiles upon GABA signaling modulation, the level of JNK and p38 phosphorylation was increased by inhibition of $GABA_B$ receptor in IAT (Figure 49). These results imply that IAT selective GABA response would play key roles in the regulation of adipose tissue inflammation as well as monocyte recruitment.

GABA treatment improves glucose metabolism via reduced inflammatory responses in IAT

Since accumulated reports have suggested that inflammatory macrophage infiltration is strongly associated with insulin resistance (Kirk et al., 2008; Lumeng et al., 2007a; Patsouris et al., 2008), I asked the question whether prolonged modulation of GABA signaling might affect glucose metabolism in DIO. Two-week daily administration of GABA or Sac in DIO mice did not alter body weights and fat

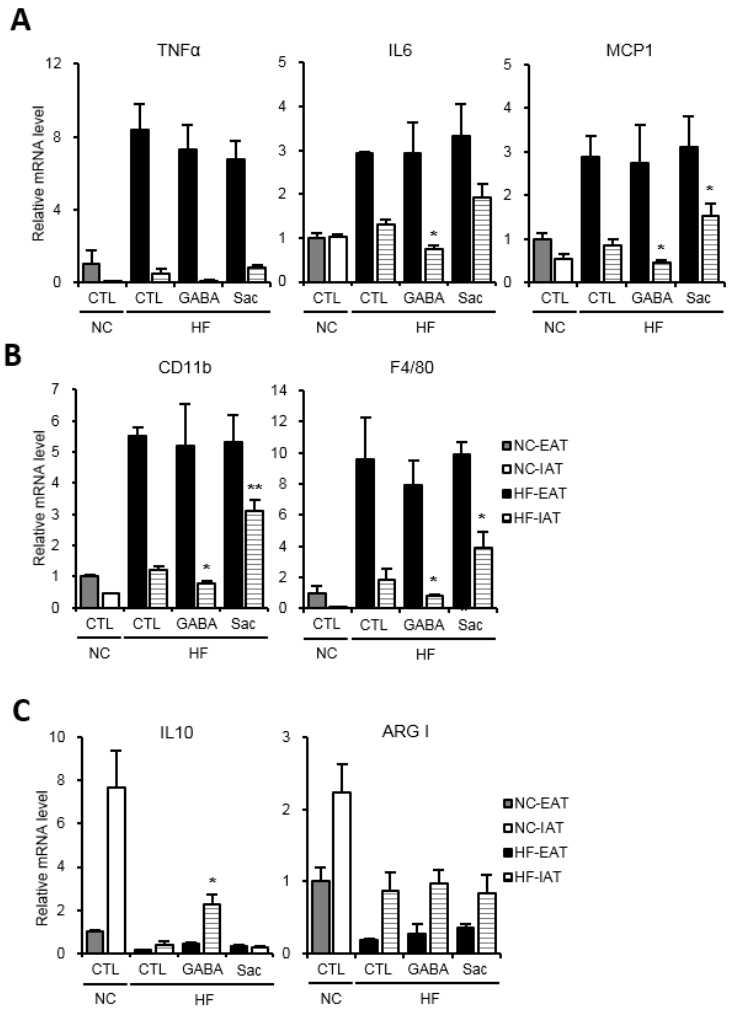

Figure 48

The effect of $GABA_B$ response on the gene expressions of adipose tissue inflammatory response. Relative mRNA levels in EAT and IAT were measured by modulation of GABA signaling. (A) Relative mRNA level of pro-inflammatory cytokine expressions such as TNFα, IL6, and MCP1. (B) Relative mRNA level of CD11b and F4/80. (C) anti-inflammatory genes such as IL10 and ARG I were measured by quantitative real time-PCR.

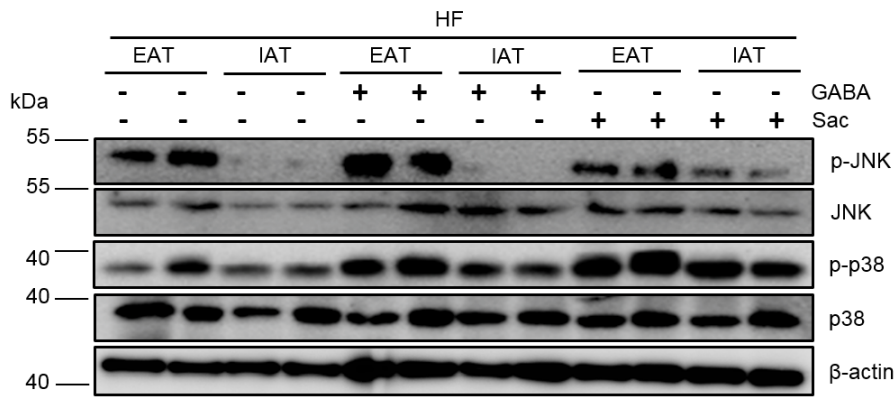

Figure 49

The effect of $GABA_B$ response on adipose tissue inflammatory signaling. Western blot images of inflammatory signaling. p-JNK and p-p38 were measured in EAT and IAT upon modulation of GABA. Total JNK, total p38, and β-actin were used as controls.

mass (Figure 50A and 50B). However, the levels of blood glucose were modulated within 3 days of GABA administration (Figure 50C). More importantly, GABA treated DIO mice improved glucose tolerances whereas inhibition of $GABA_B$ receptor with Sac slightly but significantly aggravated glucose tolerance (Figure 50D). In IAT, I found that adipose tissue inflammation was selectively altered upon GABA signaling agonist or antagonist (Figure 51). To examine whether the effects of GABA on glucose metabolism might be associated with improved insulin resistance, I performed glucose uptake by using of fluorescent glucose bioprobe (GB-Cy3), and radio-labeled 2-deoxyglucose in EAT and IAT. As shown in Figure 52, the level of insulin dependent glucose uptakes in IAT was significantly enhanced by GABA stimulation (Figure 52A and 52C) while such effects were not observed in EAT (Figure 52B and 52D). These data propose that GABA dependent mitigation of macrophage recruitment in IAT would contribute to amelioration of glucose metabolism in obesity.

In IAT, GABA stimulated ADSCs contribute to suppression of ATM infiltration

To confirm whether SVCs would respond to GABA than adipocytes in IAT, fractionated adipocytes and SVCs from EAT and IAT were tested for monocyte migration (Figure 53A). The degree of monocyte migration in conditioned media of SVC was significantly reduced in IAT (Figure 53B). On the other hand, the number of migrated cells was not reduced in adipocytes group (Figure 53C). These data led me further investigate which cell type(s) in SVC would participate in the reduction

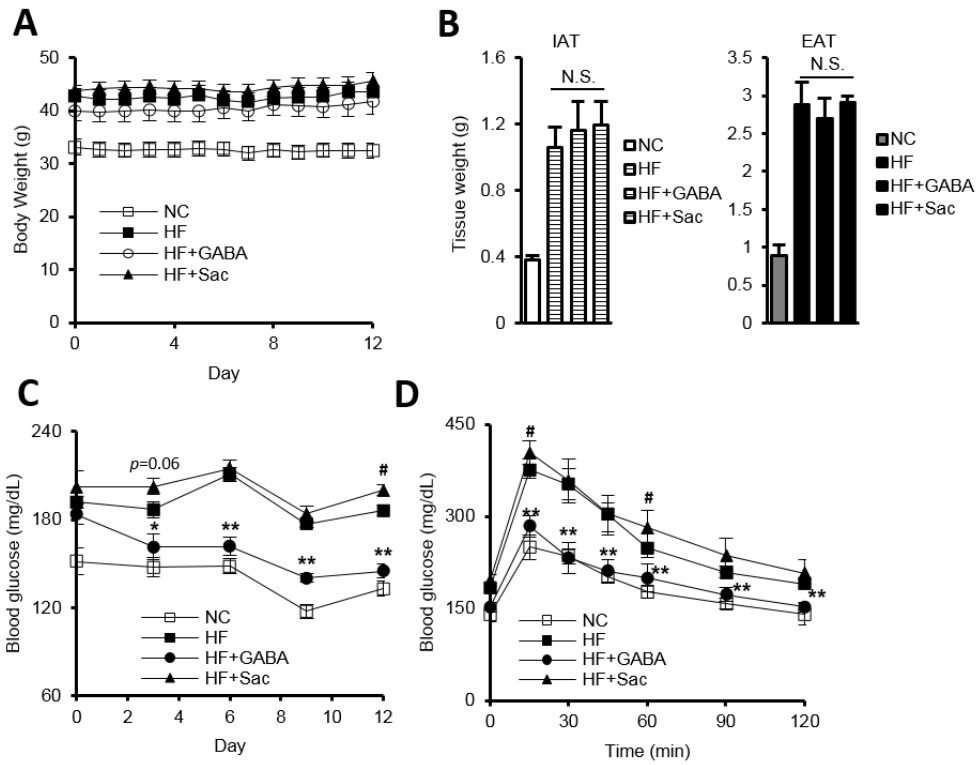

Figure 50

The prolonged effects of GABA signaling on obesity and glucose metabolism. GABA and Sac were daily injected into DIO mice. (A) Body weights and (B) adipose tissue weight of GABA and Sac treated DIO mice. (C) Blood glucose was measured in every 3 days during the experimental period. (D) At the 7 days of GABA and Sac treatment, mice were given an intraperitoneal glucose tolerance test.

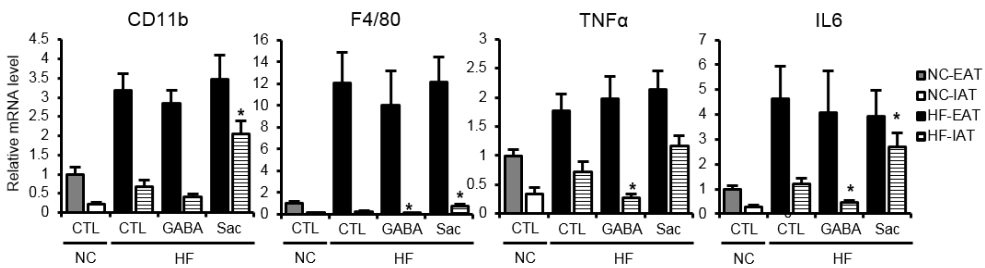

Figure 51

The prolonged effects of GABA signaling on adipose tissue inflammation. Relative mRNA levels of ATM markers (CD11b and F4/80) and inflammatory cytokines (TNFα and IL6) in EAT and IAT upon GABA treatment for 2 weeks.

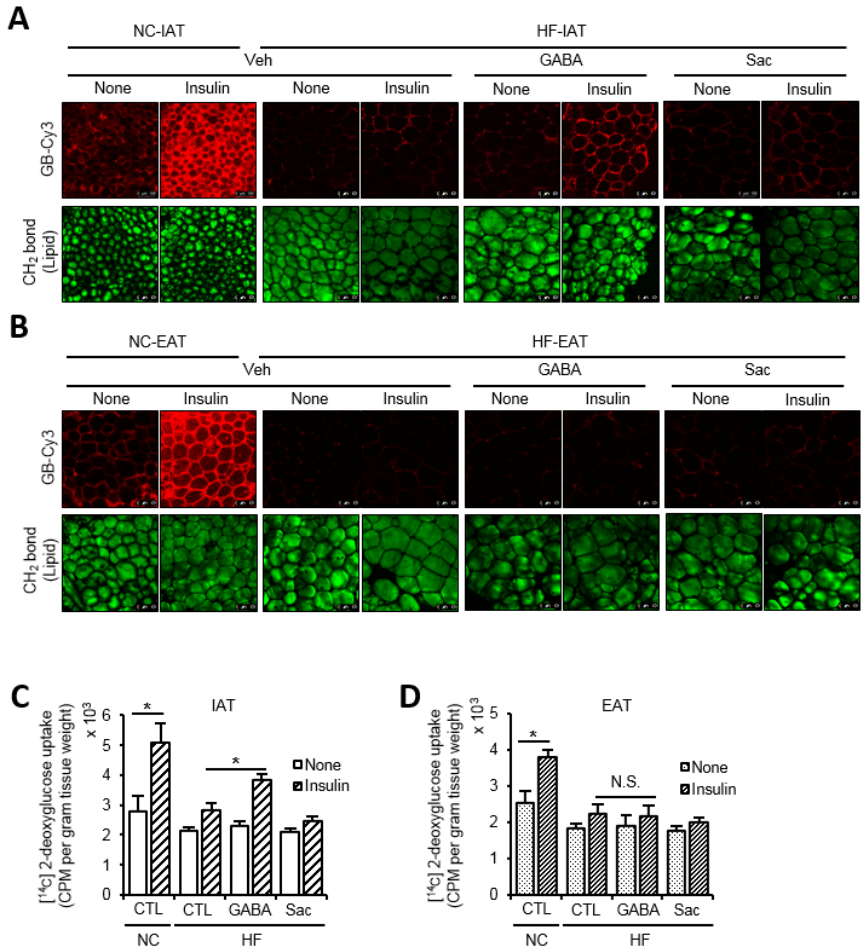

Figure 52

Fat-depot specific amelioration of insulin resistance by modulation of GABA signaling. At the end of experimental period, EAT and IAT were isolated and stimulated with insulin. Glucose uptakes in (A) IAT and (B) EAT were visualized by glucose bioprobe (GB-Cy3; Red). Adipose tissue lipid droplets (Green) were envisioned by CARS microscopy. (F) Measurement of insulin dependent 2-^{14}C deoxyglucose (2-[^{14}C]DG) uptake in (C) IAT and (D) EAT upon modulation of GABA signaling.

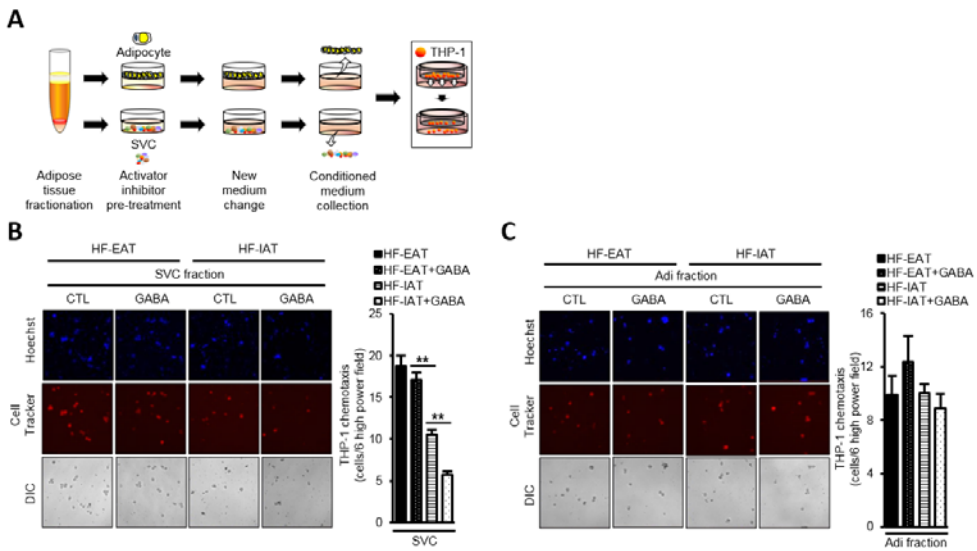

Figure 53

Monocytes chemotaxis of adipocytes and SVCs of EAT and IAT upon modulation of GABA responses. (A) An experimental strategy of THP-1 chemotaxis in adipocyte and SVC upon GABA. Measurement of monocyte migration in (B) SVCs and (C) adipocytes of EAT and IAT. Quantification of the number of cells is indicated in the right panel of each figure.

of THP-1 migration. Intriguingly, I found that $CD31^-$, $CD34^+$, and $Sca\text{-}1^+$ ADSCs expressed high levels of GABBR1 and other GABA related genes (Figure 54A). Among those genes, the mRNA level of GABBR1 was significantly greater in IAT derived ADSCs than EAT derived ADSCs (Figure 54A). Since IAT derived SVCs are more likely to differentiate into adipocytes than EAT derived SVCs (Joe et al., 2009), the number of ADSCs between two fat-depots was measured. Consistent with the previous report (Joe et al., 2009), IAT had more $CD31^-$, $CD34^+$, and $Sca\text{-}1^+$ ADSCs than EAT (Figure 54B). These findings led me to investigate whether IAT derived ADSCs would respond to GABA and suppress monocyte migration. As shown in Figure 54C, IAT derived ADSCs were likely to repress monocyte chemotaxis upon GABAB receptor signaling agonism. Meanwhile, treatment to IAT derived ADSCs elevate the number of migrated monocytes. However, EAT originated ADSCs did not exhibit any difference in monocyte migration in the presence of GABA agonist or antagonist. (Figure 54D). Due to the high level of GABBR1 in adipose-derived $CD4^+$ T cells, I estimated the level of monocyte migration by using conditioned media from these cells with GABA stimulation. However, conditioned media of GABA activated CD4+ T cells did not alter the level of monocyte chemotaxis (Figure 54E). Therefore, these data imply that ADSCs might contribute to fat-depot specific difference in ATM infiltration and inflammatory responses in obesity.

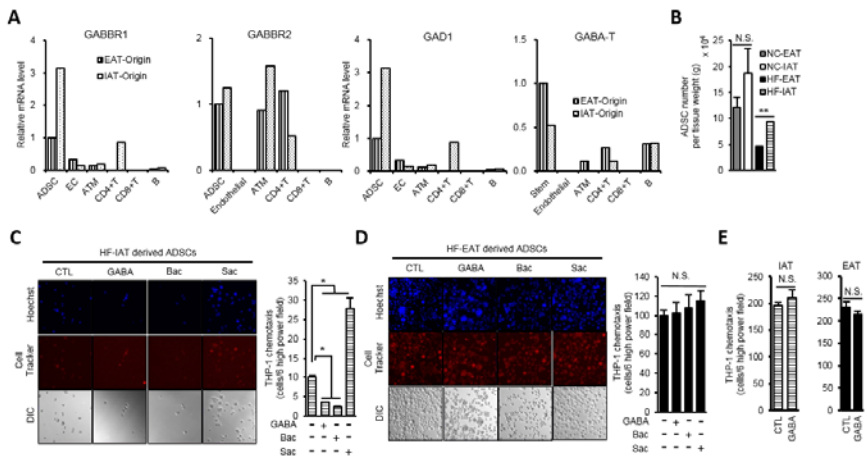

Figure 54

Identification of ADSCs as GABA responsive cell. (A) Relative mRNA levels of GABBR1, GABBR2, and GAD1 in SVC comprising cells such as ADSCs, endothelial cells (EC; $CD31^+$), ATM, $CD4^+$ T cells ($CD3^+$, $CD8^-$, and $CD4^+$), $CD8^+$ T cells ($CD3^+$, $CD4^+$, and $CD8^+$), and B cells ($CD3^-$ and $B220^+$). Each cell group was pooled from six individual mice. (B) Flow cytometry of ADSC in adipose tissues. Total ADSC numbers are counted and calibrated by gram fat mass in each fat-depots of NC and HF fed mice. (C and D) Measurement of THP-1 chemotaxis in the conditioned media of ADSCs by modulation of GABA signaling. In DIO mice, Each of IAT (C) and EAT (D) derived ADSC was pre-treated with GABA, Bac and Sac for the conditioned media prior to loading of THP-1 cells to trans-wells. Representative images are exhibited (left), and quantifications are indicated (right) of each figure. (E) Measurement of chemotactic activity by $CD4^+$ T cells upon GABA treatment. Mean values with $*p < 0.05$ and $**p < 0.01$ were considered significant. N.S., not significant.

DISCUSSION

Epidemiological and clinical approaches have reported that visceral and subcutaneous fat tissues are differentially associated with metabolic disorders (Alfadda et al., 2012; Kovacova et al., 2012). Accumulated evidence has shown that visceral adipose tissues are prone to be pro-inflammatory in obesity (Cartier et al., 2008; Miller et al., 2011; Qiang et al., 2016). For instance, the level of TNFα and IL6 in plasma is positively correlated with visceral adiposity in human (Cartier et al., 2008). Recently, it has been reported that visceral adipose tissue appears to regulate pro-inflammatory responses via TRIP-Br2 (Qiang et al., 2016). On the other hand, the findings from fat tissue transplantation have suggested that subcutaneous adipose tissue would play crucial roles against metabolic complications unlike visceral fat tissues (Foster et al., 2013; Tran et al., 2008). These findings led me to investigate the underlying mechanisms of subcutaneous adipose tissues in the regulation of energy metabolism. In this study, I have observed different effects of subcutaneous adipose tissue versus visceral adipose tissue on the regulation of macrophage infiltration and inflammatory responses via fat-depot selective GABA responses. Consistent with previous reports, I have shown that IAT recruited less macrophage infiltration than EAT. In obesity, the fat-depot specific ATM numbers were due to ATM infiltration rather than proliferation or apoptosis of resident ATMs Here, I have tried to elucidate cellular origins or populations that would mediate less fat-depot selective macrophage infiltration, particularly in obese IAT. Current transplantation

approaches indicated that fat tissue environmental factors would not be crucial factor to confer different degrees of macrophage infiltration at EAT and IAT. Rather, obesity induced fat-depot specific ATM infiltration would be due to the intrinsic characteristics of selective fat-depot composing specific cell populations. Although it has been demonstrated that IAT transplantation improves metabolic parameters in recipients, ATM infiltration in recipient fat tissues was not largely affected by transplanted fat depots. Since metabolic parameters were not observed in transplanted IAT, it remains to be investigated the potential mechanisms of donor IAT in the regulation of recipient metabolic abnormalities.

GABA is one of the principal neurotransmitters in central nervous system (Roberts and Frankel, 1950). This inhibitory neurotransmitter is essential in normal brain functions such as information processing, neuronal plasticity, and activity (Magnaghi et al., 2008; Schuler et al., 2001). GABA transmits the neuronal signaling via GABA receptors, $GABA_A$ receptor and $GABA_B$ receptor. $GABA_A$ receptor is a chloride ion channel composed of 19 subunits (Macdonald and Olsen, 1994). On the other hand, $GABA_B$ receptor, a member of G-protein coupled receptor, controls post-synaptic neurons via regulation of various kinase activities (Kerr and Ong, 1995). In pathophysiological conditions, GABAergic medications targeting GABA receptors have been utilized to treat psychological disorders such as nervous anxiety, alcohol withdrawal, and epilepsy (Bowery et al., 2002; Cryan and Kaupmann, 2005). In contrast to its well-known functions in brain, the roles of GABA in peripheral tissues has been recently reported (Ben-Othman et al., 2017; Bhat et al., 2010; Soltani et al., 2011; Xie et al., 2014). For example, GABA stimulation reduces inflammatory

response and oxidative stress in immune cells (Bhat et al., 2010; Xie et al., 2014). In pancreas, GABA has been associated with proliferation of β-cells on type 1 diabetes (Ben-Othman et al., 2017; Soltani et al., 2011). In this study, I have demonstrated that fat-depot selective GABA sensitivity would be involved in the suppression of ATM infiltration in IAT. By analyses of transcriptomes between EAT- and IAT-derived adipocytes and SVCs, I noticed that GABAergic signaling and its downstream cascades might be distinct in IAT and EAT. In obese IAT, pharmacological stimulation or inhibition of $GABA_B$ receptors reduced or aggravated, respectively, macrophage infiltration. Moreover, insulin dependent glucose uptake capacity was enhanced in IAT of GABA stimulated DIO mice. These data revealed that fat-depot selective GABA responses, at least in part, would contribute to improvement of whole body glucose metabolism and insulin resistance associated with reduced pro-inflammatory response in IAT. Recently, it has been reported that oral administration of GABA improves whole body glucose metabolism and ATM accumulation in visceral adipose tissue, associated with decreased body weight gains (Tian et al., 2011). Although this study exhibits similar results of GABA effects on the energy metabolism, the response of GABA in visceral fat tissue seems to conflict with my results. There are several possibilities to explain this discrepancy. Firstly, Tian et al., orally administered GABA from the beginning of HF feeding whereas I used intraperitoneal injections of GABA to mice after long-term HF feeding. Secondly, because GABBR1 expressions between EAT and IAT were comparable in NC and early DIO (data not shown), I have speculated that fat-depot specific GABA responses might be developed in the progression of obesity. In

this regard, precise role of GABA in the regulation of energy metabolism has to be elucidated in further study.

Recently, it has been reported that ADSCs are able to secrete GABA (Urrutia et al., 2016), which is consistent with my observation in adipose tissue level. Although high level of GABA is present in brain, it appears that low level of circulating GABA and fat tissue producing GABA might influence fat-depot selective macrophage recruitment in obesity. Since direct effects of GABA on macrophage recruitment were not observed, it needs to be investigated by which GABA sensitive IAT could reduce macrophage recruitment in obese IAT.

Mesenchymal stem cells (MSCs) have multipotency to differentiate into osteoblasts, myocytes, and adipocytes with self-proliferative activity (Friedenstein et al., 1974). MSCs also contribute to maintenance and wound healing in several tissues such as bone, muscle, and adipose tissue (Campagnoli et al., 2001; Im et al., 2005). Moreover, MSCs have been subjected to investigate inflammatory responses in addition to their pluripotency (Bernardo and Fibbe, 2013). ADSCs are known to be quite similar with mesenchymal stem cells with marker gene expressions including Sca-1, CD73, CD90, and CD105 (Banas et al., 2007). Among the other cell types comprising SVCs, I found that ADSCs abundantly expressed GABBR1 and GABAergic gene expressions. In particular, the mRNA levels of GABBR1 were significantly higher in ADSCs from IAT than ADSCs from EAT. Several lines of evidence support the idea that fat-depot specific characteristics of ADSCs would be different in subcutaneous and visceral adipose tissues. Firstly, early onset of obesity

is associated with rapid proliferation of ADSCs in EAT (Jeffery et al., 2015). Secondly, IAT has a higher potency of adipogenesis than EAT (Joe et al., 2009). Lastly, Wilms' tumor 1, an important transcription factor for development, is specifically expressed in SVCs of EAT (Chau et al., 2014). In addition to the previous findings, I found a novel function of depot-specific ADSCs to suppress macrophage recruitment associated with GABA stimulation in IAT. Although the molecular mechanisms to suppress macrophage recruitments in ADSCs from IAT are not yet elucidated, I would like to propose that potential pathways might be eligible to explain GABA signaling in ADSCs from IAT. For instance, it has been shown that GABA binding to $GABA_B$ receptors activates Gαi/o subunit in neuronal synapse. In turn, Gαi/o inhibits adenylyl cyclase to repress PKA phosphorylation (Gassmann and Bettler, 2012). In parallel, $GABA_B$ receptors are able to modulate Akt/PKB and PKC signaling (Tu et al., 2010; Zhang et al., 2015). Here, I discovered that IAT derived ADSCs could inhibit macrophage recruitment and inflammation in response to GABA signals. However, it remains to be investigated downstream signaling of $GABA_B$ receptor in ADSCs derived from IAT due to their signaling complexity.

Together, I demonstrate that adipose tissue macrophage recruitment would be differentially regulated by GABA responses in IAT. Moreover, ADSCs from IAT inhibited macrophage infiltration in response to GABA stimulation in DIO. Thus, these findings may provide an insight into the understanding of fat-depot specific roles on the metabolic control via regulation of macrophage infiltration and inflammatory responses in obesity.

CONCLUSION AND PERSPECTIVES

Insulin resistance is an important risk factor for metabolic diseases such as hyperlipidemia, hyper tension, type 2 diabetes, certain cancers, and cardiovascular diseases. Since obesity and insulin resistance are tightly associated, enormous efforts have been made to elucidate underlying mechanisms the two phenomena. Among several causal factors of insulin resistance, gut microbiota and adipose tissue inflammation have been raised as key factors. Nonetheless, the precise roles of gut microbiota and fat-depot specific contribution in the regulation of insulin resistance have not been thoroughly understood. In the first chapter, I have developed a mouse model of gut microbiota alteration to elucidate how Firmicutes and Bacteroidetes could affect glucose metabolism. In the second chapter, I have demonstrated out that fat-depot specific ATM infiltration and inflammatory responses would be resulted from GABA sensitivity in subcutaneous ADSCs. Together, these results provide new insights to understand novel mechanisms how insulin resistance could be modulated in obesity.

1. Gut microbiota and obesity-induced insulin resistance

Compelling evidences demonstrate that Firmicutes and Bacteroidetes, two major phyla are correlated with host energy metabolism in obesity (Ley et al., 2005b). To understand potential roles of those two major phyla in the regulation of energy

metabolism, a mouse model that depletion in Firmicutes and Bacteroidetes is required. Thus, I established a mouse model of gut microbiota alteration with V and B in drinking water to alter gut microbiota. Although many studies have shown that GF and pharmacological gut microbiota depletion are associated with reduced body weight gain in obesity, V + B treated DIO mice did not change body weight gains upon HF. Meanwhile, glucose metabolism and insulin resistance were significantly improved in Firmicutes and Bacteroidetes depleted DIO mice. Furthermore, I discovered that a novel mediator between commensal bacteria and host insulin resistance. In serum and intestine, the level of gut hormone a gut hormone, GLP-1 was significantly augmented in Firmicutes and Bacteroidetes depleted DIO mice. Additionally, in DIO, depletion of Firmicutes and Bacteroidetes increased TCA, which led to stimulate GLP-1. Although I have not been able to find the specific intestinal microbial species involved in the regulation of TCA synthesis in gut, it is plausible to propose a novel mechanism by which certain intestinal microbial groups might contribute to the regulation of host energy metabolism in DIO (Figure 55).

Previously, it has been reported that GF mice and gut microbiota depleted mice alleviate insulin resistance as well as inflammatory response (Cani et al., 2008b; Murphy et al., 2013a). In this study, I demonstrated that there no significant changes in adipose tissue mass, body weight gains, and inflammatory responses between NH and Ab-NH groups. Also, I could not observe any improvement of gut leakage which has been a crucial phenomenon of mitigation of endotoxemia and inflammation in obesity (Cani et al., 2007). Although combination of V and B significantly reduced

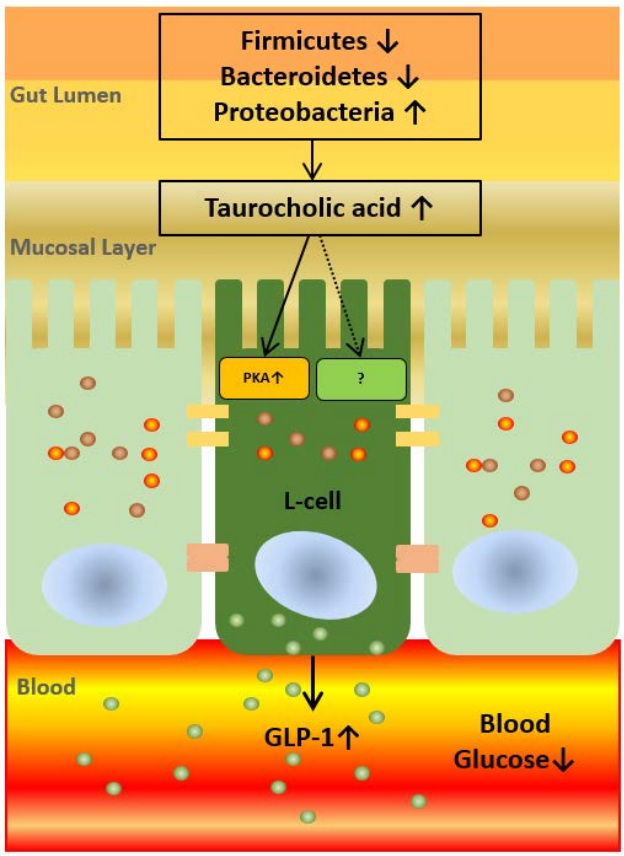

Figure 55

A schematic model in the regulation of glucose metabolism by alteration of gut microbiota. Reductions in Firmicutes and Bacteroidetes enhance bile component, TCA, which activates L-cells in distal gut via PKA dependent and independent manner. TCA stimulated L-cells increase synthesis and secretion of GLP-1 to ameliorate glucose metabolism in DIO mice.

total abundance of gut microbiota, I could not exclude the possibility that considerable amounts of other gut microorganisms might be present in my gut microbiota altered mouse model. Thus, it is feasible that other gut microbial populations might be involved in the control of gut barrier integrity.

Previously, patients with type 2 diabetes are relatively enriched with Gram-negative bacteria which belong to Bacteroidetes and Proteobacteria phyla (Larsen et al., 2010; Suez et al., 2014). Additionally, such increases in gut microbiota are associated with endotoxemia via enhanced plasma LPS leading to oxidative stress and inflammation in host (Cani et al., 2007). In particular, gastrointestinal integrity appears to aggravate host inflammatory response via dysbiosis of gut microbiota (Bode and Bode, 2005). Although there was a significant elevation in abundance of Proteobacteria interlocking to reduction of Firmicutes and Bacteroidetes, the effects of such alteration in gut microbiota would be limited to obesity-mediated gut leakage and endotoxemia. To identify which gut microbial populations might be involved in the regulation of host gut barrier integrity, it is necessary to develop various mouse models of selective depletion of individual gut microbial species or phylum.

It has been shown that prebiotics stimulate GLP-1 secretion, and gut microbiota acts as a mediator by fermenting the prebiotics into short chain fatty acids to induce GLP-1 (Cani et al., 2009; Musso et al., 2010; Tolhurst et al., 2012). In this study, Ab-NH group augmented gut metabolites including creatine, sulfotyrosine, and TCA, which stimulate secretion of GLP-1 in human L-cell line. Thus, I suggest that an increase in TCA would be a crucial factor in elucidating improved glucose

metabolism in host. In addition to TCA, other gut metabolites have been reported that certain metabolite would be beneficial for host energy homeostasis. For instance, sulfotyrosine represses protein tyrosine phosphatase 1B (Desmarais et al., 1998). Since insulin receptor belongs to receptor tyrosine kinase, sulfotyrosine might contribute to insulin signaling. Furthermore, creatine is linked to increased GLUT4 expression in muscle and thermogenesis in beige adipocytes ('t Eijnde et al., 2001; Kazak et al., 2015). As Firmicutes and Bacteroidetes were deeply associated with alteration of gut metabolites which could modulate GLP-1 in L-cells, I would like to propose underlying mechanisms how specific gut populations interact with hosts in the regulation of energy homeostasis. These findings would enhance our understandings of the interaction between commensal bacteria and host upon nutritional status.

2. Fat-depot specific inflammation and insulin resistance

The clinical description of obesity has been based on measurements, such as body fat mass, that estimate total body fat contents. Adipose tissues are anatomically and functionally divided into brown adipose tissues and WAT (Choe et al., 2016). Unlike brown adipose tissue, WAT is prone to store extra energy in the form of lipids. When adipose tissues are inflamed in obesity, the storage functions appeared to shift into the release of free fatty acids (Faty et al., 2012; Zhang et al., 1996). In addition to increased lipolysis in obesity, insulin resistance is further aggravated by adipose

tissue inflammation (Chawla et al., 2011; Ferrante, 2007). Accumulating evidence has revealed that not all of adipose tissues are alike and metabolic risks are deeply correlated with the anatomical location as well as whole body adiposity (Arner, 2005; Montague et al., 1998). The major anatomical white fat-depots are largely divided into visceral and subcutaneous adipose tissues and different fat-depots are distinct with respect to unique roles in metabolic regulation in addition to fat-storage function. In obesity, visceral adipose tissues are prone to be inflammatory than subcutaneous adipose tissues (Harman-Boehm et al., 2007). I have studied the distinct patterns of ATM accumulation between EAT and IAT in DIO and genetically obese mice. Although the degrees of ATM proliferation and apoptosis were significantly elevated in obese mice, $Ki67^+$ and Annexin V^+ ATM were similar between EAT and IAT. However, *in vivo* tracing of exogenous monocytes has revealed that Ds-Red^+ ATMs were increased in EAT, but not in IAT. Thus, these data prompted me to propose that fat-depot specific ATM accumulation might be due to the difference in the capacity of infiltration rather than ATM proliferation or apoptosis. Accordantly, in transplantation experiments I found that the number of ATM infiltration was higher in transplanted donor EAT than IAT regardless of recipient adipose loci. Therefore, it is plausible to speculate that intrinsic characteristics of adipose tissues would be important in the regulation of ATM infiltration than microenvironmental factors surrounding each fat-depot.

3. GABA responses in the regulation of immunity and energy

metabolism

In physiological process, GABA is well studied as an inhibitory neurotransmitter. Although many studies have revealed the roles of GABA in neuronal signaling, recent reports have shown that GABA signaling would play roles in peripheral organs such as the testes, gastrointestinal tract, ovaries, placenta, uterus and adrenal medulla (Gladkevich et al., 2006). Also, it has been shown that GABAergic genes such as GAD1, GAD2, GABA-T, GABA co-transporters, $GABA_A$ and $GABA_B$ receptor subunits are detected in various types of immune cells (Bhat et al., 2010; Crowley et al., 2015; Tian et al., 2004). Although underlying mechanisms are still unknown, most GABAergic stimulation in immune cells is converged to anti-inflammatory responses (Bhat et al., 2010; Crowley et al., 2015; Duthey et al., 2010; Soltani et al., 2011). With RNA-sequencing data, I proposed that 'GABAergic synapse' in KEGG pathway might be differentially regulated in EAT and IAT. In DIO, IAT reduced monocyte migration upon GABA stimuli whereas such effect was considerably diminished in EAT. Additionally, selective agonism and antagonism of GABA receptors exhibited that $GABA_B$ signaling would be considered as a crucial mediator for fat-depot specific ATM infiltration.

Among various SVC cells including ADSCs, ECs, ATMs, T and B lymphocytes, the level of GABAergic gene expressions were abundant in ADSCs whereas most other isolated cells comprising SVC did not express GABAergic genes. Further, ADSCs originated from IAT could selectively repress monocyte migration upon GABA signaling. Consequently, I would like to suggest a novel finding that fat-depot

specific ADSCs would be able to regulate immune responses as well as adipogenesis in fat tissues.

In conclusion, I suggest that alteration of gut microbiota and the roles of subcutaneous adipose tissue would be crucial factors to regulate obesity-induced insulin resistance together. The first chapter showed that Firmicutes and Bacteroidetes would provoke insulin resistance in obesity via a negative regulation of GLP-1. Alteration of gut microbiota with antibiotics is associated with complexed changes of metabolites in intestine. In obesity, a bile derivative, TCA would stimulate GLP-1 secretion which would mitigate insulin resistance. In the second chapter, I have elucidated a novel mechanisms how subcutaneous adipose tissues would be less inflammatory in obesity. In subcutaneous adipose tissue, selective $GABA_B$ signaling in ADSCs ameliorated ATM infiltration and inflammatory responses which are risk factors for insulin resistance in obesity. Therefore, I believe that this work would broaden our understanding of pathophysiological regulators in the control of glucose metabolism and insulin sensitivity in obesity.

REFERENCE

't Eijnde, B.O., Urso, B., Richter, E.A., Greenhaff, P.L., and Hespel, P. (2001). Effect of oral creatine supplementation on human muscle GLUT4 protein content after immobilization. Diabetes *50*, 18-23.

Alberti, K.G.M.M., Zimmet, P.Z., and Consultation, W. (1998). Definition, diagnosis and classification of diabetes mellitus and its complications part 1: Diagnosis and classification of diabetes mellitus - Provisional report of a WHO consultation. Diabetic Med *15*, 539-553.

Alfadda, A.A., Sallam, R.M., Chishti, M.A., Moustafa, A.S., Fatma, S., Alomaim, W.S., Al-Naami, M.Y., Bassas, A.F., Chrousos, G.P., and Jo, H. (2012). Differential patterns of serum concentration and adipose tissue expression of chemerin in obesity: Adipose depot specificity and gender dimorphism. Mol Cells *33*, 591-596.

Amano, S.U., Cohen, J.L., Vangala, P., Tencerova, M., Nicoloro, S.M., Yawe, J.C., Shen, Y.F., Czech, M.P., and Aouadi, M. (2014). Local Proliferation of Macrophages Contributes to Obesity-Associated Adipose Tissue Inflammation. Cell Metab *19*, 162-171.

Arner, P. (2005). Human fat cell lipolysis: Biochemistry, regulation and clinical role. Best Pract Res Cl En *19*, 471-482.

Arumugam, M., Raes, J., Pelletier, E., Le Paslier, D., Yamada, T., Mende, D.R., Fernandes, G.R., Tap, J., Bruls, T., Batto, J.M., *et al.* (2011). Enterotypes of the human gut microbiome. Nature *473*, 174-180.

Asterholm, I.W., Tao, C., Morley, T.S., Wang, Q.A., Delgado-Lopez, F., Wang, Z.V., and Scherer, P.E. (2014). Adipocyte Inflammation Is Essential for Healthy Adipose Tissue Expansion and Remodeling. Cell Metab *20*, 103-118.

Austin, R.L., Rune, A., Bouzakri, K., Zierath, J.R., and Krook, A. (2008). SiRNA-mediated reduction of inhibitor of nuclear factor-kappa B kinase prevents tumor necrosis factor-alpha-induced insulin resistance in human skeletal muscle. Diabetes *57*, 2066-2073.

Backhed, F., Ding, H., Wang, T., Hooper, L.V., Koh, G.Y., Nagy, A., Semenkovich, C.F., and Gordon, J.I. (2004a). The gut microbiota as an environmental factor that regulates fat storage. P Natl Acad Sci USA *101*, 15718-15723.

Backhed, F., Ding, H., Wang, T., Hooper, L.V., Koh, G.Y., Nagy, A., Semenkovich, C.F., and Gordon, J.I. (2004b). The gut microbiota as an environmental factor that regulates fat storage. Proc Natl Acad Sci U S A *101*, 15718-15723.

Backhed, F., Manchester, J.K., Semenkovich, C.F., and Gordon, J.I. (2007). Mechanisms underlying the resistance to diet-induced obesity in germ-free mice. P Natl Acad Sci USA *104*, 979-984.

Bacon, A.E., McGrath, S., Fekety, R., and Holloway, W.J. (1991). In vitro synergy studies with Clostridium difficile. Antimicrob Agents Chemother *35*, 582-583.

Baeuerle, P.A., and Henkel, T. (1994). Function Amd Activation of Nf-Kappa-B in the Immune-System. Annu Rev Immunol *12*, 141-179.

Baggio, L.L., and Drucker, D.J. (2007). Biology of incretins: GLP-1 and GIP. Gastroenterology *132*, 2131-2157.

Banas, A., Teratani, T., Yamamoto, Y., Tokuhara, M., Takeshita, F., Quinn, G., Okochi, H., and Ochiya, T. (2007). Adipose tissue-derived mesenchymal stem cells as a source of human hepatocytes. Hepatology *46*, 219-228.

Becattini, S., Taur, Y., and Pamer, E.G. (2016). Antibiotic-Induced Changes in the Intestinal Microbiota and Disease. Trends Mol Med *22*, 458-478.

Ben-Othman, N., Vieira, A., Courtney, M., Record, F., Gjernes, E., Avolio, F., Hadzic,

B., Druelle, N., Napolitano, T., Navarro-Sanz, S., *et al.* (2017). Long-Term GABA Administration Induces Alpha Cell-Mediated Beta-like Cell Neogenesis. Cell *168*, 73-+.

Bernardo, M.E., and Fibbe, W.E. (2013). Mesenchymal Stromal Cells: Sensors and Switchers of Inflammation. Cell Stem Cell *13*, 392-402.

Bhat, R., Axtell, R., Mitra, A., Miranda, M., Lock, C., Tsien, R.W., and Steinman, L. (2010). Inhibitory role for GABA in autoimmune inflammation. P Natl Acad Sci USA *107*, 2580-2585.

Bode, C., and Bode, J.C. (2005). Activation of the innate immune system and alcoholic liver disease: Effects of ethanol per se or enhanced intestinal translocation of bacterial toxins induced by ethanol? Alcoholism-Clinical and Experimental Research *29*, 166s-171s.

Bode, J.G., Ehlting, C., and Haussinger, D. (2012). The macrophage response towards LPS and its control through the p38(MAPK)-STAT3 axis. Cell Signal *24*, 1185-1194.

Bowery, N.G., Bettler, B., Froestl, W., Gallagher, J.P., Marshall, F., Raiteri, M., Bonner, T.I., and Enna, S.J. (2002). International Union of Pharmacology. XXXIII. Mammalian gamma-aminobutyric acid(B) receptors: Structure and function. Pharmacol Rev *54*, 247-264.

Brubaker, P.L. (2006). The glucagon-like peptides: pleiotropic regulators of nutrient homeostasis. Ann N Y Acad Sci *1070*, 10-26.

Bu, D.F., Erlander, M.G., Hitz, B.C., Tillakaratne, N.J.K., Kaufman, D.L., Wagnermcpherson, C.B., Evans, G.A., and Tobin, A.J. (1992). 2 Human Glutamate Decarboxylases, 65-Kda Gad and 67-Kda Gad, Are Each Encoded by a Single Gene. P Natl Acad Sci USA *89*, 2115-2119.

Campagnoli, C., Roberts, I.A.G., Kumar, S., Bennett, P.R., Bellantuono, I., and Fisk, N.M. (2001). Identification of mesenchymal stem/progenitor cells in human first-trimester fetal blood, liver, and bone marrow. Blood *98*, 2396-2402.

Campbell, J.E., and Drucker, D.J. (2013a). Pharmacology, physiology, and mechanisms of incretin hormone action. Cell Metab *17*, 819-837.

Campbell, J.E., and Drucker, D.J. (2013b). Pharmacology, Physiology, and Mechanisms of Incretin Hormone Action. Cell Metab *17*, 819-837.

Cani, P.D., Amar, J., Iglesias, M.A., Poggi, M., Knauf, C., Bastelica, D., Neyrinck, A.M., Fava, F., Tuohy, K.M., Chabo, C., *et al.* (2007). Metabolic endotoxemia initiates obesity and insulin resistance. Diabetes *56*, 1761-1772.

Cani, P.D., Bibiloni, R., Knauf, C., Neyrinck, A.M., Neyrinck, A.M., Delzenne, N.M., and Burcelin, R. (2008a). Changes in gut microbiota control metabolic endotoxemia-induced inflammation in high-fat diet-induced obesity and diabetes in mice. Diabetes *57*, 1470-1481.

Cani, P.D., Bibiloni, R., Knauf, C., Waget, A., Neyrinck, A.M., Delzenne, N.M., and Burcelin, R. (2008b). Changes in gut microbiota control metabolic endotoxemia-induced inflammation in high-fat diet-induced obesity and diabetes in mice. Diabetes *57*, 1470-1481.

Cani, P.D., Lecourt, E., Dewulf, E.M., Sohet, F.M., Pachikian, B.D., Naslain, D., De Backer, F., Neyrinck, A.M., and Delzenne, N.M. (2009). Gut microbiota fermentation of prebiotics increases satietogenic and incretin gut peptide production with consequences for appetite sensation and glucose response after a meal. Am J Clin Nutr *90*, 1236-1243.

Cartier, A., Lemieux, I., Almeras, N., Tremblay, A., Bergeron, J., and Despres, J.P. (2008). Visceral obesity and plasma glucose-insulin homeostasis: Contributions of interleukin-6 and tumor necrosis factor-alpha in men. J Clin Endocr Metab *93*, 1931-

1938.

Chau, Y.Y., Bandiera, R., Serrels, A., Martinez-Estrada, O.M., Qing, W., Lee, M., Slight, J., Thornburn, A., Berry, R., McHaffie, S., *et al.* (2014). Visceral and subcutaneous fat have different origins and evidence supports a mesothelial source. Nat Cell Biol *16*, 367-+.

Chawla, A., Nguyen, K.D., and Goh, Y.P.S. (2011). Macrophage-mediated inflammation in metabolic disease. Nat Rev Immunol *11*, 738-749.

Cho, C.H., Koh, Y.J., Han, J., Sung, H.K., Lee, H.J., Morisada, T., Schwendener, R.A., Brekken, R.A., Kang, G., Oike, Y., *et al.* (2007). Angiogenic role of LYVE-1-positive macrophages in adipose tissue. Circ Res *100*, E47-E57.

Cho, I., Yamanishi, S., Cox, L., Methe, B.A., Zavadil, J., Li, K., Gao, Z., Mahana, D., Raju, K., Teitler, I., *et al.* (2012). Antibiotics in early life alter the murine colonic microbiome and adiposity. Nature *488*, 621-626.

Choe, S.S., Huh, J.Y., Hwang, I.J., Kim, J.I., and Kim, J.B. (2016). Adipose Tissue Remodeling: its Role in energy Metabolism and Metabolic Disorders. Front Endocrinol *7*.

Choe, S.S., Shin, K.C., Ka, S., Lee, Y.K., Chun, J.S., and Kim, J.B. (2014). Macrophage HIF-2 alpha Ameliorates Adipose Tissue Inflammation and Insulin Resistance in Obesity. Diabetes *63*, 3359-3371.

Christakis, N.A., and Fowler, J.H. (2007). The spread of obesity in a large social network over 32 years. New Engl J Med *357*, 370-379.

Chun, J., Kim, K.Y., Lee, J.-H., and Choi, Y. (2010). The analysis of oral microbial communities of wild-type and toll-like receptor 2-deficient mice using a 454 GS FLX Titanium pyrosequencer. BMC Microbiol *10*, 101.

Cohen, P., and Spiegelman, B.M. (2015). Brown and Beige Fat: Molecular Parts of

a Thermogenic Machine. Diabetes *64*, 2346-2351.

Colca, J.R., McDonald, W.G., Waldon, D.J., Leone, J.W., Lull, J.M., Bannow, C.A., Lund, E.T., and Mathews, W.R. (2004). Identification of a novel mitochondrial protein ("mitoNEET") cross-linked specifically by a thiazolidinedione photoprobe. Am J Physiol-Endoc M *286*, E252-E260.

Collado, M.C., Isolauri, E., Laitinen, K., and Salminen, S. (2008). Distinct composition of gut microbiota during pregnancy in overweight and normal-weight women. Am J Clin Nutr *88*, 894-899.

Cook, J.B., and Nathan, P.W. (1967). On Site of Action of Diazepam in Spasticity in Man. J Neurol Sci *5*, 33-&.

Crowley, T., Fitzpatrick, J.M., Kuijper, T., Cryan, J.F., O'Toole, O., O'Leary, O.F., and Downer, E.J. (2015). Modulation of TLR3/TLR4 inflammatory signaling by the GABAB receptor agonist baclofen in glia and immune cells: relevance to therapeutic effects in multiple sclerosis. Front Cell Neurosci *9*.

Cryan, J.F., and Kaupmann, K. (2005). Don't worry 'B' happy!: a role for GABA(B) receptors in anxiety and depression. Trends Pharmacol Sci *26*, 36-43.

Dandona, P., Aljada, A., and Bandyopadhyay, A. (2004). Inflammation: the link between insulin resistance, obesity and diabetes. Trends Immunol *25*, 4-7.

de La Serre, C.B., Ellis, C.L., Lee, J., Hartman, A.L., Rutledge, J.C., and Raybould, H.E. (2010). Propensity to high-fat diet-induced obesity in rats is associated with changes in the gut microbiota and gut inflammation. Am J Physiol-Gastr L *299*, G440-G448.

Deacon, C.F., Nauck, M.A., Toft-Nielsen, M., Pridal, L., Willms, B., and Holst, J.J. (1995a). Both subcutaneously and intravenously administered glucagon-like peptide I are rapidly degraded from the NH2-terminus in type II diabetic patients and in

healthy subjects. Diabetes *44*, 1126-1131.

Deacon, C.F., Nauck, M.A., Toftnielsen, M., Pridal, L., Willms, B., and Holst, J.J. (1995b). Both Subcutaneously and Intravenously Administered Glucagon-Like Peptide-I Are Rapidly Degraded from the Nh2-Terminus in Type-Ii Diabetic-Patients and in Healthy-Subjects. Diabetes *44*, 1126-1131.

Deacon, C.F., Plamboeck, A., Moller, S., and Holst, J.J. (2002a). GLP-1-(9-36) amide reduces blood glucose in anesthetized pigs by a mechanism that does not involve insulin secretion. Am J Physiol-Endoc M *282*, E873-E879.

Deacon, C.F., Plamboeck, A., Moller, S., and Holst, J.J. (2002b). GLP-1-(9-36) amide reduces blood glucose in anesthetized pigs by a mechanism that does not involve insulin secretion. Am J Physiol Endocrinol Metab *282*, E873-879.

Desmarais, S., Jia, Z.C., and Ramachandran, C. (1998). Inhibition of protein tyrosine phosphatases PTP1B and CD45 by sulfotyrosyl peptides. Arch Biochem Biophys *354*, 225-231.

Despres, J.P., and Lemieux, I. (2006). Abdominal obesity and metabolic syndrome. Nature *444*, 881-887.

Ding, X.F., Luo, Y., Zhang, X., Zheng, H.D., Yang, X., Yang, X.X., and Liu, M.L. (2016). IL-33-driven ILC2/eosinophil axis in fat is induced by sympathetic tone and suppressed by obesity. J Endocrinol *231*, 35-48.

Donath, M.Y., and Shoelson, S.E. (2011). Type 2 diabetes as an inflammatory disease. Nat Rev Immunol *11*, 98-107.

Drew, C.A., Johnston, G.A.R., and Weatherby, R.P. (1984). Bicuculline-Insensitive Gaba Receptors - Studies on the Binding of (-)-Baclofen to Rat Cerebellar Membranes. Neurosci Lett *52*, 317-321.

Drucker, D.J., and Brubaker, P.L. (1989). Proglucagon Gene-Expression Is

Regulated by a Cyclic Amp-Dependent Pathway in Rat Intestine. P Natl Acad Sci USA *86*, 3953-3957.

Duthey, B., Hubner, A., Diehl, S., Boehncke, S., Pfeffer, J., and Boehncke, W.H. (2010). Anti-inflammatory effects of the GABA(B) receptor agonist baclofen in allergic contact dermatitis. Exp Dermatol *19*, 661-666.

Ehses, J.A., Lacraz, G., Giroix, M.H., Schmidlin, F., Coulaud, J., Kassis, N., Irminger, J.C., Kergoat, M., Portha, B., Homo-Delarche, F., *et al.* (2009). IL-1 antagonism reduces hyperglycemia and tissue inflammation in the type 2 diabetic GK rat. P Natl Acad Sci USA *106*, 13998-14003.

Eng, R.H.K., Ng, K., and Smith, S.M. (1993). Susceptibility of Resistant Enterococcus-Faecium to Unusual Antibiotics. J Antimicrob Chemother *31*, 609-610.

Enrique-Tarancon, G., Castan, I., Morin, N., Marti, L., Abella, A., Camps, M., Casamitjana, R., Palacin, M., Testar, X., Degerman, E., *et al.* (2000). Substrates of semicarbazide-sensitive amine oxidase co-operate with vanadate to stimulate tyrosine phosphorylation of insulin-receptor-substrate proteins, phosphoinositide 3-kinase activity and GLUT4 translocation in adipose cells. Biochem J *350*, 171-180.

Fang, S., Suh, J.M., Reilly, S.M., Yu, E., Osborn, O., Lackey, D., Yoshihara, E., Perino, A., Jacinto, S., Lukasheva, Y., *et al.* (2015). Intestinal FXR agonism promotes adipose tissue browning and reduces obesity and insulin resistance. Nat Med *21*, 71-77.

Faty, A., Ferre, P., and Commans, S. (2012). The Acute Phase Protein Serum Amyloid A Induces Lipolysis and Inflammation in Human Adipocytes through Distinct Pathways. Plos One *7*.

Ferrante, A.W. (2007). Obesity-induced inflammation: a metabolic dialogue in the language of inflammation. J Intern Med *262*, 408-414.

Feuerer, M., Herrero, L., Cipolletta, D., Naaz, A., Wong, J., Nayer, A., Lee, J., Goldfine, A.B., Benoist, C., Shoelson, S., *et al.* (2009). Lean, but not obese, fat is enriched for a unique population of regulatory T cells that affect metabolic parameters. Nat Med *15*, 930-U137.

Foster, M.T., Softic, S., Caldwell, J., Kohli, R., de Kloet, A.D., and Seeley, R.J. (2013). Subcutaneous Adipose Tissue Transplantation in Diet-Induced Obese Mice Attenuates Metabolic Dysregulation While Removal Exacerbates It. Physiological reports *1*.

Friedenstein, A.J., Deriglasova, U.F., Kulagina, N.N., Panasuk, A.F., Rudakowa, S.F., Luria, E.A., and Rudakow, I.A. (1974). Precursors for Fibroblasts in Different Populations of Hematopoietic Cells as Detected by Invitro Colony Assay Method. Exp Hematol *2*, 83-92.

Gassmann, M., and Bettler, B. (2012). Regulation of neuronal GABA(B) receptor functions by subunit composition. Nat Rev Neurosci *13*, 380-394.

Gealekman, O., Guseva, N., Hartigan, C., Apotheker, S., Gorgoglione, M., Gurav, K., Tran, K.-V., Straubhaar, J., Nicoloro, S., Czech, M.P., *et al.* (2011). Depot-Specific Differences and Insufficient Subcutaneous Adipose Tissue Angiogenesis in Human Obesity. Circulation *123*, 186-U173.

Gesta, S., Tseng, Y.H., and Kahn, C.R. (2007). Developmental origin of fat: Tracking obesity to its source. Cell *131*, 242-256.

Gladkevich, A., Korf, J., Hakobyan, V.P., and Melkonyan, K.V. (2006). The peripheral GABAergic system as a target in endocrine disorders. Auton Neurosci-Basic *124*, 1-8.

Grundy, S.M. (2004). Obesity, metabolic syndrome, and cardiovascular disease. J Clin Endocr Metab *89*, 2595-2600.

Guilherme, A., Virbasius, J.V., Puri, V., and Czech, M.P. (2008). Adipocyte dysfunctions linking obesity to insulin resistance and type 2 diabetes. Nat Rev Mol Cell Bio *9*, 367-377.

Hall, S.S. (1994). The Coming Plague - Newly Emerging Diseases in a World out of Balance - Garrett,L. New York Times Book Review, 13-&.

Harman-Boehm, I., Bluher, M., Redel, H., Sion-Vardy, N., Ovadia, S., Avinoach, E., Shai, I., Kloting, N., Stumvoll, M., Bashan, N., *et al.* (2007). Macrophage infiltration into omental versus subcutaneous fat across different populations: Effect of regional adiposity and the comorbidities of obesity. J Clin Endocr Metab *92*, 2240-2247.

Herlaar, E., and Brown, Z. (1999). p38 MAPK signalling cascades in inflammatory disease. Mol Med Today *5*, 439-447.

Hildebrandt, M.A., Hoffmann, C., Sherrill-Mix, S.A., Keilbaugh, S.A., Hamady, M., Chen, Y.Y., Knight, R., Ahima, R.S., Bushman, F., and Wu, G.D. (2009). High-Fat Diet Determines the Composition of the Murine Gut Microbiome Independently of Obesity. Gastroenterology *137*, 1716-1724.

Hill, A.A., Anderson-Baucum, E.K., Kennedy, A.J., Webb, C.D., Yull, F.E., and Hasty, A.H. (2015). Activation of NF-kappa B drives the enhanced survival of adipose tissue macrophages in an obesogenic environment. Mol Metab *4*, 665-677.

Hirosumi, J., Tuncman, G., Chang, L.F., Gorgun, C.Z., Uysal, K.T., Maeda, K., Karin, M., and Hotamisligil, G.S. (2002). A central role for JNK in obesity and insulin resistance. Nature *420*, 333-336.

Hocking, S.L., Stewart, R.L., Brandon, A.E., Stuart, E., Suryana, E., Blaber, S., Medynskyj, M., Herbert, B., Cooney, G.J., and Swarbrick, M.M. (2014). Intra-abdominal Transplantation of Subcutaneous Adipose Tissue in Mice Prevents High-Fat Diet-induced Inflammation and Glucose Intolerance. Diabetes *63*, A435-A435.

Holst, J.J. (2007). The physiology of glucagon-like peptide 1. Physiol Rev *87*, 1409-1439.

Holt, J.A., Luo, G.Z., Billin, A.N., Bisi, J., McNeill, Y.Y., Kozarsky, K.F., Donahee, M., Wang, D.Y., Mansfield, T.A., Kliewer, S.A., *et al.* (2003). Definition of a novel growth factor-dependent signal cascade for the suppression of bile acid biosynthesis. Gene Dev *17*, 1581-1591.

Hotamisligil, G.S., Arner, P., Caro, J.F., Atkinson, R.L., and Spiegelman, B.M. (1995). Increased Adipose-Tissue Expression of Tumor-Necrosis-Factor-Alpha in Human Obesity and Insulin-Resistance. J Clin Invest *95*, 2409-2415.

Hotamisligil, G.S., Shargill, N.S., and Spiegelman, B.M. (1993). Adipose Expression of Tumor-Necrosis-Factor-Alpha - Direct Role in Obesity-Linked Insulin Resistance. Science *259*, 87-91.

Huh, J.Y., Kim, J.I., Park, Y.J., Hwang, I.J., Lee, Y.S., Sohn, J.H., Lee, S.K., Alfadda, A.A., Kim, S.S., Choi, S.H., *et al.* (2013). A Novel Function of Adipocytes in Lipid Antigen Presentation to iNKT Cells. Mol Cell Biol *33*, 328-339.

Hwang, I., Park, Y.J., Kim, Y.R., Kim, Y.N., Ka, S., Lee, H.Y., Seong, J.K., Seok, Y.J., and Kim, J.B. (2015). Alteration of gut microbiota by vancomycin and bacitracin improves insulin resistance via glucagon-like peptide 1 in diet-induced obesity. Faseb J *29*, 2397-2411.

Im, G.I., Shin, Y.W., and Lee, K.B. (2005). Do adipose tissue-derived mesenchymal stem cells have the same osteogenic and chondrogenic potential as bone marrow-derived cells? Osteoarthr Cartilage *13*, 845-853.

Inagaki, T., Choi, M., Moschetta, A., Peng, L., Cummins, C.L., McDonald, J.G., Luo, G., Jones, S.A., Goodwin, B., Richardson, J.A., *et al.* (2005). Fibroblast growth factor 15 functions as an enterohepatic signal to regulate bile acid homeostasis. Cell Metab *2*, 217-225.

Jeffery, E., Church, C.D., Holtrup, B., Colman, L., and Rodeheffer, M.S. (2015). Rapid depot-specific activation of adipocyte precursor cells at the onset of obesity. Nat Cell Biol *17*, 376-+.

Jeong, H.W., Lee, J.W., Kim, W.S., Choe, S.S., Shin, H.J., Lee, G.Y., Shin, D., Lee, J.H., Choi, E.B., Lee, H.K., *et al.* (2010). A nonthiazolidinedione peroxisome proliferator-activated receptor alpha/gamma dual agonist CG301360 alleviates insulin resistance and lipid dysregulation in db/db mice. Molecular pharmacology *78*, 877-885.

Jinnouchi, H., Sugiyama, S., Yoshida, A., Hieshima, K., Kurinami, N., Suzuki, T., Miyamoto, F., Kajiwara, K., Matsui, K., and Jinnouchi, T. (2015). Liraglutide, a Glucagon-Like Peptide-1 Analog, Increased Insulin Sensitivity Assessed by Hyperinsulinemic-Euglycemic Clamp Examination in Patients with Uncontrolled Type 2 Diabetes Mellitus. J Diabetes Res.

Jo, H., Choe, S.S., Shin, K.C., Jang, H., Lee, J.H., Seong, J.K., Back, S.H., and Kim, J.B. (2013). Endoplasmic reticulum stress induces hepatic steatosis via increased expression of the hepatic very low-density lipoprotein receptor. Hepatology *57*, 1366-1377.

Joe, A.W.B., Yi, L., Even, Y., Vogl, A.W., and Rossi, F.M.V. (2009). Depot-Specific Differences in Adipogenic Progenitor Abundance and Proliferative Response to High-Fat Diet. Stem Cells *27*, 2563-2570.

Judex, S., Luu, Y.K., Ozcivici, E., Adler, B., Lublinsky, S., and Rubin, C.T. (2010). Quantification of adiposity in small rodents using micro-CT. Methods *50*, 14-19.

Kahn, B.B., and Flier, J.S. (2000). Obesity and insulin resistance. J Clin Invest *106*, 473-481.

Kanda, H., Tateya, S., Tamori, Y., Kotani, K., Hiasa, K.I., Kitazawa, R., Kitazawa, S., Miyachi, H., Maeda, S., Egashira, K., *et al.* (2006). MCP-1 contributes to

macrophage infiltration into adipose tissue, insulin resistance, and hepatic steatosis in obesity. J Clin Invest *116*, 1494-1505.

Kanehisa, M., and Goto, S. (2000). KEGG: Kyoto Encyclopedia of Genes and Genomes. Nucleic Acids Res *28*, 27-30.

Kazak, L., Chouchani, E.T., Jedrychowski, M.P., Erickson, B.K., Shinoda, K., Cohen, P., Vetrivelan, R., Lu, G.Z., Laznik-Bogoslavski, D., Hasenfuss, S.C., *et al.* (2015). A Creatine-Driven Substrate Cycle Enhances Energy Expenditure and Thermogenesis in Beige Fat. Cell *163*, 643-655.

Kerr, D.I.B., and Ong, J. (1995). Gaba(B) Receptors. Pharmacol Therapeut *67*, 187-246.

Kerr, D.I.B., Ong, J., Johnston, G.A.R., Abbenante, J., and Prager, R.H. (1988). 2-Hydroxy-Saclofen - an Improved Antagonist at Central and Peripheral Gabab Receptors. Neurosci Lett *92*, 92-96.

Kim, J.I., Huh, J.Y., Sohn, J.H., Choe, S.S., Lee, Y.S., Lim, C.Y., Jo, A., Park, S.B., Han, W.P., and Kim, J.B. (2015). Lipid-Overloaded Enlarged Adipocytes Provoke Insulin Resistance Independent of Inflammation. Mol Cell Biol *35*, 1686-1699.

Kim, J.Y., De Wall, E.V., Laplante, M., Azzara, A., Trujillo, M.E., Hofmann, S.M., Schraw, T., Durand, J.L., Li, H., Li, G., *et al.* (2007). Obesity-associated improvements in metabolic profile through expansion of adipose tissue. J Clin Invest *117*, 2621-2637.

Kim, K.H., Yoon, J.M., Choi, A.H., Kim, W.S., Lee, G.Y., and Kim, J.B. (2009). Liver X Receptor Ligands Suppress Ubiquitination and Degradation of LXR alpha by Displacing BARD1/BRCA1. Mol Endocrinol *23*, 466-474.

Kim, O.S., Cho, Y.J., Lee, K., Yoon, S.H., Kim, M., Na, H., Park, S.C., Jeon, Y.S., Lee, J.H., Yi, H., *et al.* (2012). Introducing EzTaxon-e: a prokaryotic 16S rRNA gene

sequence database with phylotypes that represent uncultured species. Int J Syst Evol Microbiol *62*, 716-721.

Kim, S.H., and Plutzky, J. (2016). Brown Fat and Browning for the Treatment of Obesity and Related Metabolic Disorders. Diabetes Metab J *40*, 12-21.

Kirk, E.A., Sagawa, Z.K., McDonald, T.O., O'Brien, K.D., and Heinecke, J.W. (2008). Monocyte chemoattractant protein-1 deficiency fails to restrain macrophage infiltration into adipose tissue. Diabetes *57*, 1254-1261.

Kissebah, A.H., and Krakower, G.R. (1994). Regional Adiposity and Morbidity. Physiol Rev *74*, 761-811.

Kobayashi, M., Ikegami, H., Fujisawa, T., Nojima, K., Kawabata, Y., Noso, S., Babaya, N., Itoi-Babaya, M., Yamaji, K., Hiromine, Y., *et al.* (2007). Prevention and treatment of obesity, insulin resistance, and diabetes by bile acid-binding resin. Diabetes *56*, 239-247.

Kovacova, Z., Tencerova, M., Roussel, B., Wedellova, Z., Rossmeislova, L., Langin, D., Polak, J., and Stich, V. (2012). The impact of obesity on secretion of adiponectin multimeric isoforms differs in visceral and subcutaneous adipose tissue. Int J Obesity *36*, 1360-1365.

Kusminski, C.M., Holland, W.L., Sun, K., Park, J., Spurgin, S.B., Lin, Y., Askew, G.R., Simcox, J.A., McClain, D.A., Li, C., *et al.* (2012). MitoNEET-driven alterations in adipocyte mitochondrial activity reveal a crucial adaptive process that preserves insulin sensitivity in obesity. Nat Med *18*, 1539-U1144.

Langmead, B., and Salzberg, S.L. (2012). Fast gapped-read alignment with Bowtie 2. Nat Methods *9*, 357-359.

Larsen, N., Vogensen, F.K., van den Berg, F.W.J., Nielsen, D.S., Andreasen, A.S., Pedersen, B.K., Abu Al-Soud, W., Sorensen, S.J., Hansen, L.H., and Jakobsen, M.

(2010). Gut Microbiota in Human Adults with Type 2 Diabetes Differs from Non-Diabetic Adults. PLoS One *5*.

Lauffer, L.M., Lakoubov, R., and Brubaker, P.L. (2009). GPR119 Is Essential for Oleoylethanolamide-Induced Glucagon-Like Peptide-1 Secretion From the Intestinal Enteroendocrine L-Cell. Diabetes *58*, 1058-1066.

Law, C.W., Chen, Y.S., Shi, W., and Smyth, G.K. (2014). voom: precision weights unlock linear model analysis tools for RNA-seq read counts. Genome Biol *15*.

Lee, Y.C., Brubaker, P.L., and Drucker, D.J. (1990). Developmental and Tissue-Specific Regulation of Proglucagon Gene-Expression. Endocrinology *127*, 2217-2222.

Lee, Y.H., Petkova, A.P., and Granneman, J.G. (2013). Identification of an Adipogenic Niche for Adipose Tissue Remodeling and Restoration. Cell Metab *18*, 355-367.

Lee, Y.S., Li, P.P., Huh, J.Y., Hwang, I.J., Lu, M., Kim, J.I., Ham, M., Talukdar, S., Chen, A., Lu, W.J., *et al.* (2011). Inflammation Is Necessary for Long-Term but Not Short-Term High-Fat Diet Induced Insulin Resistance. Diabetes *60*, 2474-2483.

Ley, R.E., Backhed, F., Turnbaugh, P., Lozupone, C.A., Knight, R.D., and Gordon, J.I. (2005a). Obesity alters gut microbial ecology. Proc Natl Acad Sci U S A *102*, 11070-11075.

Ley, R.E., Backhed, F., Turnbaugh, P., Lozupone, C.A., Knight, R.D., and Gordon, J.I. (2005b). Obesity alters gut microbial ecology. P Natl Acad Sci USA *102*, 11070-11075.

Li, B., and Dewey, C.N. (2011). RSEM: accurate transcript quantification from RNA-Seq data with or without a reference genome. Bmc Bioinformatics *12*.

Li, G.L., Xie, C., Lu, S.Y., Nichols, R.G., Tian, Y., Li, L.C., Patel, D., Ma, Y.Y.,

Brocker, C.N., Yan, T.T., *et al.* (2017). Intermittent Fasting Promotes White Adipose Browning and Decreases Obesity by Shaping the Gut Microbiota. Cell Metab *26*, 672-+.

Lim, G.E., and Brubaker, P.L. (2006). Glucagon-like peptide 1 secretion by the L-cell - The view from within. Diabetes *55*, S70-S77.

Lingohr, M.K., Buettner, R., and Rhodes, C.J. (2002). Pancreatic beta-cell growth and survival--a role in obesity-linked type 2 diabetes? Trends Mol Med *8*, 375-384.

Liu, J., Divoux, A., Sun, J., Zhang, J., Clement, K., Glickman, J.N., Sukhova, G.K., Wolters, P.J., Du, J., Gorgun, C.Z., *et al.* (2009). Genetic deficiency and pharmacological stabilization of mast cells reduce diet-induced obesity and diabetes in mice. Nat Med *15*, 940-U144.

Ludwig, D.D.S. (2002). The glycemic index - Physiological mechanisms relating to obesity, diabetes, and cardiovascular disease. Jama-J Am Med Assoc *287*, 2414-2423.

Lumeng, C.N., Bodzin, J.L., and Saltiel, A.R. (2007a). Obesity induces a phenotypic switch in adipose tissue macrophage polarization. J Clin Invest *117*, 175-184.

Lumeng, C.N., DeYoung, S.M., Bodzin, J.L., and Saltiel, A.R. (2007b). Increased inflammatory properties of adipose tissue macrophages recruited during diet-induced obesity. Diabetes *56*, 16-23.

Macdonald, M.J., and Fahien, L.A. (1988). Glyceraldehyde Phosphate and Methyl-Esters of Succinic Acid 2 New Potent Insulin Secretagogues. Diabetes *37*, 997-999.

Macdonald, R.L., and Olsen, R.W. (1994). Gaba(a) Receptor Channels. Annu Rev Neurosci *17*, 569-602.

Magnaghi, V., Ballabio, M., Camozzi, F., Colleoni, M., Consoli, A., Gassmann, M., Lauria, G., Motta, M., Procacci, P., Trovato, A.E., *et al.* (2008). Altered peripheral myelination in mice lacking GABA(B) receptors. Mol Cell Neurosci *37*, 599-609.

Makishima, M., Okamoto, A.Y., Repa, J.J., Tu, H., Learned, R.M., Luk, A., Hull, M.V., Lustig, K.D., Mangelsdorf, D.J., and Shan, B. (1999). Identification of a nuclear receptor for bile acids. Science *284*, 1362-1365.

Martin, F.P., Dumas, M.E., Wang, Y., Legido-Quigley, C., Yap, I.K., Tang, H., Zirah, S., Murphy, G.M., Cloarec, O., Lindon, J.C., *et al.* (2007). A top-down systems biology view of microbiome-mammalian metabolic interactions in a mouse model. Mol Syst Biol *3*, 112.

Matsumoto, M., Kibe, R., Ooga, T., Aiba, Y., Kurihara, S., Sawaki, E., Koga, Y., and Benno, Y. (2012). Impact of intestinal microbiota on intestinal luminal metabolome. Sci Rep *2*, 233.

Meigs, J.B., Wilson, P.W., Sullivan, L., Fox, C.S., and D'Agostino, R.B. (2005). Metabolic syndrome accounts for increased risk of type 2 diabetes or cardiovascular disease associated with overall obesity. Circulation *111*, E200-E200.

Membrez, M., Blancher, F., Jaquet, M., Bibiloni, R., Cani, P.D., Burcelin, R.G., Corthesy, I., Mace, K., and Chou, C.J. (2008a). Gut microbiota modulation with norfloxacin and ampicillin enhances glucose tolerance in mice. FASEB J *22*, 2416-2426.

Membrez, M., Blancher, F., Jaquet, M., Bibiloni, R., Cani, P.D., Burcelin, R.G., Corthesy, I., Mace, K., and Chou, C.J. (2008b). Gut microbiota modulation with norfloxacin and ampicillin enhances glucose tolerance in mice. Faseb J *22*, 2416-2426.

Mendez, J.D., and Balderas, F. (2001). Regulation of hyperglycemia and dyslipidemia by exogenous L-arginine in diabetic rats. Biochimie *83*, 453-458.

Mestdagh, R., Dumas, M.E., Rezzi, S., Kochhar, S., Holmes, E., Claus, S.P., and Nicholson, J.K. (2012). Gut Microbiota Modulate the Metabolism of Brown Adipose Tissue in Mice. J Proteome Res *11*, 620-630.

Metchnikoff, E. (1908). The prolongation of life (New York & London: G. P. Putman's Sons).

Miller, N.E., Michel, C.C., Nanjee, M.N., Olszewski, W.L., Miller, I.P., Hazell, M., Olivecrona, G., Sutton, P., Humphreys, S.M., and Frayn, K.N. (2011). Secretion of adipokines by human adipose tissue in vivo: partitioning between capillary and lymphatic transport. Am J Physiol-Endoc M *301*, E659-E667.

Miyazaki, Y., Mahankali, A., Matsuda, M., Mahankali, S., Hardies, J., Cusi, K., Mandarino, L.J., and DeFronzo, R.A. (2002). Effect of pioglitazone on abdominal fat distribution and insulin sensitivity in type 2 diabetic patients. J Clin Endocr Metab *87*, 2784-2791.

Montague, C.T., Prins, J.B., Sanders, L., Zhang, J.L., Sewter, C.P., Digby, J., Byrne, C.D., and O'Rahilly, S. (1998). Depot-related gene expression in human subcutaneous and omental adipocytes. Diabetes *47*, 1384-1391.

Muegge, B.D., Kuczynski, J., Knights, D., Clemente, J.C., Gonzalez, A., Fontana, L., Henrissat, B., Knight, R., and Gordon, J.I. (2011). Diet Drives Convergence in Gut Microbiome Functions Across Mammalian Phylogeny and Within Humans. Science *332*, 970-974.

Muller, T.D., Nogueiras, R., Andermann, M.L., Andrews, Z.B., Anker, S.D., Argente, J., Batterham, R.L., Benoit, S.C., Bowers, C.Y., Broglio, F., *et al.* (2015). Ghrelin. Mol Metab *4*, 437-460.

Murphy, E.F., Cotter, P.D., Hogan, A., O'Sullivan, O., Joyce, A., Fouhy, F., Clarke, S.F., Marques, T.M., O'Toole, P.W., Stanton, C., *et al.* (2013a). Divergent metabolic outcomes arising from targeted manipulation of the gut microbiota in diet-induced obesity. Gut *62*, 220-226.

Murphy, E.F., Cotter, P.D., Hogan, A., O'Sullivan, O., Joyce, A., Fouhy, F., Clarke, S.F., Marques, T.M., O'Toole, P.W., Stanton, C., *et al.* (2013b). Divergent metabolic

outcomes arising from targeted manipulation of the gut microbiota in diet-induced obesity. Gut *62*, 220-226.

Muscelli, E., Mari, A., Casolaro, A., Camastra, S., Seghieri, G., Gastaldelli, A., Holst, J.J., and Ferrannini, E. (2008). Separate impact of obesity and glucose tolerance on the incretin effect in normal subjects and type 2 diabetic patients. Diabetes *57*, 1340-1348.

Musso, G., Gambino, R., and Cassader, M. (2010). Obesity, Diabetes, and Gut Microbiota The hygiene hypothesis expanded? Diabetes Care *33*, 2277-2284.

Nguyen, M.T.A., Favelyukis, S., Nguyen, A.K., Reichart, D., Scott, P.A., Jenn, A., Liu-Bryan, R., Glass, C.K., Neels, J.G., and Olefsky, J.M. (2007). A subpopulation of macrophages infiltrates hypertrophic adipose tissue and is activated by free fatty acids via toll-like receptors 2 and 4 and JNK-dependent pathways. J Biol Chem *282*, 35279-35292.

Nikolaidis, L.A., Elahi, D., Shen, Y.T., and Shannon, R.P. (2005). Active metabolite of GLP-1 mediates myocardial glucose uptake and improves left ventricular performance in conscious dogs with dilated cardiomyopathy. American Journal of Physiology-Heart and Circulatory Physiology *289*, H2401-H2408.

Nishimura, S., Manabe, I., Nagasaki, M., Eto, K., Yamashita, H., Ohsugi, M., Otsu, M., Hara, K., Ueki, K., Sugiura, S., *et al.* (2009). CD8(+) effector T cells contribute to macrophage recruitment and adipose tissue inflammation in obesity. Nat Med *15*, 914-U116.

Odegaard, J.I., and Chawla, A. (2011). Alternative Macrophage Activation and Metabolism. Annu Rev Pathol-Mech *6*, 275-297.

Odegaard, J.I., Ricardo-Gonzalez, R.R., Eagle, A.R., Vats, D., Morel, C.R., Goforth, M.H., Subramanian, V., Mukundan, L., Ferrante, A.W., and Chawla, A. (2008). Alternative M2 activation of Kupffer cells by PPAR delta ameliorates obesity-

induced insulin resistance. Cell Metab *7*, 496-507.

Oh, D.Y., Morinaga, H., Talukdar, S., Bae, E.J., and Olefsky, J.M. (2012). Increased Macrophage Migration Into Adipose Tissue in Obese Mice. Diabetes *61*, 346-354.

Olefsky, J.M., and Glass, C.K. (2010a). Macrophages, inflammation, and insulin resistance. Annu Rev Physiol *72*, 219-246.

Olefsky, J.M., and Glass, C.K. (2010b). Macrophages, Inflammation, and Insulin Resistance. Annu Rev Physiol *72*, 219-246.

Olpe, H.R., Karlsson, G., Pozza, M.F., Brugger, F., Steinmann, M., Vanriezen, H., Fagg, G., Hall, R.G., Froestl, W., and Bittiger, H. (1990). Cgp 35348 - a Centrally Active Blocker of Gaba-B Receptors. Eur J Pharmacol *187*, 27-38.

Parlevliet, E.T., van Weenen, J.E.D., Romijn, J.A., and Pijl, H. (2010). GLP-1 treatment reduces endogenous insulin resistance via activation of central GLP-1 receptors in mice fed a high-fat diet. Am J Physiol-Endoc M *299*, E318-E324.

Patsouris, D., Li, P.P., Thapar, D., Chapman, J., Olefsky, J.M., and Neels, J.G. (2008). Ablation of CD11c-Positive Cells Normalizes Insulin Sensitivity in Obese Insulin Resistant Animals. Cell Metab *8*, 301-309.

Permana, P.A., Menge, C., and Reaven, P.D. (2006). Macrophage-secreted factors induce adipocyte inflammation and insulin resistance. Biochem Biophys Res Commun *341*, 507-514.

Petersen, K.F., Dufour, S., Befroy, D., Lehrke, M., Hendler, R.E., and Shulman, G.I. (2005). Reversal of nonalcoholic hepatic steatosis, hepatic insulin resistance, and hyperglycemia by moderate weight reduction in patients with type 2 diabetes. Diabetes *54*, 603-608.

Pols, T.W.H., Auwerx, J., and Schoonjans, K. (2010). Targeting the TGR5-GLP-1 pathway to combat type 2 diabetes and non-alcoholic fatty liver disease. Gastroen

Clin Biol *34*, 270-273.

Pouliot, M.C., Despres, J.P., Nadeau, A., Moorjani, S., Prudhomme, D., Lupien, P.J., Tremblay, A., and Bouchard, C. (1992). Visceral Obesity in Men - Associations with Glucose-Tolerance, Plasma-Insulin, and Lipoprotein Levels. Diabetes *41*, 826-834.

Qiang, G.F., Kong, H.W., Fang, D.F., McCann, M., Yang, X.Y., Du, G.H., Bluher, M., Zhu, J.F., and Liew, C.W. (2016). The obesity-induced transcriptional regulator TRIP-Br2 mediates visceral fat endoplasmic reticulum stress-induced inflammation. Nat Commun *7*.

Rajilic-Stojanovic, M., and de Vos, W.M. (2014). The first 1000 cultured species of the human gastrointestinal microbiota. Fems Microbiol Rev *38*, 996-1047.

Ramkhelawon, B., Hennessy, E.J., Menager, M., Ray, T.D., Sheedy, F.J., Hutchison, S., Wanschel, A., Oldebeken, S., Geoffrion, M., Spiro, W., *et al.* (2014). Netrin-1 promotes adipose tissue macrophage retention and insulin resistance in obesity. Nat Med *20*, 377-+.

Ranganath, L.R., Beety, J.M., Morgan, L.M., Wright, J.W., Howland, R., and Marks, V. (1996). Attenuated GLP-1 secretion in obesity: Cause or consequence? Gut *38*, 916-919.

Rao, S., Kupfer, Y., Pagala, M., Chapnick, E., and Tessler, S. (2011). Systemic absorption of oral vancomycin in patients with Clostridium difficile infection. Scand J Infect Dis *43*, 386-388.

Roberts, E., and Frankel, S. (1950). Gamma-Aminobutyric Acid in Brain - Its Formation from Glutamic Acid. J Biol Chem *187*, 55-63.

Rose, W.C. (1911). Mucic acid and intermediary carbohydrate metabolism. J Biol Chem *10*, 16.

Rosen, E.D., and Spiegelman, B.M. (2006). Adipocytes as regulators of energy

balance and glucose homeostasis. Nature *444*, 847-853.

Russell, D.W. (2003). The enzymes, regulation, and genetics of bile acid synthesis. Annu Rev Biochem *72*, 137-174.

Saltiel, A.R., and Kahn, C.R. (2001). Insulin signalling and the regulation of glucose and lipid metabolism. Nature *414*, 799-806.

Savage, D.C. (1977). Microbial ecology of the gastrointestinal tract. Annu Rev Microbiol *31*, 107-133.

Schaffler, A., Muller-Ladner, U., Scholmerich, J., and Buchler, C. (2006). Role of adipose tissue as an inflammatory organ in human diseases. Endocr Rev *27*, 449-467.

Schuler, V., Luscher, C., Blanchet, C., Klix, N., Sansig, G., Klebs, K., Schmutz, M., Heid, J., Gentry, C., Urban, L., *et al.* (2001). Epilepsy, hyperalgesia, impaired memory, and loss of pre- and postsynaptic GABA(B) responses in mice lacking GABA(B(1)). Neuron *31*, 47-58.

Schulz, M.D., Atay, C., Heringer, J., Romrig, F.K., Schwitalla, S., Aydin, B., Ziegler, P.K., Varga, J., Reindl, W., Pommerenke, C., *et al.* (2014). High-fat-diet-mediated dysbiosis promotes intestinal carcinogenesis independently of obesity. Nature *514*, 508-+.

Schwiertz, A., Taras, D., Schafer, K., Beijer, S., Bos, N.A., Donus, C., and Hardt, P.D. (2010). Microbiota and SCFA in lean and overweight healthy subjects. Obesity *18*, 190-195.

Seale, P., Conroe, H.M., Estall, J., Kajimura, S., Frontini, A., Ishibashi, J., Cohen, P., Cinti, S., and Spiegelman, B.M. (2011). Prdm16 determines the thermogenic program of subcutaneous white adipose tissue in mice. J Clin Invest *121*, 96-105.

Siviero-Miachon, A.A., Spinola-Castro, A.M., Lee, M.L.D., Monteiro, C.M.D., Carvalho, A.C.D., Calixto, A.R., Geloneze, B., and Guerra-Junior, G. (2015).

Subcutaneous adipose tissue plays a beneficial effect on subclinical atherosclerosis in young survivors of acute lymphocytic leukemia. Vasc Health Risk Man *11*, 479-488.

Soltani, N., Qiu, H.M., Aleksic, M., Glinka, Y., Zhao, F., Liu, R., Li, Y.M., Zhang, N., Chakrabarti, R., Ng, T., *et al.* (2011). GABA exerts protective and regenerative effects on islet beta cells and reverses diabetes. P Natl Acad Sci USA *108*, 11692-11697.

Suarez-Zamorano, N., Fabbiano, S., Chevalier, C., Stojanovic, O., Colin, D.J., Stevanovic, A., Veyrat-Durebex, C., Tarallo, V., Rigo, D., Germain, S., *et al.* (2015). Microbiota depletion promotes browning of white adipose tissue and reduces obesity. Nat Med *21*, 1497-+.

Suez, J., Korem, T., Zeevi, D., Zilberman-Schapira, G., Thaiss, C.A., Maza, O., Israeli, D., Zmora, N., Gilad, S., Weinberger, A., *et al.* (2014). Artificial sweeteners induce glucose intolerance by altering the gut microbiota. Nature *514*, 181-+.

Svendsen, B., and Holst, J.J. (2016). Regulation of gut hormone secretion. Studies using isolated perfused intestines. Peptides *77*, 47-53.

Swann, J.R., Want, E.J., Geier, F.M., Spagou, K., Wilson, I.D., Sidaway, J.E., Nicholson, J.K., and Holmes, E. (2011). Systemic gut microbial modulation of bile acid metabolism in host tissue compartments. Proc Natl Acad Sci U S A *108 Suppl 1*, 4523-4530.

Talukdar, S., Oh, D.Y., Bandyopadhyay, G., Li, D.M., Xu, J.F., McNelis, J., Lu, M., Li, P.P., Yan, Q.Y., Zhu, Y.M., *et al.* (2012). Neutrophils mediate insulin resistance in mice fed a high-fat diet through secreted elastase. Nat Med *18*, 1407-+.

Tang, W.H.W., Wang, Z.E., Levison, B.S., Koeth, R.A., Britt, E.B., Fu, X.M., Wu, Y.P., and Hazen, S.L. (2013). Intestinal Microbial Metabolism of Phosphatidylcholine and Cardiovascular Risk. New Engl J Med *368*, 1575-1584.

Tarca, A.L., Draghici, S., Khatri, P., Hassan, S.S., Mittal, P., Kim, J.S., Kim, C.J., Kusanovic, J.P., and Romero, R. (2009). A novel signaling pathway impact analysis. Bioinformatics *25*, 75-82.

Tian, J., Dang, H.N., Yong, J., Chui, W.S., Dizon, M.P.G., Yaw, C.K.Y., and Kaufman, D.L. (2011). Oral Treatment with gamma-Aminobutyric Acid Improves Glucose Tolerance and Insulin Sensitivity by Inhibiting Inflammation in High Fat Diet-Fed Mice. Plos One *6*.

Tian, J.D., Lu, Y.X., Zhang, H.W., Chau, C.H., Dang, H.N., and Kaufman, D.L. (2004). gamma-aminobutyric acid inhibits T cell autoimmunity and the development of inflammatory responses in a mouse type 1 diabetes model. J Immunol *173*, 5298-5304.

Tolhurst, G., Heffron, H., Lam, Y.S., Parker, H.E., Habib, A.M., Diakogiannaki, E., Cameron, J., Grosse, J., Reimann, F., and Gribble, F.M. (2012). Short-Chain Fatty Acids Stimulate Glucagon-Like Peptide-1 Secretion via the G-Protein-Coupled Receptor FFAR2. Diabetes *61*, 364-371.

Tran, T.T., Yamamoto, Y., Gesta, S., and Kahn, C.R. (2008). Beneficial effects of subcutaneous fat transplantation on metabolism. Cell Metab *7*, 410-420.

Tu, H., Okamoto, A.Y., and Shan, B. (2000). FXR, a bile acid receptor and biological sensor. Trends Cardiovas Med *10*, 30-35.

Tu, H.J., Xu, C.J., Zhang, W.H., Liu, Q.Y., Rondard, P., Pin, J.P., and Liu, J.F. (2010). GABA(B) Receptor Activation Protects Neurons from Apoptosis via IGF-1 Receptor Transactivation. J Neurosci *30*, 749-759.

Turnbaugh, P.J., Hamady, M., Yatsunenko, T., Cantarel, B.L., Duncan, A., Ley, R.E., Sogin, M.L., Jones, W.J., Roe, B.A., Affourtit, J.P., *et al.* (2009). A core gut microbiome in obese and lean twins. Nature *457*, 480-U487.

Turnbaugh, P.J., Ley, R.E., Mahowald, M.A., Magrini, V., Mardis, E.R., and Gordon, J.I. (2006). An obesity-associated gut microbiome with increased capacity for energy harvest. Nature *444*, 1027-1031.

Turner, M.D., Nedjai, B., Hurst, T., and Pennington, D.J. (2014). Cytokines and chemokines: At the crossroads of cell signalling and inflammatory disease. Bba-Mol Cell Res *1843*, 2563-2582.

Urrutia, M., Fernandez, S., Gonzalez, M., Vilches, R., Rojas, P., Vasquez, M., Kurte, M., Vega-Letter, A.M., Carrion, F., Figueroa, F., *et al.* (2016). Overexpression of Glutamate Decarboxylase in Mesenchymal Stem Cells Enhances Their Immunosuppressive Properties and Increases GABA and Nitric Oxide Levels. Plos One *11*.

Vahl, T.P., Paty, B.W., Fuller, B.D., Prigeon, R.L., and D'Alessio, D.A. (2003). Effects of GLP-1-(7-36)NH(2), GLP-1-(7-37), and GLP-1-(9-36)NH(2) on intravenous glucose tolerance and glucose-induced insulin secretion in healthy humans. J Clin Endocr Metab *88*, 1772-1779.

Van Eldere, J., Celis, P., De Pauw, G., Lesaffre, E., and Eyssen, H. (1996). Tauroconjugation of cholic acid stimulates 7 alpha-dehydroxylation by fecal bacteria. Appl Environ Microbiol *62*, 656-661.

Vijay-Kumar, M., Aitken, J.D., Carvalho, F.A., Cullender, T.C., Mwangi, S., Srinivasan, S., Sitaraman, S.V., Knight, R., Ley, R.E., and Gewirtz, A.T. (2010). Metabolic syndrome and altered gut microbiota in mice lacking Toll-like receptor 5. Science *328*, 228-231.

Walter, J., and Ley, R. (2011). The Human Gut Microbiome: Ecology and Recent Evolutionary Changes. Annual Review of Microbiology, Vol 65 *65*, 411-429.

Wang, Z.N., Klipfell, E., Bennett, B.J., Koeth, R., Levison, B.S., Dugar, B., Feldstein, A.E., Britt, E.B., Fu, X.M., Chung, Y.M., *et al.* (2011). Gut flora metabolism of

phosphatidylcholine promotes cardiovascular disease. Nature *472*, 57-U82.

Warren, J.R., and Marshall, B. (1983). Unidentified curved bacilli on gastric epithelium in active chronic gastritis. Lancet *1*, 1273-1275.

Watala, C., Kazmierczak, P., Dobaczewski, M., Przygodzki, T., Bartus, M., Lomnicka, M., Slominska, E.M., Durackova, Z., and Chlopicki, S. (2009). Anti-diabetic effects of 1-methylnicotinamide (MNA) in streptozocin-induced diabetes in rats. Pharmacol Rep *61*, 86-98.

Waterston, R.H., Lindblad-Toh, K., Birney, E., Rogers, J., Abril, J.F., Agarwal, P., Agarwala, R., Ainscough, R., Alexandersson, M., An, P., *et al.* (2002). Initial sequencing and comparative analysis of the mouse genome. Nature *420*, 520-562.

Weisberg, S.P., McCann, D., Desai, M., Rosenbaum, M., Leibel, R.L., and Ferrante, A.W. (2003). Obesity is associated with macrophage accumulation in adipose tissue. J Clin Invest *112*, 1796-1808.

Wellen, K.E., and Hotamisligil, G.S. (2003). Obesity-induced inflammatory changes in adipose tissue. J Clin Invest *112*, 1785-1788.

WHO (2017). Obesity and overweight. World Health Organization (WHO).

Willms, B., Werner, J., Holst, J.J., Orskov, C., Creutzfeldt, W., and Nauck, M.A. (1996). Gastric emptying glucose responses, and insulin secretion after a liquid test meal: Effects of exogenous glucagon-like peptide-1 (GLP-1)-(7-36) amide in type 2 (noninsulin-dependent) diabetic patients. J Clin Endocr Metab *81*, 327-332.

Winer, D.A., Winer, S., Shen, L., Wadia, P.P., Yantha, J., Paltser, G., Tsui, H., Wu, P., Davidson, M.G., Alonso, M.N., *et al.* (2011). B cells promote insulin resistance through modulation of T cells and production of pathogenic IgG antibodies. Nat Med *17*, 610-U134.

Wolf, M., Muller, T., Dandekar, T., and Pollack, J.D. (2004). Phylogeny of

Firmicutes with special reference to Mycoplasma (Mollicutes) as inferred from phosphoglycerate kinase amino acid sequence data. Int J Syst Evol Microbiol *54*, 871-875.

Wu, T., Bound, M.J., Standfield, S.D., Gedulin, B., Jones, K.L., Horowitz, M., and Rayner, C.K. (2013a). Effects of rectal administration of taurocholic acid on glucagon-like peptide-1 and peptide YY secretion in healthy humans. Diabetes Obesity & Metabolism *15*, 474-477.

Wu, T.Z., Bound, M.J., Standfield, S.D., Jones, K.L., Horowitz, M., and Rayner, C.K. (2013b). Effects of Taurocholic Acid on Glycemic, Glucagon-like Peptide-1, and Insulin Responses to Small Intestinal Glucose Infusion in Healthy Humans. J Clin Endocr Metab *98*, E718-E722.

Xie, Q.W., Kashiwabara, Y., and Nathan, C. (1994). Role of Transcription Factor Nf-Kappa-B/Rel in Induction of Nitric-Oxide Synthase. J Biol Chem *269*, 4705-4708.

Xie, Z.X., Xia, S.F., and Le, G.W. (2014). Gamma-aminobutyric acid improves oxidative stress and function of the thyroid in high-fat diet fed mice. J Funct Foods *8*, 76-86.

Xu, X.J., Gauthier, M.S., Hess, D.T., Apovian, C.M., Cacicedo, J.M., Gokce, N., Farb, M., Valentine, R.J., and Ruderman, N.B. (2012). Insulin sensitive and resistant obesity in humans: AMPK activity, oxidative stress, and depot-specific changes in gene expression in adipose tissue. J Lipid Res *53*, 792-801.

Yuan, M.S., Konstantopoulos, N., Lee, J.S., Hansen, L., Li, Z.W., Karin, M., and Shoelson, S.E. (2001). Reversal of obesity- and diet-induced insulin resistance with salicylates or targeted disruption of IKK beta. Science *293*, 1673-1677.

Zhang, B., Berger, J., Hu, E.I., Szalkowski, D., WhiteCarrington, S., Spiegelman, B.M., and Moller, D.E. (1996). Negative regulation of peroxisome proliferator-activated receptor-gamma gene expression contributes to the antiadipogenic effects

of tumor necrosis factor-alpha. Mol Endocrinol *10*, 1457-1466.

Zhang, W.H., Xu, C.J., Tu, H.J., Wang, Y.Y., Sun, Q., Hu, P., Hu, Y.J., Rondard, P., and Liu, J.F. (2015). GABA(B) receptor upregulates fragile X mental retardation protein expression in neurons. Sci Rep-Uk *5*.

국문 초록

주요 소화기관인 소장은 외부에서 흡수한 영양분의 분해 및 체내 흡수를 통하여 체내 에너지를 공급하는 역할을 담당하며, 지방조직은 외부에서 유입된 잉여 에너지를 지질 형태로 저장함으로써 체내 에너지 항상성을 조절한다. 또한, 소장과 지방조직은 체내 영양 상태에 따라 다양한 호르몬을 분비하여 전신적 에너지 대사를 능동적으로 조절하는데 관여한다. 최근 연구결과에 따르면, 장내 미생물은 비만 및 인슐린 민감도 조절에 중요한 요인 중 하나로 연구되고 있다. 다양한 장내미생물 중 대부분을 차지하는 Firmicutes 및 Bacteroidetes 문(門)은 비만이 유도되면 상대적 비율이 변화한다. 선행연구결과에서 장내미생물이 없는 생쥐는 대조군과 대비하여 고지방식이 투여시 비만 및 인슐린 저항성이 대조군 대비 개선됨이 보고되었다. 그럼에도 불구하고 Firmicutes 및 Bacteroidetes 두 門에 의한 비만 및 에너지 대사 조절에 대한 분자수준의 기전 연구는 명확하게 규명된 바가 없다.

비만이 유도되면 지방조직 내 염증반응이 증가한다. 지방조직내 염증반응 증가는 인슐린 저항성 유도의 주요 원인 중 하나로 알려져 있다. 다양한 지방조직 가운데 내장지방조직 비대화는 대사성 질환 발병률과 높은 양의 상관관계를 가진다. 반면 피하지방조직은 에너지 대사 항상성

조절에 긍정적 역할로 기여한다. 흥미롭게도 비만 개체에서 내장지방조직과 피하지방조직은 염증반응의 양상이 다르게 나타남이 알려져 있다. 그럼에도 불구하고 내장지방조직과 피하지방조직 간 상이한 염증반응의 원인에 대한 기전 연구는 부족한 상황이다. 본 학위논문 연구에서는 대사성 질환 유발에 중요한 인슐린 저항성 조절 기전을 다각적 측면에서 규명하기 위하여 장내미생물 및 지방조직의 역할과 조절 기전을 연구하고자 하였다.

본 논문의 1장에서는 Firmicutes와 Bacteroidetes에 의한 비만 및 인슐린 민감도 조절을 조사하기 위하여 Firmicutes와 Bacteroidetes가 선택적으로 감소된 생쥐 모델을 구축하였다. 이 생쥐 모델은 전체 장내미생물이 제거된 (germ-free) 생쥐와 달리, 고지방성 식이 투여에 의한 비만이 개선되지 않았음에도 불구하고 인슐린 저항성은 현저히 개선되었다. 또한 장내 미생물의 변화와 맞물려 담즙 성분 가운데 taurocholic 산이 증가하였다. 흥미롭게도 taurocholic 산은 장 호르몬 glucagon-like peptide 1 (GLP-1)을 증가시킴으로써 인슐린 저항성을 완화시켰다. 이상의 결과들은 Firmicutes 및 Bacteroidetes가 소장의 GLP-1 분비를 조절함으로써 체내 에너지 대사 조절에 기여할 수 있음을 제시하였다.

본 논문의 2장에서는 비만 개체에서 지방조직 위치 특이성에 따른 염증반응 차이를 관찰하고 그 원인을 분석하였다. 비만 유도시 피하지방

조직은 내장지방조직 대비 대식세포 침투율이 낮았다. 지방조직 이식수술 실험을 통해 지방조직 위치 특이성에 따른 대식세포 침투 차이는 지방조직 고유의 내재적 특성에 기인할 수 있음을 추론하였다. 나아가 내장 및 피하 지방조직은 Gamma (γ)-amino butyric acid (GABA)의 신호전달경로가 다르게 조절됨을 발견하였다. 피하 및 내장지방조직에 GABA 자극을 가했을 경우 피하지방조직 특이적으로 대식세포 및 지방조직 염증반응이 억제되었고 동시에 인슐린 저항성이 개선됨을 관찰함으로써 지방조직 위치 특이적 대식세포 침투 조절에 GABA 신호가 관여하여 체내 에너지 대사 조절이 가능함을 규명하였다. 이와 더불어 피하지방조직 특이적 GABA 신호에 대한 대식세포 침투 억제효과는 피하지방조직 내 지방줄기세포와 연관되어 있음을 관찰하였다.

본 연구를 통하여 장내 미생물과 피하지방조직은 비만에서 유도된 인슐린 저항성 및 당 대사를 조절할 수 있음을 새로이 제안하였다. 이를 통하여 비만으로부터 유도되는 인슐린 저항성의 기전적 이해를 도모하였다. 그러므로 장내미생물 및 피하지방조직의 GABA 신호전달 조절은 인슐린 저항성으로 인한 대사성 질환 극복의 새로운 표적이 될 수 있음을 제안한다.

주요어: **인슐린 저항성**, **장내미생물**, Firmicutes, Bacteroidetes, **피하지방조직**, **내장지방조직**, **염증반응**, **대식세포**, GABA, **지방줄기세포**

학번: 2008-22701